Regina A. Schmidt

Masses and Decay Widths of Hadron Resonances with Explicit Pionic Contributions

DISSERTATION

zur Erlangung des Doktorgrades der Naturwissenschaften

Institut für Physik
Fachbereich Theoretische Physik
Karl-Franzens-Universität Graz

Betreuung:
Univ.- Prof. Dr. Willibald Plessas

Graz/2018

Präambel

Ich, Regina A. Schmidt, bestätige, dass es sich bei der hier vorgelegten Dissertation um eine Originalarbeit handelt, die von mir selbständig angefertigt und abgefasst wurde.

Abstract

In this thesis we aim at studying hadron resonances with explicit mesonic degrees of freedom. We work in the framework of relativistic quantum mechanics and develop a coupled-channels formalism. This allows to include mesonic degrees of freedom by coupling to specific hadronic decay channels.

The present work focusses on baryons, more specifically on the nucleon N and the $\Delta(1232)$ resonance. In particular, we investigate pionic effects in the masses and hadronic structures of these baryon states.

First we study the influence of π degrees of freedom by coupling the N and Δ to channels with explicit pions on the macroscopic/hadronic level. We employ the coupled-channels formalism to construct a Poincaré-invariant mass operator in matrix form. Thereby we achieve the dressing of a bare N and a bare Δ by π loops. We obtain the pionic effects on the N and Δ masses, where the latter becomes complex and produces a finite decay width. The results depend on πNN and $\pi N\Delta$ vertex form factors and corresponding coupling constants, for which we use in the first instance model prescriptions from the literature. While one-π loop effects in the N mass turn out to be similar, namely, of the order of about 100 MeV, for all cases, they vary a lot for the Δ resonance mass and decay width. Two-π channels produce only minor effects.

An analogous study is then carried out on the microscopic quark level. For this purpose a relativistic coupled-channels constituent-quark model is constructed that couples three-quark states to a channel with an additional π. This allows to calculate explicit pionic effects consistently in both the masses as well as vertex form factors and coupling constants. In this attempt we arrive at results for the strong decay width of the Δ in good agreement with experiment and obtain the hadronic structures of both the N and the Δ similar to phenomenological models.

Contents

Part I.

Introduction

1. Hadron Resonances

1.1. Motivation

With regard to the strong interaction hadron physics is governed by quantum chromodynamics (QCD). Due to a running coupling constant, which gets smaller and smaller towards higher energies, it can be solved accurately in the high-energy regime by perturbative methods. At low energies alternative approaches have to be followed. All of them, however, require either approximations or model assumptions. While lattice QCD in principle leads to correct solutions, it is still limited, e. g., due to finite lattice spacings, volume size restrictions, and large quark masses. Often one resorts to effective methods. They rely on assumptions about the active degrees of freedom and on the type of dynamics. A traditional effective approach consists in the constituent-quark model (CQM). Modern versions are set up in a relativistic framework, assume constituent quarks as quasiparticles with dynamical masses, and design their interactions according to the low-energy properties of QCD, such as dynamical breaking of chiral symmetry (sbχs). While mesons are considered as quark-antiquark systems, baryons are viewed to consist of three quarks. The spectra of both types of hadrons are calculated from confined systems. Therefore excited states are described as excited bound states rather than as true resonances. This leads to shortcomings in the hadronic decay widths, even though the spectra of the resonance energies can be largely reproduced, see e. g. Ref. [Sen06].

In the present thesis the pertinent limitations should be removed. We aim at a relativistic theory in combination with a coupled-channels (CC) approach. This will allow to take mesonic degrees of freedom into account by coupling to decay channels. The final result will be a CC relativistic constituent-quark model (RCQM). It should provide for a more appropriate description of hadron resonances. These states will then be represented by complex poles in the (unphysical sheet) of the energy plane rather than as poles on the negative real axis, namely, excited bound states.

1.1.1. Short Account of Hadron-Resonance Phenomenology

Resonances are observed in all fields of the quantum world such as atomic, nuclear, and particle physics. In their simplest form they show up as sharp peaks in scattering cross sections as a function of energy. If so and if the peak is isolated, all the desired properties of a resonance may be extracted, for instance, via employing a Breit-Wigner parametrization. However, if the peaks are highly overlapping, more refined methods have to be applied to extract the resonance information, see Ref. [P$^+$16].

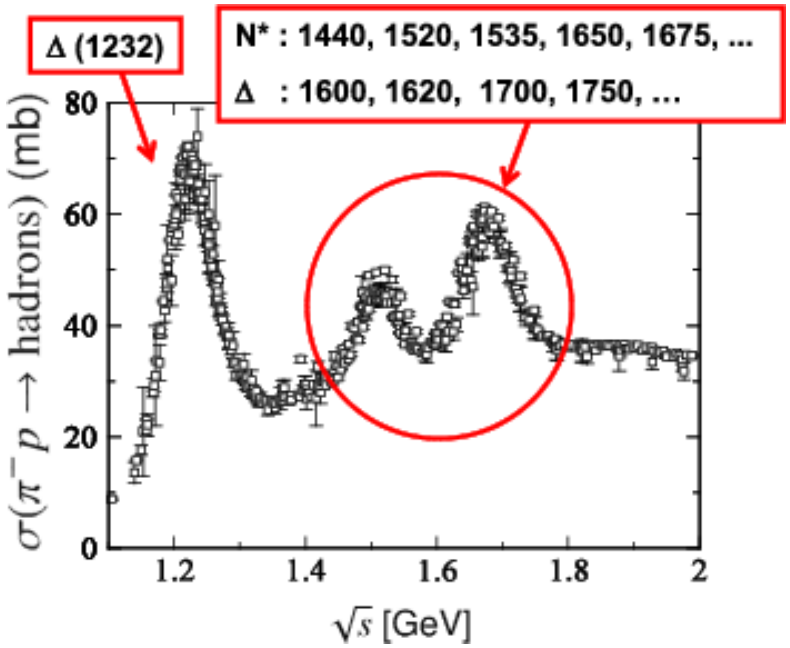

Figure 1.1.: Peaks in the $\pi^- p$ total cross sections as presented in Ref. [Kam12]. The first peak is known to be produced by the $\Delta(1232)$, while the second and third peaks contain more than 10 excited nucleon states. As can be seen, they are highly overlapping in energy.

Since in the following chapters we shall mainly focus on the Δ resonance, we give in Fig. 1.1 the example of the total cross section of the $\pi^- p$ reaction. The first peak is an isolated one, namely the $\Delta(1232)$, and a standart Breit-Wigner parametrization can be applied to extract information about it, in particular the resonance energy and the decay width. The second and third peaks are an example for highly overlapping resonances, since they contain more than 10 excited N^* states.

One may wonder, how one first got aware of hadron resonances and in particular the $\Delta(1232)$. Resorting to a standard text book of particle physics [CG09], we learn that most of the discovered resonances before 1952 had lifetimes of about 10^{-10} sec and traveled a distinctive distance in bubble chambers before decaying. Due to following developments of particle accelerators and measurement procedures, more and more new resonances have been determined experimentally. Such resonances may have lifetimes of down to $\frac{\hbar}{100}$ MeV $\sim 10^{-25}$ sec corresponding to decay widths Γ of a few hundreds of MeV and less. They are often also termed "particles" even though they are unstable.

The first resonance in hadron physics was observed due to striking differences between the $\pi^+ p$ and $\pi^- p$ total cross sections. The one for the $\pi^+ p \to \pi^+ p$ scattering was much larger than the one for the $\pi^- p \to \pi^- p$ case as is depicted in Fig. 1.2. Many more measurements of similar type had subsequently been performed, and one associ-

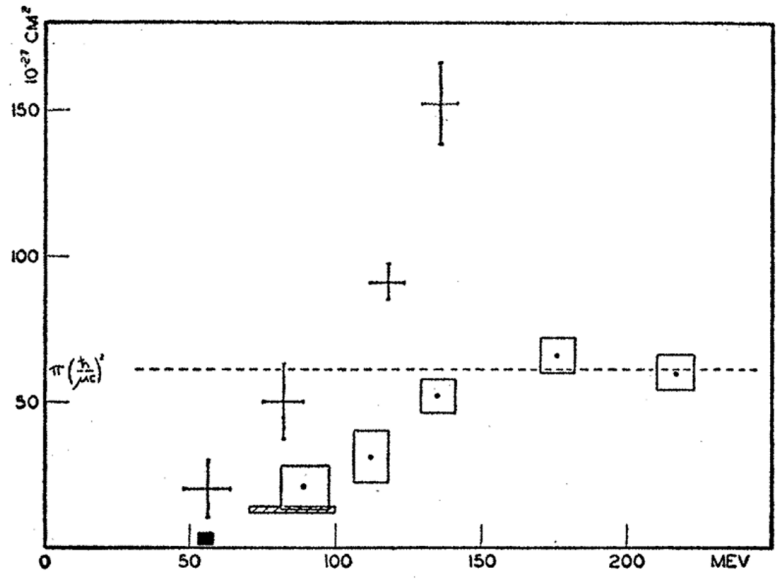

Figure 1.2.: Detection of the first resonance in hadronic physics due to strong distinctions in comparing total cross sections of $\pi^+ p \to \pi^+ p$ (crosses) and $\pi^- p \to \pi^- p$ (boxes) scattering processes. Figure taken from Ref. [AFLN52]

ated the resonance with a new "particle", the $\Delta(1232)$. A final answer was reached in Ref. [ABFS56].

1.1.2. Theoretical Description of Resonances

In theory there are various ways, how resonances can be defined and understood. For the beginning let us follow the guiding thread in Ref. [Tay83].

As already indicated, resonances are very striking phenomena in the field of quantum scattering. They are correlated to (metastable) states of a system that has a sufficiently large energy to break up into two or more subsystems. An example for such an event of a collision process, where the lifetime of the system of particle and target is larger than the collision time, may be pictured as in Fig. 1.3.

However, as stated in Ref. [EL07] there are several formal ways in which the problem can be approached. The two most common concepts are so-called "scattering resonances" and "resolvent resonances".

The concept of scattering resonances is connected with the definition of time delay as in Ref. [KNKJ04]: There time delay is a measure of the collision time in a scattering reaction that can be calculated directly from the phase shift or the scattering-matrix. It has a close connection to the appearance of an unstable intermediate state – a resonance – which, due to its finite lifetime, "delays" the reaction process. Using this kind of approach to extract resonances, usually a partial-wave analysis of scattering data is performed and by fitting the cross section data one obtains the energy-dependent

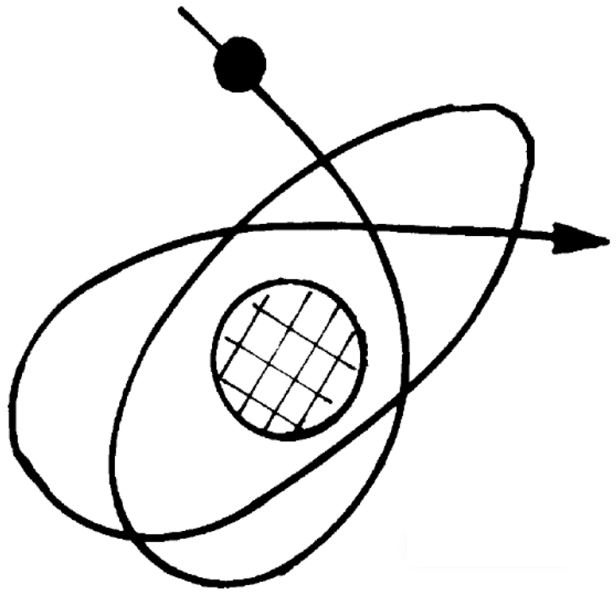

Figure 1.3.: Enhanced time delay in a scattering process due to the formation of a metastable state according to Ref. [Moi98].

amplitude, i. e. the transition matrix T.

The complex T-matrix contains all the information of the resonant and non-resonant scattering. Locating the poles of the latter on the unphysical energy sheet and studying the Argand diagrams of the complex T-matrix leads to the determination of resonance parameters.

In contrast, in extracting resolvent resonances one is performing an analytical continuation of the resolvent to the unphysical sheets of the complex energy plane and searching for poles there. The two approaches are, of course, related to each other and are even shown to be identical in certain regimes; for more details see Ref. [EL07].

There are several techniques for locating such poles, a very common one being the method of complex scaling [Moi98]. It consists of rotating the poles from the lower half-plane of the unphysical energy sheet beyond the cut of scattering energies, so that the imaginary part of the resonance location becomes positive.

1.2. Mesons and Baryons as $Q\overline{Q}$ and QQQ Systems

Before proceeding to the essentials of our work, namely, considering a CC theory for a more appropriate description of hadron resonances, let us shortly review what has so far been achieved regarding excited hadrons. While all approaches to QCD have

encountered shortcomings in dealing with resonances, we shall here only exemplify the case of CQMs, since we shall later on focus only on the extension of this type of approach to include additional mesonic (decay) channels.

For the CQM the original degrees of freedom of QCD, namely the quarks and gluons, are replaced by effective ones and one tries to take over only those properties of the full theory that are assumed to be the most relevant ones. The interaction between Q respectively $\overline{Q}$ constituent quarks consists of a potential that is confining them inside the hadron. Some additional interaction is assumed to provide the proper hyperfine splittings in the spectra as observed experimentally. Two types of hyperfine interactions have mostly been investigated, namely, the one-gluon exchange (OGE) and the Goldstone-boson exchange (GBE) interactions. Contrary to OGE, the latter is mediated by the exchange of pseudoscalar mesons, which are assumed to be the Goldstone bosons of spontaneous breaking of chiral symmetry.

In CQMs mesons are viewed as $Q\overline{Q}$ and baryons as QQQ systems. Due to the confining interaction such a theory, in principle, can only provide for (bound) ground and excited states and in principle no decay of such states to hadronic decay channels can explicitly be foreseen. Still, one has tried to extract resonance decay widths, e. g. Ref. [Sen06]. However, they may only be seen as transitions among excited states or from an excited to a ground state. The calculated decay widths have to be viewed with this caution. In the following we summarize the main features of meson and baryon spectra as well as their decay characteristics, mainly following the works of the Graz goup as in Refs. [Tho98], [Wag98] and, [Sen06].

The Graz group has considered the GBE RCQM both for mesons and baryons. In order to get familiar with this approach, I have first recalculated within this thesis all the meson and baryon spectra using the stochastic variational method (SVM) Ref. [SV98].

1.2.1. Meson Spectra

While the GBE hyperfine interaction was first designed for baryons as QQQ systems (Refs. [GPVW98] and [GPP$^+$98]), one was interested, if the same dynamical concept worked also for mesons as $Q\overline{Q}$ systems. Therefore a G-parity transformation was employed to the GBE pseudoscalar meson-exchange interaction. This should allow to transfer the GBE dynamics already fixed by baryon spectroscopy also to $Q\overline{Q}$ mesonic systems. In addition to adapting the confinement to $Q\overline{Q}$ all parameters were kept the same except for the V_0, which determines the ground state of the spectra, in case of mesons, the ρ mass.[1]

I have taken the GBE $Q\overline{Q}$ potential as defined in [Tho98] and recalculated the spectra of various mesons. The results are shown Fig. 1.4. As can be seen, the vector mesons are described quite well, but in the case of pseudoscalar mesons further improvements are called for.

[1] Note that in the concept of GBE dynamics the π as the meson with the lowest mass is considered as a fundamental particle (Goldstone boson) rather than a $Q\overline{Q}$ state.

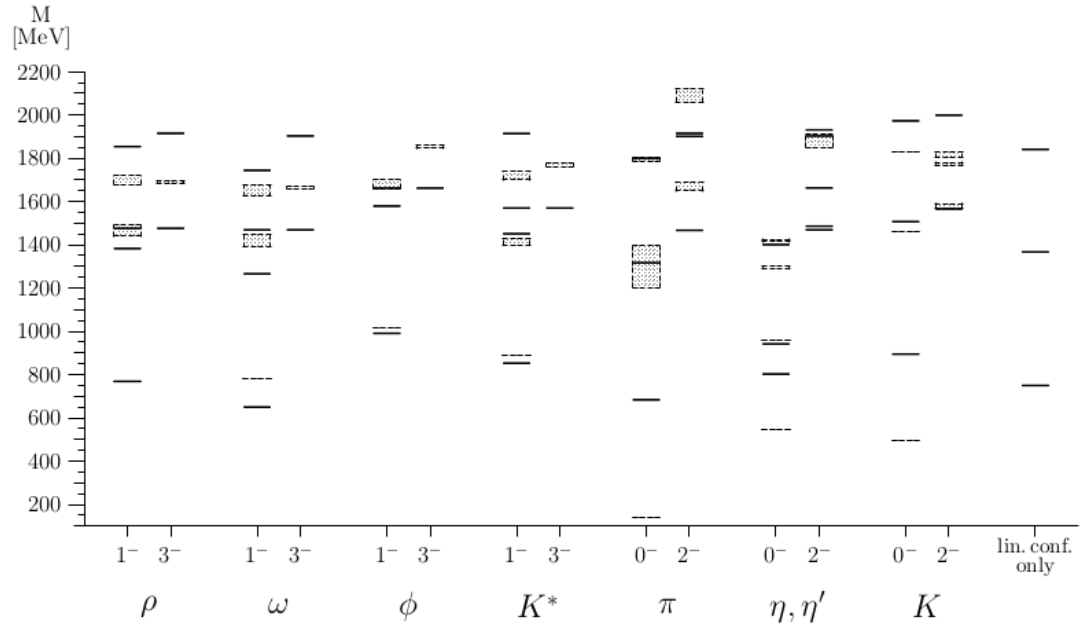

Figure 1.4.: Meson spectra for the GBE RCQM [Tho98]. The states are characterized by J^P with J the total angular momentum and P the parity. The solid lines represent the theoretical levels. The dashed boxed are the experimental data with their uncertainties as taken from Ref. [A$^+$08].

1.2.2. Baryon Spectra

In the same way I recalculated the baryon spectra as QQQ systems with the original GBE interaction ([GPVW98], [GPP$^+$98]). Considering the baryon excitations with u, d, and s flavors I could well reproduce the spectra already known in particular from the PhD theses of Refs. [Wag98] and [Sen06] using the SVM. The results are summarized in Fig. 1.5. In addition in Tabs. 1.1 and 1.2 I quote the numerical values of the GBE RCQM for N and Δ excitations. There a comparison is also given to a variant ot the relativistic OGE RCQM as parametrized in Ref. [TWDP01]. Since we shall later on, in the work with the CC theory, be concerned especially with the N and Δ, a comparison to experiment is given here too.

	Theory				Experiment	
Baryon	J^P	L,S	GBE [MeV]	OGE [MeV]	Mass [MeV]	J^P
N	$\frac{1}{2}^+$	$0,\frac{1}{2}$	939	939	938 – 940	$\frac{1}{2}^+$
$N(1440)$	$\frac{1}{2}^+$	$0,\frac{1}{2}$	1459	1577	1420 – 1470	$\frac{1}{2}^+$
$N(1520)$	$\frac{3}{2}^-$	$1,\frac{1}{2}$	1519	1521	1515 – 1525	$\frac{3}{2}^-$
$N(1535)$	$\frac{1}{2}^-$	$1,\frac{1}{2}$	1519	1521	1525 – 1545	$\frac{1}{2}^-$
$N(1650)$	$\frac{1}{2}^-$	$1,\frac{3}{2}$	1647	1690	1645 – 1670	$\frac{1}{2}^-$
$N(1675)$	$\frac{5}{2}^-$	$1,\frac{3}{2}$	1647	1690	1670 – 1680	$\frac{5}{2}^-$
$N(1700)$	$\frac{3}{2}^-$	$1,\frac{3}{2}$	1647	1690	1650 – 1750	$\frac{3}{2}^-$
$N(1710)$	$\frac{1}{2}^+$	$0,\frac{1}{2}$	1776	1859	1680 – 1740	$\frac{1}{2}^+$

Table 1.1.: Ground and excited N states from the GBE RCQM [GPVW98, GPP$^+$98] in comparison to the OGE RCQM in a variant of Ref. [TWDP01] and to experiment.

	Theory				Experiment	
Baryon	J^P	L,S	GBE [MeV]	OGE [MeV]	Mass [MeV]	J^P
Δ	$\frac{3}{2}^+$	$0,\frac{3}{2}$	1240	1231	1231 – 1233	$\frac{3}{2}^+$
$\Delta(1600)$	$\frac{3}{2}^+$	$0,\frac{3}{2}$	1718	1854	1550 – 1700	$\frac{3}{2}^+$
$\Delta(1620)$	$\frac{1}{2}^-$	$1,\frac{1}{2}$	1642	1621	1600 – 1660	$\frac{1}{2}^-$
$\Delta(1700)$	$\frac{3}{2}^-$	$1,\frac{1}{2}$	1642	1621	1670 – 1750	$\frac{3}{2}^-$

Table 1.2.: Ground and excited Δ states. Same description as in Tab. 1.1.

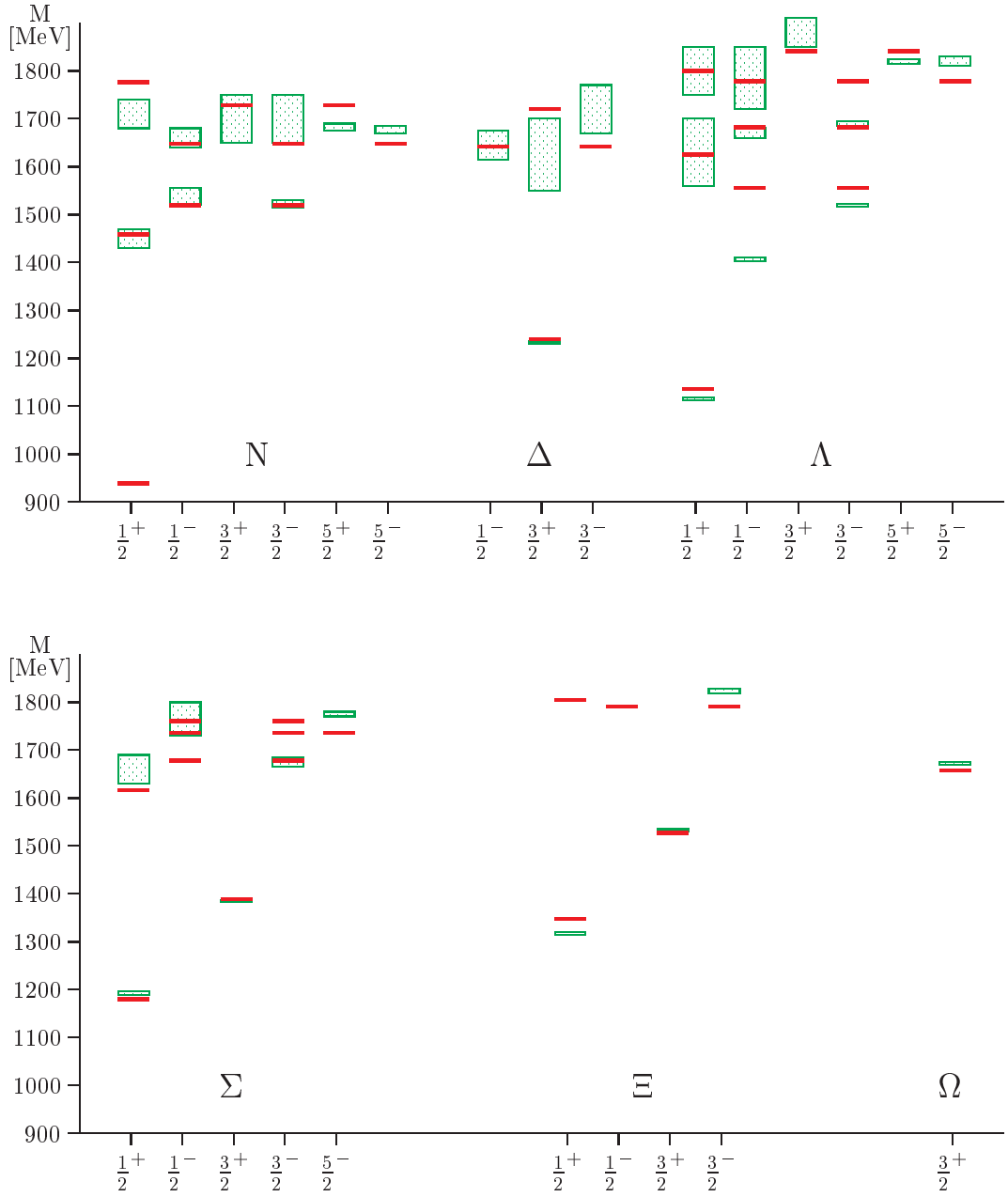

Figure 1.5.: Energy levels (solid lines) of all light and strange baryons from the GBE RCQM [GPVW98, GPP+98] in comparison to experimental data with their uncertainties (shaded boxes).

1.3. Synopsis

After this introduction about hadron resonances, we shall first discuss in Part. II, how hadron resonances may be treated within a relativistic CC approach. Particularly, we shall discuss the point form of relativistic quantum mechanics and its advantages for or our purposes in Ch. 2. In Ch. 3 the CC framework will be introduced and the benefits of treating resonances within a CC approach will be emphasized.

Part III contains the practical application of the CC framework to dynamically coupling pionic channels to the N and to the Δ, respectively. First, in Ch. 4 this is done for the N, and the π effects on its mass are discussed. In Ch. 5 we consider further pionic channels and their effects on the N mass.

The coupling of the Δ to the πN channel is treated in Ch. 6, where the pionic effects on the bare Δ mass as well as on the naturally appearing resonance decay width are discussed. Further pionic effects are considered in Ch. 7.

In Part IV the framework introduced in Part II is applied on the microscopic quark level to extract in a consistent manner strong vertex form factors and corresponding coupling constants within a CC approach. An analytical expression of the optical potential in terms of constituent-quark degrees of freedom is given in Ch. 8. In Ch. 9 the CC form factors are used as input to consistently obtain the π loop effects on the N mass. Furthermore the effects on the Δ mass and the $\Delta \to \pi N$ decay width are discussed.

We summarize in Part V and also present an outlook to possible further investigations.

The final Part VI contains the appendix, with specifying the notation and giving basic relations, a list of figures, the bibliography, and an acknowledgment.

Part II.

Hadron Resonances in a Coupled-Channels Approach

2. Point-Form Relativistic Quantum Mechanics

In this chapter we present the basic framework of our theory and discuss its benefits as well as possible drawbacks.

With relativistic quantum mechanics (RQM) we mean a quantum theory with a finite number of degrees of freedom (particles) that is invariant under Poincaré transformations. It can be rigorously formulated on a Hilbert space.

Dirac in his paper *Forms of Relativistic Dynamics* [Dir49] defined three forms of RQM with maximal invariant subgroups (stability groups) in the Poincaré group. He called them instant form (IF), front form (FF), and point form (PF) conferring to the hypersurfaces in Minkowski space that are left invariant under certain Poincaré transformations. Each of this forms have particular operators that may be kept free of interactions. They are called kinematical and correspond to the transformations in the stability group. The interaction-dependent ones are called Hamiltonians. For our work we adhere to point-form RQM (PFRQM). For details not discussed here we refer, for instance, to Refs. [KP91], [Kra01], and [BKSZ08].

2.1. The Poincaré Group

In the framework of RQM the symmetry transformations connecting different inertial systems form the Lorentz group. These transformations preserve the proper time between two events in Minkowski space. In particular they are called Lorentz transformations Λ^{μ}_{ν} with $\det \Lambda = 1$, consisting of three-dimensional spatial rotations together with the three-dimensional rotation-less canonical boosts. Adding the continuous four-dimensional space-time translations a^{μ} they lead to the proper, orthochronous Poincaré group (Λ, a). Hence, a general Poincaré transformation can be written as

$$x^{\mu} \to x'^{\mu} = \Lambda^{\mu}_{\nu} x^{\nu} + a^{\mu}. \tag{2.1}$$

They define the Poincaré transformation in Minkowski space with a^{μ} being a constant four-vector and Λ^{μ}_{ν} being a constant (4×4)-matrix.

Every element of the Poincaré group can be exponentially expressed in terms of its generators. There are the four-momentum operator P^{μ} with $\mu = 0, 1, 2, 3$ as generator of space-time translations, the K^{j} with $j = 1, 2, 3$ as generators of the Lorentz-boosts and the total angular momentum operator J^{j} as generators of spatial rotations again with $j = 1, 2, 3$. All these generators satisfy the algebra of the corresponding Lie group by the

following commutation relations

$$\left[J^i, J^j\right] = i\epsilon^{ijk}J^k, \quad \left[K^i, K^j\right] = i\epsilon^{ijk}J^k, \quad \left[J^i, K^j\right] = i\epsilon^{ijk}K^k, \quad [P^\mu, P^\nu] = 0,$$
$$\left[K^i, P^j\right] = i\delta^{ij}P^0, \quad \left[J^i, P^j\right] = i\epsilon^{ijk}P^k, \quad \left[K^i, P^0\right] = -iP^i, \quad \left[J^i, P^0\right] = 0 \tag{2.2}$$

with ϵ_{ijk} the Levi-Civita symbol and δ_{ij} the Kronecker delta.

The relations in Eq. (2.2) can be reformulated by using $J^{0i} := K^i$ and $J^{ij} := \epsilon^{ijk}J^k$ to end up with

$$\left[P_\mu, P_\nu\right] = 0, \tag{2.3}$$

$$\left[J_{\mu\nu}, P_\kappa\right] = i\left(g_{\nu\kappa}P_\mu - g_{\mu\kappa}P_\nu\right), \tag{2.4}$$

$$\left[J_{\mu\nu}, J_{\kappa_\lambda}\right] = -i\left(g_{\mu\kappa}J_{\nu\lambda} - g_{\nu\kappa}J_{\mu\lambda} + g_{\nu\lambda}J_{\mu\kappa} - g_{\mu\lambda}J_{\nu\kappa}\right), \tag{2.5}$$

see among others also [Bie11], [Kra01], and [Sen06]. Details about the definition of the metric tensor $g_{\mu\nu}$ can be found in App. A.

2.2. Point Form and the Bakamjian-Thomas Construction

The stability group in PF is the Lorentz group. It leaves the hyperboloid $x^\mu x_\mu = \tau^2$ and in particular the point x_μ invariant. The four-momentum operator P^μ is interaction-dependent and all the components of the latter may all be called Hamiltonians. Hence, the Schrödinger equation can also be generalized by replacing the Hamiltonian by the four-momentum operator leading to the following eigenvalue equation

$$P^\mu|\Psi\rangle = p^\mu|\Psi\rangle. \tag{2.6}$$

As discussed in Ref. [Kli03], with a given unitary operator U_Λ serving as representation for a Lorentz transformation Λ the four-momentum operator P_μ has to satisfy the following point-form equations

$$\left[P_\mu, P_\nu\right] = 0, \tag{2.7}$$

$$U_\Lambda P_\mu U_\Lambda^{-1} = \left(\Lambda^{-1}\right)_\mu^\nu P_\nu \tag{2.8}$$

whith $P_\mu P^\mu = M^2$.

We are now aiming at multi-particle momentum eigenstates and their Lorentz transformation properties. First, we start with considering single-particle momentum states defined as

$$P^\mu|p,\sigma\rangle = p^\mu|p,\sigma\rangle \tag{2.9}$$

for a spin-$\frac{1}{2}$ particle with four-momentum p and spin projection σ. These states have the following Lorentz transformation properties

$$U_\Lambda|p,\sigma\rangle = \sum_{\sigma'=\pm\frac{1}{2}} |\Lambda p,\sigma'\rangle D^{\frac{1}{2}}_{\sigma'\sigma}\left[R_W(p,\Lambda)\right] \tag{2.10}$$

where $R_W(p,\Lambda)$ is a Wigner rotation defined as

$$R_W(p,\Lambda) = B^{-1}(\Lambda v)\Lambda B(v). \tag{2.11}$$

The four-velocity appearing in Eq. (2.11) is given as

$$v = \frac{p}{m} = \begin{pmatrix} v^0 \\ \vec{v} \end{pmatrix}, \qquad v^0 = \sqrt{1+\vec{v}^2} \tag{2.12}$$

and $B(v)$ is a Lorentz boost defined as

$$B(v) = \begin{pmatrix} v^0 & \vec{v}^T \\ \vec{v} & \mathbb{1}_3 + \frac{v^0-1}{v^2}\vec{v}\otimes\vec{v}^T \end{pmatrix}. \tag{2.13}$$

$D^{\frac{1}{2}}_{\sigma'\sigma}$ are the standard Wigner D-functions, and more information on them can be found, for example, in Ref. [VMK88].

In order to generalize from single-particle states to multi-particle states it is convenient to use velocity states instead of usual multi-particle momentum states. In the latter, each D-function happens to depend on a different Wigner rotation. Therefore the coupling of spins and orbital angular momenta cannot be done like in the standard nonrelativistic case. The construction of velocity states and their properties will be discussed in Sec. 2.3.

Now we shall consider the Bakamjian-Thomas construction, [BT53]. It is a convenient way to introduce interactions. One steps out from a free mass operator and replaces it by an interacting one. In PF it means that through the relation

$$P^\mu = V^\mu M \tag{2.14}$$

all the four-momentum operators get interaction-dependent. Still they satisfy Eqs. (2.7) and (2.8). The interacting mass operator is expressed as

$$M = M_{free} + M_{int}. \tag{2.15}$$

Its eigenvalue equation

$$M|\Psi\rangle = m|\Psi\rangle \tag{2.16}$$

is equivalent to Eq. (2.6), due to the vanishing commutator between M and P^μ.

2.3. Velocity States

In the previous section the PF of relativistic quantum mechanics was presented and one of its most prominent features is its stability group, the Lorentz group. Hence we are interested in a basis for multi-particle momentum states that have simple Lorentz-transformation properties. In this section velocity states (VS), simultaneously eigenstates of the four-velocity operator and the free n-particle mass operator M will be introduced, since they fulfill these requirements, see also [Kli98], [Kli03], and [Bie11].

General Definitions

As stated in the last section, a Lorentz transformation applied to a multi-particle state leads to difficulties by coupling all momenta and spins together to total spin or orbital angular momentum states. By defining velocity states as

$$\begin{aligned} |v;\vec{k}_i\mu_i\rangle &:= U_{B(v)}|k_1\mu_1,\ldots,k_n\mu_n\rangle \\ &= \sum_{\sigma_i}|p_1\sigma_1,\ldots,p_n\sigma_n\rangle\prod_i^n D_{\sigma_i,\mu_i}\left(R_{W_i}\right) \end{aligned} \tag{2.17}$$

it can be shown that velocity states have more convenient Lorentz transformation properties:

$$\begin{aligned} U_\Lambda|v;\vec{k}_i\mu_i\rangle &= U_\Lambda U_{B(v)}|k_1\mu_1,\ldots,k_n\mu_n\rangle \\ &= U_{B(\Lambda v)}U_{R_W}|k_1\mu_1,\ldots,k_n\mu_n\rangle \\ &= \sum_{\sigma_i}|\Lambda v;R_W\vec{k}_i\mu_i'\rangle\prod_i^n D_{\mu_i',\mu_i}(R_W). \end{aligned} \tag{2.18}$$

Here, all appearing Wigner rotations in the D-functions are the same and thus spin and orbital angular momentum can be coupled just as is done nonrelativistically.

Summarizing, velocity states are multi-particle states in their overall center of momentum (CM) frame boosted to a four-velocity v. They are specified by the overall four-velocity of the n-particle system

$$v = \frac{p}{m} \tag{2.19}$$

and the individual four-momenta k_i, $i = 1,\ldots,n$. The occurring momenta are now internal momenta defined in the CM frame, which satisfy

$$\sum_{i=1}^n \vec{k}_i = 0 \tag{2.20}$$

and consequently only $n-1$ are linearly independent. The CM momenta k_i are connected to the paticle momenta p_i via the following relation

$$p_i = B(v)k_i \tag{2.21}$$

with $B(v)$ being a Lorentz boost as defined in Eq. (2.13).

Completeness and Orthogonality Relations

The completeness and orthogonality relations for velocity states with an arbitrary number of particles n read

$$\begin{aligned} \mathbb{1}_n = &\sum_{\mu_1,\mu_2,\ldots,\mu_n}\int\frac{d^3v}{(2\pi)^3v^0}\left(\prod_{i=1}^{n-1}\frac{d^3k_i}{(2\pi)^3 2\omega_i}\right)\frac{(\sum_{i=1}^n\omega_i)^3}{2\omega_n} \\ &\times|v;\vec{k}_1\mu_1,\vec{k}_2\mu_2,\ldots,\vec{k}_n\mu_n\rangle\langle v;\vec{k}_1\mu_1,\vec{k}_2\mu_2,\ldots,\vec{k}_n\mu_n| \end{aligned} \tag{2.22}$$

and

$$\begin{aligned}&\langle v;\vec{k}_1\mu_1,\vec{k}_2\mu_2,\ldots,\vec{k}_n\mu_n|v';\vec{k}'_1\mu'_1,\vec{k}'_2\mu'_2,\ldots,\vec{k}'_n\mu'_n\rangle\\&\quad=\frac{(2\pi)^3 2\omega_n}{(\sum_{i=1}^n\omega_i)^3}v^0\delta^3(\vec{v}-\vec{v}')\left(\prod_{i=1}^{n-1}(2\pi)^3 2\omega_i\delta^3(\vec{k}_i-\vec{k}'_i)\right)\prod_{i=1}^{n}\delta_{\mu_i\mu'_i}\end{aligned}\tag{2.23}$$

with

$$\omega_i=\sqrt{m_i^2+\vec{k}_i^2}.\tag{2.24}$$

For more details see, e. g., Ref. [Bie11].

3. Relativistic Coupled-Channels Formalism

As discussed in Ch. 1, until now a proper description of hadronic resonances and the corresponding decay widths within the framework of RCQM has not yet been achieved, see, e.g., Ref. [SCPS17] and references therein. Likewise, other models and theories too struggle with describing resonances in a proper manner. The CC framework will help in describing hadron resonances and in particular hadronic decays within the framework of RCQM in a more realistic way.

3.1. Coupled-Channels Mass Operator and Eigenvalue Equation

Originally the CC approach was developed and applied, e.g., for nuclear reactions, such as nucleon-nucleus scattering, in order to take into account the effects of open channels over a wider range of scattering energies [Fes62]. In his concluding remarks, Feshbach stated that, among other applications, the formalism should be useful in few-body physics.

If a single-channel treatment with a fixed number of degrees of freedom is not enough to describe the system under investigation, one may introduce the effects of further channels by a generalized formalism still defined on a Hilbert space but now extended by additional contributing degrees of freedom.

In order to describe resonances in RQM we aim at solving the eigenvalue equation for the interaction-dependent mass operator. This operator will now be defined in the CC framework to allow the description of resonances, in particular the description of hadronic decays in taking the additional degrees of freedom (decay channels) explicitly into account.

Our starting point is the multi-channel mass operator that is defined on a Hilbert space that is a direct sum of the single-channel Hilbert spaces. The most general CC mass-eigenvalue equation according to this multi-channel mass operator is written in the following form

$$\begin{pmatrix} M_1 & K_{12} & \cdots \\ K_{12}^{\dagger} & M_2 & \cdots \\ \vdots & \vdots & \ddots \end{pmatrix} \begin{pmatrix} \Psi_1 \\ \Psi_2 \\ \vdots \end{pmatrix} = m \begin{pmatrix} \Psi_1 \\ \Psi_2 \\ \vdots \end{pmatrix} \tag{3.1}$$

where "1" denotes channel one, "2" channel two and so on. On the diagonal, the mass operator in the first channel describes, for example, a baryon, e. g., the nucleon or it

may describe a two- or three-quark cluster. The one in the second channel describes, for example, the nucleon plus an additional particle but it may also describe a two- or three-quark cluster and an additional particle and so forth.

The off-diagonal entries of the mass operator are vertex operators providing the coupling between the different channels. In the next section it will be shown, how these operators can be identified with Lagrangian densities taken from quantum field theory to describe particle production and absorption.

The m appearing in Eq. (3.1) corresponds to the mass eigenvalues of the system. The CC problem is a Hermitian one with real eigenvalues.

Feshbach Reduction

A Feshbach reduction may be applied in order so solve the mass-eigenvalue equation (3.1). In the first step of the procedure, the CC equation has to be multiplied out to end up with a system of equations, which are of course coupled to each other. These equations have to be reduced such that one finally ends up with one single equation, which will in general no longer represent a Hermitian eigenvalue problem

$$M_1|\psi_1\rangle + K_{12}\,(m - M_2 - \dots)^{-1}\,K_{12}^{\dagger}|\psi_1\rangle = m|\psi_1\rangle. \tag{3.2}$$

If the considered particle is a resonance (above a decay threshold) then it may decay into a lower lying state and an additional particle. Hence, the resulting mass eigenvalue m will assume complex values as soon as m reaches some model-dependent threshold. Its real part is describing the position of the resonance and two times its imaginary part can be identified with the resonance decay width.

3.2. Vertex Interaction

Our central interest is the description of hadron resonances and in particular their decays. Thus we have to consider the transition from an n- to an $(n+1)$-particle system. It will be furnished by a vertex operator K sandwiched between n- and $(n+1)$-particle states

$$\langle v;\vec{k}_1\mu_1,\vec{k}_2\mu_2,\dots,\vec{k}_n\mu_n|K|v';\vec{k}'_1\mu'_1,\vec{k}'_2\mu'_2,\dots,\vec{k}'_n\mu'_n,\vec{k}'_{n+1}\mu'_{n+1}\rangle. \tag{3.3}$$

Its dynamics can be deduced from a Lagrangian density $\mathcal{L}_I(x)$ taken from quantum field theory. It describes the coupling of an additional particle to the already existing ones.

Since $\mathcal{L}_I(x)$ is a product of free fields it transforms under Lorentz transformations as

$$U_\Lambda \mathcal{L}_I(x) U_\Lambda^{-1} = \mathcal{L}_I(\Lambda x), \tag{3.4}$$

while $\mathcal{L}_I(0)$ is a Lorentz scalar and obeys the following transformation properties

$$U_\Lambda \mathcal{L}_I(0) U_\Lambda^{-1} = \mathcal{L}_I(0). \tag{3.5}$$

Due to this property Eq. (3.3) can be written as

$$\begin{aligned}&\langle v;\vec{k}_1\mu_1,\vec{k}_2\mu_2,\ldots,\vec{k}_n\mu_n|K|v';\vec{k}'_1\mu'_1,\vec{k}'_2\mu'_2,\ldots,\vec{k}'_n\mu'_n,\vec{k}'_{n+1}\mu'_{n+1}\rangle\\&\quad\propto v^0\delta^3(\vec{v}'-\vec{v})\langle v;\vec{k}_1\mu_1,\vec{k}_2\mu_2,\ldots,\vec{k}_n\mu_n|\mathcal{L}_I(0)|v;\vec{k}'_1\mu'_1,\vec{k}'_2\mu'_2,\ldots,\vec{k}'_n\mu'_n,\vec{k}'_{n+1}\mu'_{n+1}\rangle.\end{aligned}\tag{3.6}$$

If one considers composite particles as, e. g., a baryon that is assumed to consist of three consituent quarks, the inner structure can be taken into account via multiplying the matrix element with appropriate strong vertex form factors $\mathcal{F}_I(\vec{\kappa}^{\,2})$. The latter depend on the three-momentum squared of the additional particle, here denoted by $\vec{\kappa}$.

The final vertex matrix elements we have to consider are given in general form as

$$\begin{aligned}&\langle v,\vec{k}_1\mu_1,\vec{k}_2\mu_2,\ldots,\vec{k}_n\mu_n|K|v',\vec{k}'_1\mu'_1,\vec{k}'_2\mu'_2,\ldots,\vec{k}'_n\mu'_n,\vec{k}'_{n+1}\mu'_{n+1}\rangle\\&=v^0\delta^3(\vec{v}'-\vec{v})\mathcal{F}_I(\vec{\kappa}^{\,2})\frac{(2\pi^3)}{\sqrt{\left(\sum_{i=1}^{n+1}\omega_{k'_i}\right)^3\left(\sum_{i=1}^{n}E_{k_i}\right)^3}}\\&\times\langle\vec{k}_1\mu_1,\vec{k}_2\mu_2,\ldots,\vec{k}_n\mu_n|\mathcal{L}_I(0)|\vec{k}'_1\mu'_1,\vec{k}'_2\mu'_2,\ldots,\vec{k}'_n\mu'_n,\vec{k}'_{n+1}\mu'_{n+1}\rangle.\end{aligned}\tag{3.7}$$

3.3. Previous Works Using the Coupled-Channels Approach

A Relativistic Point-Form Approach to Quark-Antiquark Systems. In order to achieve a more realistic description of resonances within a PF relativistic constituent-quark model for mesons, Krassnigg applied the CC formalism to mimic the hyperfine interaction due to GBE dynamics, Ref. [Kra01]. Within this model the lightest pseudoscalar mesons – meant to be GB of spontaneous chiral symmetry breaking – couple directly to quarks and antiquarks while the latter are assumed to be clustered by instantaneous confinement. In particular he considered a CC mass-operator eigenvalue equation on the microscopic level consisting of a bound $Q\bar{Q}$ channel and a bound $Q\bar{Q}$ + GB channel. This treatment allows for the decay of a resonance to a lower lying state and an additional GB.

In his thesis, Krassnigg applied an approximation to solve the final microscopic complex mass-operator eigenvalue equation. The contributions of GB emission and reabsorption by the same quark have been neglected due to constituent-quark mass renormalization arguments. Still, the CC treatment led to decay widths that were larger as compared to a corresponding calculation with a nonrelativistically reduced potential performed in the same work. Anyhow, it was argued that due to the applied approximation the resulting widths were still underestimating the experimentally measured ones by two orders of magnitude.

Resonances and Decay Widths Within a Relativistic Coupled Channels Approach. The attempt in Ref. [Kle10] was to apply the above-mentioned formal CC setup to a simple scalar toy model for mesons in order to check the contribution of the loop diagrams neglected in Ref. [Kra01]. It was found that, in taking all possible GB exchange contributions into account, the optical potential at microscopic level can be reinterpreted such that one ends up with the latter at the macroscopic level. This idea is pictorially shown in Fig. 3.1.

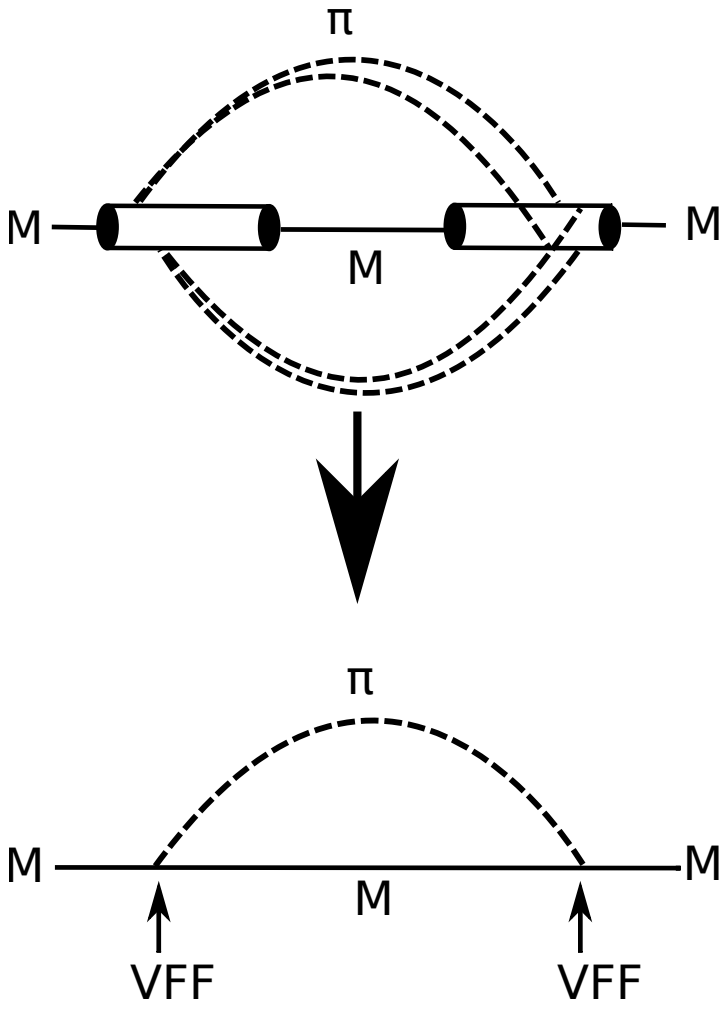

Figure 3.1.: Combining various π-exchange possibilities of the microscopic optical-potential to end up with the latter on the macroscopic level by taking the quark structure via vertex form factors (VFF) into account.

The microscopic structure is transcribed to strong form factors that show up at the vertices, when solving the macroscopic mass-eigenvalue equation. Strong vertex form factors can consistently be extracted by assuming on the one hand the mass eigenvalue equation at the microscopic level and on the other hand at the macroscopic level. In comparing the respective expressions at the vertices, strong vertex form factors can be extracted.

It was found that the simple scalar toy model leads to finite decay widths and thus made us interested in further studying this kind of ansatz to investigate hadronic resonances in a relativistic manner.

Part III.

The N and Δ Coupled to π Channels

The central aim in this thesis is a realistic description of the N ground state and the Δ resonance. In particular we want to include pionic effects and investigate, how well we can then describe the masses and decay width of the N and Δ, respectively, in good agreement with the experimental data summarized in the following figures.

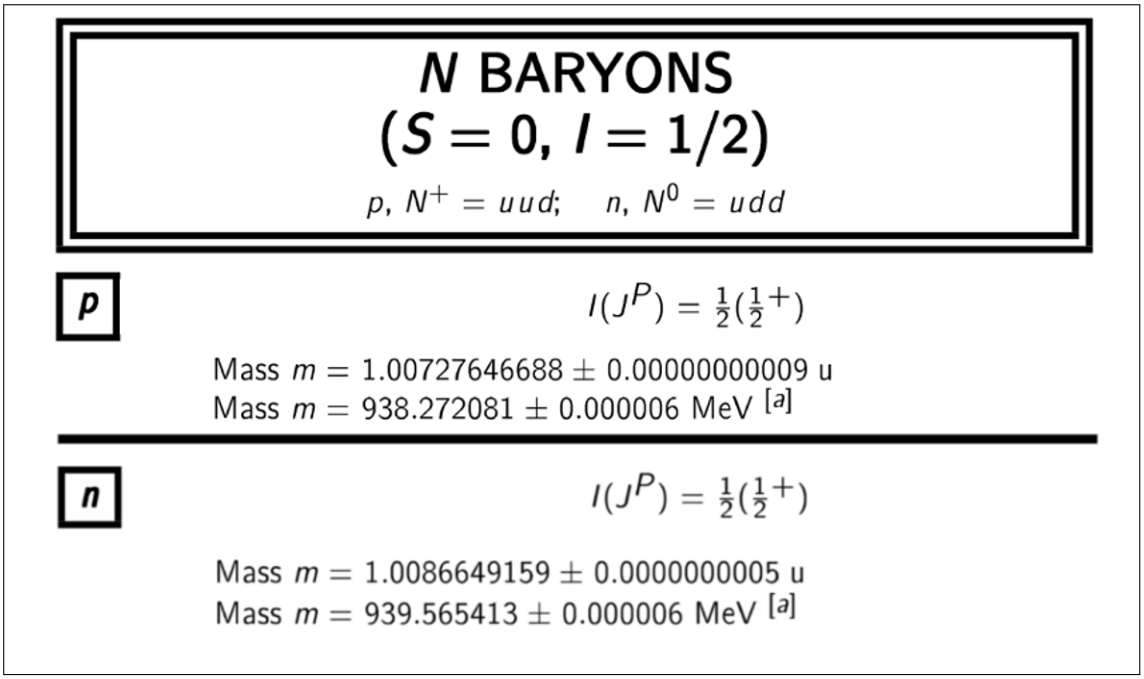

Experimental information about the N ground state from Ref. [P+16]

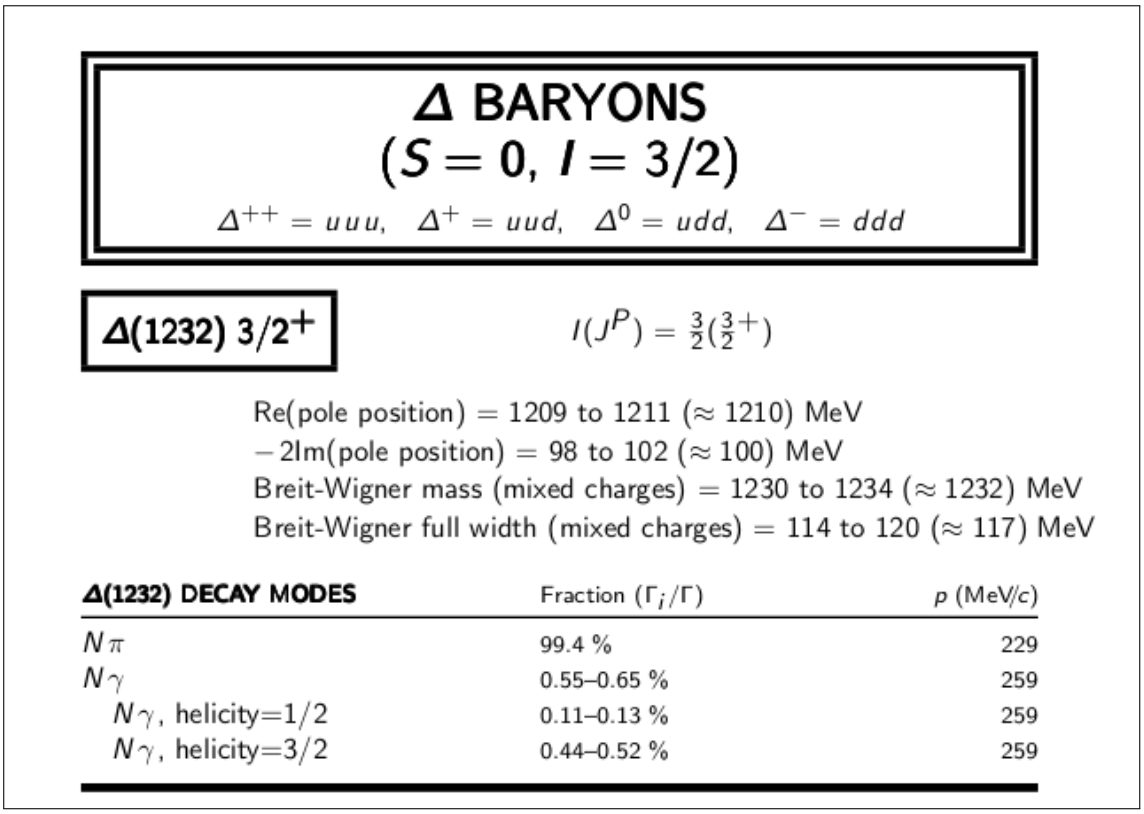

Δ BARYONS
($S = 0$, $I = 3/2$)

$\Delta^{++} = uuu$, $\Delta^{+} = uud$, $\Delta^{0} = udd$, $\Delta^{-} = ddd$

Δ(1232) 3/2⁺ $I(J^P) = \frac{3}{2}(\frac{3}{2}^+)$

Re(pole position) = 1209 to 1211 (≈ 1210) MeV
−2Im(pole position) = 98 to 102 (≈ 100) MeV
Breit-Wigner mass (mixed charges) = 1230 to 1234 (≈ 1232) MeV
Breit-Wigner full width (mixed charges) = 114 to 120 (≈ 117) MeV

Δ(1232) DECAY MODES	Fraction (Γ_i/Γ)	p (MeV/c)
$N\pi$	99.4 %	229
$N\gamma$	0.55–0.65 %	259
$N\gamma$, helicity=1/2	0.11–0.13 %	259
$N\gamma$, helicity=3/2	0.44–0.52 %	259

Experimental information about the Δ resonance from Ref. [P+16]

4. The Nucleon with Explicit One-π Contributions

4.1. Eigenvalue Equation

The first step to take into account π degrees of freedom in the nucleon consists in considering a bare nucleon $\widetilde{N}$ dressed with a π loop. To calculate the corresponding mass renormalization we start with the CC eigenvalue equation for the mass operator

$$\begin{pmatrix} M_{\widetilde{N}} & K \\ K^\dagger & M_{\widetilde{N}+\pi} \end{pmatrix} \begin{pmatrix} |\psi_N\rangle \\ |\psi_{N+\pi}\rangle \end{pmatrix} = m \begin{pmatrix} |\psi_N\rangle \\ |\psi_{N+\pi}\rangle \end{pmatrix}. \tag{4.1}$$

Here, $M_{\widetilde{N}}$ is the mass operator of the bare nucleon $\widetilde{N}$ and $M_{\widetilde{N}+\pi}$ the mass operator of the interaction-free $\pi\widetilde{N}$ system. The operators K and $K^\dagger$ furnish the coupling to the $\pi\widetilde{N}$ channel. They will rely on a Lorentz-scalar Lagrangian density $\mathcal{L}_I(0)$ (see Sec. 4.2 below).

Eq. (4.1) represents two coupled equations, one for the physical nucleon state $|\psi_N\rangle$ and one for the πN system $|\psi_{N+\pi}\rangle$:

$$\text{I}: \quad M_{\widetilde{N}}|\psi_N\rangle + K|\psi_{N+\pi}\rangle = m|\psi_N\rangle, \tag{4.2}$$

$$\text{II}: \quad K^\dagger|\psi_N\rangle + M_{\widetilde{N}+\pi}|\psi_{N+\pi}\rangle = m|\psi_{N+\pi}\rangle. \tag{4.3}$$

In order to calculate the dressed N eigenstate $|\psi_N\rangle$, we can eliminate $|\psi_{N+\pi}\rangle$ in I by using

$$|\psi_{N+\pi}\rangle = \left(m - M_{\widetilde{N}+\pi}\right)^{-1} K^\dagger|\psi_N\rangle \tag{4.4}$$

and obtain

$$M_{\widetilde{N}}|\psi_N\rangle + K\left(m - M_{\widetilde{N}+\pi}\right)^{-1} K^\dagger|\psi_N\rangle = m|\psi_N\rangle. \tag{4.5}$$

Alternatively, by eliminating $|\psi_N\rangle$ in II by

$$|\psi_N\rangle = \left(m - M_{\widetilde{N}}\right)^{-1} K|\psi_{N+\pi}\rangle \tag{4.6}$$

we can also calculate $|\psi_{N+\pi}\rangle$ through

$$M_{\widetilde{N}+\pi}|\psi_{N+\pi}\rangle + K^\dagger\left(m - M_{\widetilde{N}}\right)^{-1} K|\psi_{N+\pi}\rangle = m|\psi_{N+\pi}\rangle. \tag{4.7}$$

Both of these Eqs. (4.5) and (4.7) have the property that the searched eigenvalue m occurs also on the l.h.s.

Continuing with first calculating $|\psi_N\rangle$ we use the velocity states $|\widetilde{N}:v\rangle$ and $|\widetilde{N},\pi:v,\vec{k}_\pi\rangle$ which are eigenstates of the mass operators $M_{\widetilde{N}}$ and $M_{\widetilde{N}+\pi}$, respectively

$$M_{\widetilde{N}}|\widetilde{N}:v\rangle = m_{\widetilde{N}}|\widetilde{N}:v\rangle, \tag{4.8}$$

$$M_{\widetilde{N}+\pi}|\widetilde{N},\pi:v,\vec{k}_\pi\rangle = \left(\omega_{\widetilde{N}}+\omega_\pi\right)|\widetilde{N},\pi:v,\vec{k}_\pi\rangle. \tag{4.9}$$

They fulfill the following orthonormality and completeness relations

$$\langle\widetilde{N}:v'|\widetilde{N}:v\rangle = (2\pi)^3\, v^0\delta^3\left(\vec{v}'-\vec{v}\right)\frac{2}{m_{\widetilde{N}}^2}, \tag{4.10}$$

$$\mathbb{1}_{\widetilde{N}} = \int \frac{d^3v}{(2\pi)^3\, v^0}\frac{m_{\widetilde{N}}^2}{2}|\widetilde{N}:v\rangle\langle\widetilde{N}:v|, \tag{4.11}$$

$$\langle\widetilde{N},\pi:v',\vec{k}'_\pi|\widetilde{N},\pi:v,\vec{k}_\pi\rangle = (2\pi)^3\, v^0\delta^3\left(\vec{v}'-\vec{v}\right)\frac{2\omega_{\widetilde{N}}2\omega_\pi}{\left(\omega_{\widetilde{N}}+\omega_\pi\right)^3}(2\pi)^3\,\delta^3\left(\vec{k}'_\pi-\vec{k}_\pi\right), \tag{4.12}$$

$$\mathbb{1}_{\widetilde{N}+\pi} = \int \frac{d^3v}{(2\pi)^3\, v^0}\int\frac{d^3k_\pi}{(2\pi)^3\,2\omega_\pi}\frac{\left(\omega_\pi+\omega_{\widetilde{N}}\right)^3}{2\omega_{\widetilde{N}}}|\widetilde{N},\pi:v,\vec{k}_\pi\rangle\langle\widetilde{N},\pi:v,\vec{k}_\pi| \tag{4.13}$$

with $\omega_i = \sqrt{m_i+\vec{k}_i^2}\ \left(i=\pi,\widetilde{N}\right)$. More details about this special basis of velocity states can be found in Sec. 2.3.

By representing (4.5) with $\langle\widetilde{N}:v|$ we thus have:

$$m_{\widetilde{N}}\langle\widetilde{N}:v|\psi_N\rangle + \langle\widetilde{N}:v|K\left(m-M_{\widetilde{N}+\pi}\right)^{-1}\mathbb{1}''_{\widetilde{N}+\pi}K^\dagger\mathbb{1}'_{\widetilde{N}}|\psi_N\rangle = m\langle\widetilde{N}:v|\psi_N\rangle \tag{4.14}$$

$$\begin{aligned}
&\Rightarrow m_{\widetilde{N}}\langle\widetilde{N}:v\mid\psi_N\rangle + \int\frac{d^3v'}{(2\pi)^3\,v^{0'}}\int\frac{d^3v''}{(2\pi)^3\,v^{0''}}\int\frac{d^3k''_\pi}{(2\pi)^3\,2\omega''_\pi}\frac{\left(\omega''_\pi+\omega''_{\widetilde{N}}\right)^3}{2\omega''_{\widetilde{N}}}\frac{m'^2_{\widetilde{N}}}{2}\\
&\times\langle\widetilde{N}:v\mid K\mid\widetilde{N},\pi:v'',\vec{k}''_\pi\rangle\frac{1}{m-\omega''_{\widetilde{N}}-\omega''_\pi}\langle\widetilde{N},\pi:v'',\vec{k}''_\pi\mid K^\dagger\mid N:v'\rangle\langle\widetilde{N}:v'\mid\psi_N\rangle\\
&= m\langle\widetilde{N}:v\mid\psi_N\rangle.
\end{aligned} \tag{4.15}$$

This can shortly be written as

$$m_{\widetilde{N}}\langle\widetilde{N}:v\mid\psi_N\rangle + \int\frac{d^3v'}{(2\pi)^3\,v^{0'}}\langle\widetilde{N}:v\mid V_{opt}(m)\mid\widetilde{N}:v'\rangle\langle\widetilde{N}:v'\mid\psi_N\rangle = m\langle\widetilde{N}:v\mid\psi_N\rangle, \tag{4.16}$$

where the matrix element of the so-called optical potential $V_{opt}(m)$ is

$$\begin{aligned}
\langle\widetilde{N}:v\mid V_{opt}(m)\mid\widetilde{N}:v'\rangle &= \int\frac{d^3v''}{(2\pi)^3\,v^{0''}}\int\frac{d^3k''_\pi}{(2\pi)^3\,2\omega''_\pi}\frac{\left(\omega''_\pi+\omega''_{\widetilde{N}}\right)^3}{2\omega''_{\widetilde{N}}}\frac{m'^2_{\widetilde{N}}}{2}\\
&\times\langle\widetilde{N}:v\mid K\mid\widetilde{N},\pi:v'',\vec{k}''_\pi\rangle\frac{1}{m-\omega''_{\widetilde{N}}-\omega''_\pi}\langle\widetilde{N},\pi:v'',\vec{k}''_\pi\mid K^\dagger\mid N:v'\rangle.
\end{aligned} \tag{4.17}$$

4.2. Vertex Matrix Elements

Next we specify the $\pi\widetilde{N}\widetilde{N}$ couplings in K. At the vertices we consider both pseudovector (PV) and pseudoscalar (PS) type couplings. Thus we identify K with the Lorentz-scalar Lagrangian density $\mathcal{L}_I^{PV,PS}$ and the corresponding elements are defined by (cf. Sec. 3.2)

$$\begin{aligned}\langle\widetilde{N}\colon v|K|\widetilde{N},\pi;v',\vec{k}'_\pi\rangle = \\ v^0\delta^3(\vec{v}-\vec{v}')\frac{(2\pi)^3}{\sqrt{\left(\omega'_\pi+\omega'_{\widetilde{N}}\right)^3 m^3_{\widetilde{N}}}}\mathcal{F}_{\pi\widetilde{N}\widetilde{N}}\left(\vec{k}'^2_\pi\right)\langle\widetilde{N}|\mathcal{L}_I(0)|\widetilde{N},\pi:\vec{k}'_\pi\rangle,\end{aligned} \tag{4.18}$$

where we have used the velocity-states property $\vec{k}'_{\widetilde{N}}+\vec{k}'_\pi=0$. Since $\mathcal{L}_I(0)$ as a Lorentz scalar is relativistically invariant, we may consider the matrix element in the rest frame of the nucleon and thus $v=v'=0$. Therefore we have written the velocity states as $|\widetilde{N}\rangle$ and $|\widetilde{N},\pi:\vec{k}_\pi\rangle$. Here, the extended structure of $\pi\widetilde{N}\widetilde{N}$ vertex is taken into account by the form factor $\mathcal{F}_{\pi\widetilde{N}\widetilde{N}}\left(\vec{k}'^2_\pi\right)$, which we consider and term as a bare form factor.

4.2.1. Pseudovector Coupling

We now discuss the two vertex matrix elements

$$\langle\widetilde{N}|\mathcal{L}_I^{PV}(0)|\widetilde{N},\pi:\vec{k}_\pi\rangle, \tag{4.19}$$

$$\langle\widetilde{N},\pi:\vec{k}_\pi|\mathcal{L}_I^{PV\dagger}(0)|\widetilde{N}\rangle, \tag{4.20}$$

in detail. In the case of PV coupling we have [EW88]

$$\mathcal{L}_I^{PV}(x)=-\frac{f_{\pi\widetilde{N}\widetilde{N}}}{m_\pi}\bar{\psi}(x)\gamma^\mu\gamma_5\vec{T}\psi(x)\cdot\partial_\mu\vec{\phi}(x), \tag{4.21}$$

where $f_{\pi\widetilde{N}\widetilde{N}}$ is the bare PV $\pi\widetilde{N}\widetilde{N}$ coupling constant, ψ is the nucleon Dirac field and $\vec{\phi}$ is the π field. $\vec{T}$ is the isospin operator at the vertex.

Field operator for spin-0 particle: π

We express the π field operator by the plane-wave expansion

$$\phi(x)=\int\frac{d^3\kappa}{(2\pi)^3\,2\omega_\kappa}\left(e^{-i\kappa x}c(\kappa)+e^{i\kappa x}c^\dagger(\kappa)\right). \tag{4.22}$$

The plane waves can then be expanded in terms of partial waves. Since we consider the field at $x=0$ we take all possibillities for angular excitations into account. The commutator relations for the creation and annihilation operators read

$$[c(\kappa),c^\dagger(\kappa')]=(2\pi)^3\,2\omega_\kappa\delta^3(\vec{\kappa}-\vec{\kappa}'). \tag{4.23}$$

Dirac field operator for spin-$\frac{1}{2}$ particles: $\widetilde{N}$

Analogously, we write nucleon field operators as

$$\psi(x) = \frac{1}{(2\pi)^3}\int \frac{d^3p}{2p_0}\sum_{\sigma=\pm\frac{1}{2}}\left(e^{-ipx}u(p,\sigma)\,a(\vec{p},\sigma) + e^{ipx}v(p,\sigma)\,b^\dagger(\vec{p},\sigma)\right), \tag{4.24}$$

$$\bar{\psi}(x) = \frac{1}{(2\pi)^3}\int \frac{d^3p}{2p_0}\sum_{\sigma=\pm\frac{1}{2}}\left(e^{ipx}\bar{u}(p,\sigma)\,a^\dagger(\vec{p},\sigma) + e^{-ipx}\bar{v}(p,\sigma)\,b(\vec{p},\sigma)\right), \tag{4.25}$$

where $u(p,\sigma)$ and $v(p,\sigma)$ are Dirac spinors with momentum p and spin σ (cf. A.2) and the operators $a\left(a^\dagger\right)$ and $b\left(b^\dagger\right)$ are the annihilation (creation) operators of particles and antiparticles, respectively. The corresponding anti-commutator relations read

$$\{a(p,\sigma), a^\dagger(p',\sigma')\} = (2\pi)^3\,\delta_{\sigma\sigma'}2p_0\delta^3(\vec{p}-\vec{p}'). \tag{4.26}$$

After inserting the field expansions into Eqs. (4.19) and (4.20) and combining the terms with creation and annihilation operators one ends up with a whole bunch of terms. Since the numbers of creation and annihilation operators always have to be equal, only two will give a nonzero contribution. One of these describes the π together with a particle in the intermediate state, the other one a π and an antiparticle. The latter will not contribute here.

By using Wick's theorem in combination with the (anti)commutation properties of creation and annihilation operators one ends up with the final expressions for the vertex matrix elements

$$\langle\widetilde{N}|\mathcal{L}_I^{PV}(0)|\widetilde{N},\pi:\vec{k}_\pi\rangle = -i\sum\frac{f_{\pi\widetilde{N}\widetilde{N}}}{m_\pi}\bar{u}\left(k_{\widetilde{N}},\sigma\right)\gamma^\mu\gamma_5 I\left(\tau_{\widetilde{N}},\tau'_{\widetilde{N}},\tau_\pi\right)u\left(k'_{\widetilde{N}},\sigma'\right)(k_\pi)_\mu, \tag{4.27}$$

$$\langle\widetilde{N},\pi:\vec{k}_\pi|\mathcal{L}_I^{PV\dagger}(0)|\widetilde{N}\rangle = i\sum\frac{f_{\pi\widetilde{N}\widetilde{N}}}{m_\pi}\bar{u}\left(k'_{\widetilde{N}},\sigma'\right)\gamma^\mu\gamma_5 I\left(\tau'_{\widetilde{N}},\tau_{\widetilde{N}},\tau_\pi\right)u\left(k_{\widetilde{N}},\sigma\right)(k_\pi)_\mu. \tag{4.28}$$

The isospin matrix element $I\left(\tau_{\widetilde{N}},\tau'_{\widetilde{N}},\tau_\pi\right) = \langle\widetilde{N}|\vec{T}\cdot\vec{\pi}|\widetilde{N}'\rangle$ occurring here will be discussed in Sec. (4.2.3) below.

4.2.2. Peudoscalar Coupling

Instead of PV coupling one can also use PS coupling [EW88] in Eq. (4.19) and Eq. (4.20)

$$\mathcal{L}_I^{PS}(x) = -ig_{\pi\widetilde{N}\widetilde{N}}\bar{\psi}(x)\,\gamma_5\vec{T}\psi(x)\cdot\vec{\phi}(x). \tag{4.29}$$

Here, $g_{\pi\widetilde{N}\widetilde{N}}$ is the PS $\pi\widetilde{N}\widetilde{N}$ coupling constant and the fields are defined as above in Sec. 4.2.1. After following the same procedure as for PV coupling, the final expressions

for the matrix elements read

$$\langle \widetilde{N}|\mathcal{L}_I^{PS}(0)|\widetilde{N},\pi:\vec{k}_\pi\rangle = -i\sum g_{\pi\widetilde{N}\widetilde{N}}\bar{u}\left(k_{\widetilde{N}},\sigma\right)\gamma_5 I\left(\tau_{\widetilde{N}},\tau'_{\widetilde{N}},\tau_\pi\right)u\left(k'_{\widetilde{N}},\sigma'\right), \tag{4.30}$$

$$\langle \widetilde{N},\pi:\vec{k}_\pi|\mathcal{L}_I^{PS\dagger}(0)|\widetilde{N}\rangle = i\sum g_{\pi\widetilde{N}\widetilde{N}}\bar{u}\left(k'_{\widetilde{N}},\sigma'\right)\gamma_5 I\left(\tau'_{\widetilde{N}},\tau_{\widetilde{N}},\tau_\pi\right)u\left(k_{\widetilde{N}},\sigma\right). \tag{4.31}$$

4.2.3. Spin and Isospin Considerations

The isospin matrix element $I\left(\tau_{\widetilde{N}},\tau'_{\widetilde{N}},\tau_\pi\right) = \langle\widetilde{N}|\vec{T}\cdot\vec{\pi}|\widetilde{N}'\rangle$ appearing in Eqs. (4.27), (4.28), (4.30) and (4.31) will now discussed in great detail. It describes the isospin behavior at the vertex.

$\vec{\pi} = \left(\pi^1,\pi^2,\pi^3\right)$ has isospin $T = 1$ and $\tau = 1,0,-1$ and so the isospin triplet is defined as

$$\vec{\pi} = \begin{pmatrix} \pi^+ \\ \pi^0 \\ \pi^- \end{pmatrix}, \tag{4.32}$$

while the isospin operator $\vec{T}$ is built by the three Pauli matrices

$$\tau^1 = \begin{pmatrix} 0 & 1 \\ 1 & 0 \end{pmatrix}, \quad \tau^2 = \begin{pmatrix} 0 & -i \\ i & 0 \end{pmatrix}, \quad \tau^3 = \begin{pmatrix} 1 & 0 \\ 0 & -1 \end{pmatrix}. \tag{4.33}$$

The nucleon spinor is written as $N = \begin{pmatrix} p \\ n \end{pmatrix}$.

For the case of a proton incoming and outgoing the intermediate state can be a proton and a π^0 or a neutron and a π^+ as shown in Fig. (4.1).

Figure 4.1.: Two possible intermediate states for an incoming and outgoing proton.

Spherical Representation

In this representation the isospin operator $\vec{T}$ is defined to have the following components,

- $\tau^\pm = \mp\frac{1}{2}(\tau_1 \pm i\tau_2)$,
- $\tau_0 = \tau_3$,

namely

$$\tau^+ = -\begin{pmatrix} 0 & \sqrt{2} \\ 0 & 0 \end{pmatrix}, \quad \tau^- = \begin{pmatrix} 0 & 0 \\ \sqrt{2} & 0 \end{pmatrix}, \quad \tau^0 = \begin{pmatrix} 1 & 0 \\ 0 & -1 \end{pmatrix}, \tag{4.34}$$

where τ^+ and τ^- are usually called ladder operators.

An analogous relation holds for the $\vec{\pi}$

- $\pi^\pm = \mp\frac{1}{\sqrt{2}}(\pi_1 \pm i\pi_2)$,

(4.35)

- $\pi_0 = \pi_3$.

(4.36)

Using the definition of the scalar product for arbitrary vectors $\vec{v}$ and $\vec{w}$ in spherical representation [Car71]

$$\vec{v}\cdot\vec{w} = -v^+w^- - v^-w^+ + v^0w^0, \tag{4.37}$$

we calculate the scalar product $\vec{T}\cdot\vec{\pi}$ in $I\left(\tau_{\widetilde{N}}, \tau''_{\widetilde{N}}, \tau''_\pi\right)$ and obtain

$$\vec{T}\cdot\vec{\pi} = (-)(-)\begin{pmatrix} 0 & \sqrt{2} \\ 0 & 0 \end{pmatrix}\pi^- - \begin{pmatrix} 0 & 0 \\ \sqrt{2} & 0 \end{pmatrix}\pi^+ + \begin{pmatrix} 1 & 0 \\ 0 & -1 \end{pmatrix}\pi^0. \tag{4.38}$$

The ladder operators appearing in Eq. (4.38) obey

$$\tau^{\mu\dagger} = (-1)^\mu \tau^{-\mu}, \tag{4.39}$$

which is the hermiticity condition in spherical representation. More detailes can be found in Ref. [Car71]. The following three possible matrix elements

$$\langle n|\vec{T}\cdot\vec{\pi}|p\rangle, \quad \langle p|\left(\vec{T}\cdot\vec{\pi}\right)^\dagger|n\rangle, \quad \langle p|\vec{T}\cdot\vec{\pi}|p\rangle \tag{4.40}$$

have to be considered. Keeping in mind the characteristics of the isospin ladder operators

$$\tau^-|p\rangle = |n\rangle, \quad \tau^+|n\rangle = |p\rangle, \quad \tau^-|n\rangle = \tau^+|p\rangle = 0 \tag{4.41}$$

we get for the first matrix element in Eq. (4.40) a factor $-\sqrt{2}$, since the only contribution is the one with the π^+. For the second matrix element the term with the π^- is surviving and gives again $-\sqrt{2}$. This is true due to the minus appearing in the hermiticity condition. The third matrix element gives 1.

Eventually the diagram on the l.h.s. of Fig. (4.1) gives an isospin factor 2, the diagram on the r.h.s gives a factor 1 and in sum the isospin contribution gives an overall factor of 3.

Calculation with Clebsch-Gordan coefficients

Concerning the l.h.s. diagram of Fig. (4.1), we have to consider the matrix element

$$\langle \frac{1}{2}\frac{1}{2}|\tau^0|\frac{1}{2}\frac{1}{2}\rangle \tag{4.42}$$

at each vertex. However, for the r.h.s. diagram the following matrix elements

$$\langle \frac{1}{2}\frac{1}{2}|\tau^+|\frac{1}{2}-\frac{1}{2}\rangle, \quad \left(\langle \frac{1}{2}\frac{1}{2}|\tau^+|\frac{1}{2}-\frac{1}{2}\rangle\right)^\dagger \tag{4.43}$$

occur. They can be evaluated with the following formula (see, e.g. Refs. [DST65] and [KNLS13])

$$\langle sm_s|\tau^m|sm_s'\rangle = \langle s1m_s'm|sm_s\rangle\langle s\|\tau\|s\rangle/\sqrt{2s+1}, \tag{4.44}$$

where $\langle s1m_s'm|sm_s\rangle$ is a usual Clebsch-Gordon coefficient with $m=\pm1,0$ and $\langle s\|\tau\|s\rangle = \sqrt{6}$ is the reduced matrix element.

The Clebsch-Gordan coefficients are defined in spherical representation and so we again have to take into account the corresponding hermiticity condition for the corresponding operators.

The matrix element describing the process shown on the l.h.s. in Fig. (4.1) leads to

$$\langle \frac{1}{2}\frac{1}{2}|\tau^0|\frac{1}{2}\frac{1}{2}\rangle = \left(\langle \frac{1}{2}\frac{1}{2}|\tau^0|\frac{1}{2}\frac{1}{2}\rangle\right)^\dagger = \langle \frac{1}{2}1\frac{1}{2}0|\frac{1}{2}\frac{1}{2}\rangle\sqrt{6}/\sqrt{2} = 1. \tag{4.45}$$

The second possibility shown on the r.h.s. of Fig. (4.1) leads to

$$\begin{aligned}\langle \frac{1}{2}\frac{1}{2}|\tau^+|\frac{1}{2}-\frac{1}{2}\rangle &= \langle \frac{1}{2}1-\frac{1}{2}1|\frac{1}{2}\frac{1}{2}\rangle\sqrt{6}/\sqrt{2} = -\sqrt{2},\\ \left(\langle \frac{1}{2}\frac{1}{2}|\tau^+|\frac{1}{2}-\frac{1}{2}\rangle\right)^\dagger &= (-)\langle \frac{1}{2}-\frac{1}{2}|\tau^-|\frac{1}{2}\frac{1}{2}\rangle\\ &= (-)\langle \frac{1}{2}1\frac{1}{2}-1|\frac{1}{2}-\frac{1}{2}\rangle\sqrt{6}/\sqrt{2} = -\sqrt{2}.\end{aligned} \tag{4.46}$$

Summing the contributions of the two possibilities one ends up with an overall isospin factor of 3.

Pseudospherical Representation

The isospin operator $\vec{T}$ in pseudospherical representation has the following components,

- $\tau^\pm = \frac{1}{2}\left(\tau^1 \pm i\tau^2\right)$
- $\tau^0 = \tau^3$,

namely

$$\tau^+ = \begin{pmatrix} 0 & \sqrt{2} \\ 0 & 0 \end{pmatrix}, \quad \tau^- = \begin{pmatrix} 0 & 0 \\ \sqrt{2} & 0 \end{pmatrix}, \quad \tau^0 = \begin{pmatrix} 1 & 0 \\ 0 & -1 \end{pmatrix}. \tag{4.47}$$

An analogous relation holds for the $\vec{\pi}$,

- $\pi^\pm = \frac{1}{\sqrt{2}}\left(\pi^1 \pm i\pi^2\right)$,
- $\pi^3 = \pi^0$.

Using the definition of the scalar product in pseudosherical representation

$$\vec{v} \cdot \vec{w} = +v^+ w^- + v^- w^+ + v^0 w^0, \tag{4.48}$$

we can calculate $\vec{T} \cdot \vec{\pi}$ and get

$$\vec{T} \cdot \vec{\pi} = \begin{pmatrix} 0 & \sqrt{2} \\ 0 & 0 \end{pmatrix} \pi^- + \begin{pmatrix} 0 & 0 \\ \sqrt{2} & 0 \end{pmatrix} \pi^+ + \begin{pmatrix} 1 & 0 \\ 0 & -1 \end{pmatrix} \pi^0. \tag{4.49}$$

Now the matrix elements of Eq. (4.42) and Eq. (4.43) are evaluated in pseudospherical representation. Matrix multiplication leads to

- $$\left(p^\dagger \tau^0 p\right) = (1 \;\; 0) \begin{pmatrix} 1 & 0 \\ 0 & -1 \end{pmatrix} \begin{pmatrix} 1 \\ 0 \end{pmatrix} = 1, \tag{4.50}$$
- $$\left(p^\dagger \tau^+ n\right) = (1 \;\; 0) \begin{pmatrix} 0 & \sqrt{2} \\ 0 & 0 \end{pmatrix} \begin{pmatrix} 0 \\ 1 \end{pmatrix} = \sqrt{2}, \tag{4.51}$$
- $$\left(p^\dagger \tau^+ n\right)^\dagger = n^\dagger \tau^- p = (0 \;\; 1) \begin{pmatrix} 0 & 0 \\ \sqrt{2} & 0 \end{pmatrix} \begin{pmatrix} 1 \\ 0 \end{pmatrix} = \sqrt{2}. \tag{4.52}$$

Again an overall isospin factor of 3 results.

4.3. Solution of the Eigenvalue Equation

Now we turn to the solution of the eigenvalue equation (4.16) with the optical potential given in Eq. (4.17).

In our frame-independent theory we may assume the incoming and outgoing $\widetilde{N}$ to be at rest, so its four-momentum without the presence of the π is given by

$$k_{\widetilde{N}} = \begin{pmatrix} m_{\widetilde{N}} \\ 0 \\ 0 \\ 0 \end{pmatrix}. \tag{4.53}$$

In the intermediate region, where there is a $\widetilde{N}$ and a π, due to three-momentum conservation, we have

$$k''_{\pi} = \begin{pmatrix} \omega''_{\pi} \\ k''_{\pi} \sin\theta'' \cos\phi'' \\ k''_{\pi} \sin\theta'' \sin\phi'' \\ k''_{\pi} \cos\theta'' \end{pmatrix}, \qquad k''_{\widetilde{N}} = \begin{pmatrix} \omega''_{\widetilde{N}} \\ -k''_{\pi} \sin\theta'' \cos\phi'' \\ -k''_{\pi} \sin\theta'' \sin\phi'' \\ -k''_{\pi} \cos\theta'' \end{pmatrix} \tag{4.54}$$

with $\omega_i = \sqrt{m_i^2 + \vec{k}_i^2}$.

As already mentioned in Sec. 4.1, the eigenvalue equation (4.16) contains in the term for the optical potential Eq. (4.17) also the searched mass eigenvalue m. It means that the dynamics governing the dressed mass m also occurs in the propagator of the intermediate $\pi\widetilde{N}$ state. By solving this eigenvalue equation we therefore take into account all one-π loops including their iterations. In the view of an iterative method we can thus represent the optical potential like in Fig. 4.2.

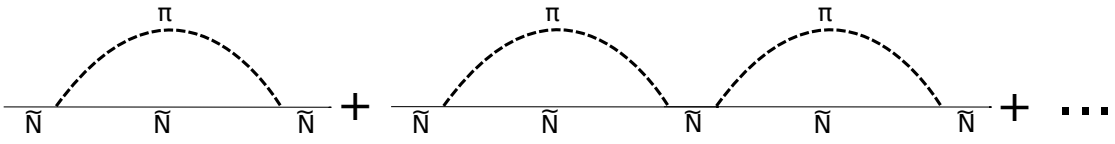

Figure 4.2.: Pictorial representation of the first- and second-order iterations of the optical potential in Eq. (4.17).

The fact that the eigenvalue m also occurs on the l. h. s. of Eq. (4.16) requires also a particular method for its practical solution. We adhere to the following procedure:

We begin by setting the dressed (physical) mass eigenvalue to m = 939 MeV and search for the bare mass $m_{\widetilde{N}}$ dictated by the eigenvalue equation. In order to find the corresponding value of $m_{\widetilde{N}}$ we use an iterative procedure. We start with an arbitrary value for $m_{\widetilde{N}}$ in the optical potential and solve Eq. (4.16). The resulting value for $m_{\widetilde{N}}$ from the first step is then reinserted into the equation and so on. When $m_{\widetilde{N}}$ becomes stable, we know that the final solution is achieved and all orders of one-π loops are included.

4.3.1. Input Vertex Form Factors

Eq. (4.16) consists of bare macroscopic quantities only. Nevertheless they have an extended structure. In order to account for them we employ vertex form factors $\mathcal{F}_{\pi\widetilde{N}\widetilde{N}}$. They are here taken from the literature. Corresponding works sometimes do not clearly distinguish between bare and dressed vertex form factors. In order to make our calculations consistent and clear-cut, we assume for the present purposes (to get an idea of the magnitudes of the π dressing effects in the N) all of the employed vertex form factors to be bare ones. In some cases [SL96] and [KNLS13] the $\mathcal{F}_{\pi\widetilde{N}\widetilde{N}}$ are definitely stated

as such, in other cases [MCP09] and [PR05b] we just assume them as bare ones.[1]

RCQM:

In Ref. [MCP09] one deduced a $\pi\widetilde{N}\widetilde{N}$ form factor microscopically from a relativistic constituent-quark model. In fact, the matrix element of a PV transition operator for the process of Fig. 4.2 was evaluated with refined three-quark wave functions. The result was parametrized by the multipole function

$$\mathcal{F}_{\pi\widetilde{N}\widetilde{N}}\left(\vec{k}_\pi^2\right) = \frac{1}{1+\left(\frac{\vec{k}_\pi}{\Lambda_1}\right)^2+\left(\frac{\vec{k}_\pi}{\Lambda_2}\right)^4} \qquad \text{(RCQM, SL and PR Multipole)} \tag{4.55}$$

with parameters given in Tab. 4.1. The same type of parametrization is used for SL and PR Multipole form factors form factors described below.

SL and KNLS:

The form factors by Sato and Lee (SL) Ref. [SL96] and by Kamano, Nakamura, Lee and Sato (KNLS), Ref. [KNLS13], were introduced and parametrized within a phenomenological meson-baryon model, where the $f_{\pi\widetilde{N}\widetilde{N}}$ coupling constant is taken to be the canonical phenomenological one as is given in Tab. 4.1.

For the reason of comparison the authors of Ref. [MCP09] cast the form factor of SL into the form of Eq. (4.55) with parameters given in Tab. 4.1. We adopt this parametrization of the SL form factor also in our work, while for the KNLS form factor we use their original form

$$\mathcal{F}_{\pi\widetilde{N}\widetilde{N}}\left(\vec{k}_\pi^2\right) = \left(\frac{\Lambda^2}{\vec{k}_\pi^2+\Lambda^2}\right)^2 \qquad \text{(KNLS)}, \tag{4.56}$$

again with parameters given in Tab. 4.1.

Polinder Rijken (PR):

In Ref. [PR05a] form factors of a Gaussian type were introduced. The cut-off parameters were fixed in Ref. [PR05b] by fitting the Nijmegen soft-core (NSC) πN model to the energy-dependent SM95 partial wave analysis [ASWP95]. As can be seen in Tab. 4.1, the $\pi\widetilde{N}\widetilde{N}$ coupling constant differs very much from the other parametrizations and also the dependence on $\vec{k}_\pi^2$ is much different, see Fig. 4.3.

Here, we consider the PR form factors according to two different parametrizations, the original Gaussian one

$$\mathcal{F}_{\pi\widetilde{N}\widetilde{N}}\left(\vec{k}_\pi^2\right) = \exp^{-\vec{k}_\pi^2/\Lambda^2} \qquad \text{(PR Gauss)}, \tag{4.57}$$

[1] In the 8th chapter below we shall produce vertex form factors ourselves consistently with a microscopic CC constituent-quark model.

and the multipole reparametrization with formula (4.55) by [MCP09]. The corresponding parameters are again given in Tab. 4.1.

The dependences of the various vertex form factors on the three-momenutm $\vec{k}_\pi^2$ can be seen from Fig. 4.3.

	RCQM	SL	KNLS	PR Gauss	PR Multipole
$\frac{f^2_{\pi\widetilde{N}\widetilde{N}}}{4\pi}$	0.0691	0.08	0.08	0.013	0.013
λ_1	0.451	0.453			0.940
λ_2	0.931	0.641			1.102
Λ			0.656	0.665	

Table 4.1.: Coupling constants and parameters for the $\pi\widetilde{N}\widetilde{N}$ vertex form factors according to different models in the literature. Here and everywhere throughout this thesis the dimensions of the cut-off parameters are GeV. For the abbreviations see the text.

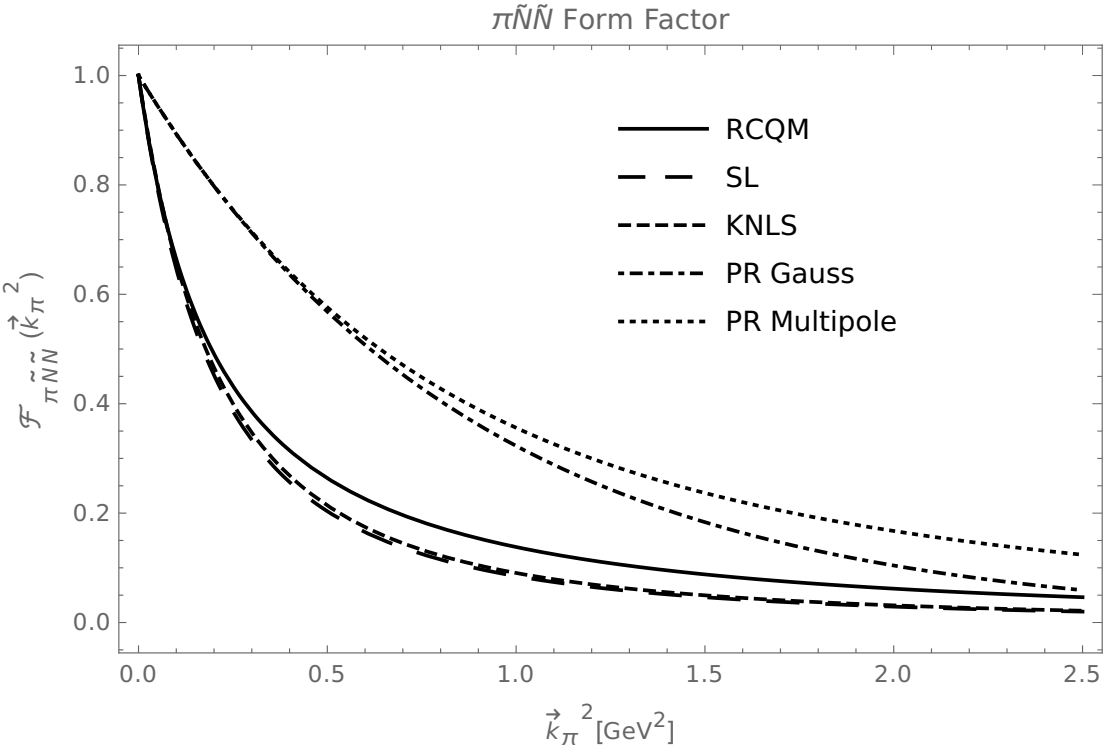

Figure 4.3.: $\pi\widetilde{N}\widetilde{N}$ form factor parametrizations as functions of the three-momentum squared from various models in the literature.

4.4. Results and Discussion

We now give the results for the one-π loop effects on the N mass from our CC theory using the $\pi\widetilde{N}\widetilde{N}$ vertex form factor models discussed above.

	RCQM	SL	KNLS	PR Gauss	PR Multipole
m_N	939	939	939	939	939
$m_{\widetilde{N}}$	1067	1031	1037	1025	1051
$m_N - m_{\widetilde{N}}$	-128	-92	-98	-86	-112

Table 4.2.: π loop effects on the nucleon mass m_N from coupling to the πN channel ($m_{\widetilde{N}}$ being the bare mass and m_N the dressed (physical) one). All values given in MeV. The π mass is always assumed to be m_π=139 MeV.

As can be seen from Tab. 4.2 the obtained values for the bare N masses vary between $m_{\widetilde{N}} = 1025$ MeV, for the PR Gauss form-factor parametrization, and $m_{\widetilde{N}} = 1067$ MeV, for the RCQM case. This leads to one-π loop effects between 86 and 128 MeV. Note that the mass of the N dressed in this manner is always resulting as $m_N = 939$ MeV, i. e. the mass of the physical N. We observe that the one-π loop dressing effect, which always reduces the mass from the bare to the physical N, is of the same order of magnitude of about 100 MeV, varying up and down by approximately 20%. The differences are due to the different momentum dependences of the $\pi\widetilde{N}\widetilde{N}$ vertex form factors (see Fig. 4.3) and the different sizes of the πN coupling constants (cf. Tab. 4.1). Consequently, the results are more or less the same for the SL and KNLS cases. In corresponding form-factor models the same value for the πN coupling constant of $\frac{f^2_{\pi N\Delta}}{4\pi} = 0.08$, as extracted from phenomenology, is assumed and the form-factor dependences on the momentum are very similar. The RCQM form factor falls off slower, while the coupling constant is about the same. As a result the dressing effect is bigger by about 20%. The form factor dependences of the PR model are quite distinct with a very slow fall-off towards higher momenta. Still, the dressing effects are smaller especially for the PR Gaussian parametrization. This is caused by a rather small πN coupling constant.

We note that the dressing effect on the N mass was also investigated by Polinder and Rijken in Ref. [PR05b], however, in a completely different, nonrelativistic approach. They obtained a rather large dressing effect of $m_N - m_{\widetilde{N}} = -248$ MeV.

On the other hand, π effects on the N mass were also studied by Pascalutsa and Tjon in Ref. [PT00]. They employed a relativistic theory and produced a π dressing effect of -151 MeV, i. e. about 18% higher than the RCQM.

Having established the one-π loop effects on the N mass by our relativistic CC theory, we may ask, if additional pionic effects influence the N dressing. In this regard we my think of two-π loops or interactions in the πN channel.

5. The Nucleon with Additional Pionic Contributions

The CC model considered in the previous chapter is only the simplest way of including explicit π degrees of freedom. Here we investigate the possible role of further π effects. In particular, we first add an additional interaction-free $\pi\pi\widetilde{N}$ channel and subsequently we consider also interactions in the $\pi\widetilde{N}$ and $\pi\pi\widetilde{N}$ channels.

5.1. Additional $\pi\pi\widetilde{N}$ Channel

The extended CC mass operator with an additional interaction-free $\pi\pi\widetilde{N}$ channel reads:

$$\begin{pmatrix} M_{\widetilde{N}} & K & 0 \\ K^\dagger & M_{\widetilde{N}+\pi} & K \\ 0 & K^\dagger & M_{\widetilde{N}+\pi+\pi} \end{pmatrix} \begin{pmatrix} |\psi_N\rangle \\ |\psi_{N+\pi}\rangle \\ |\psi_{N+\pi+\pi}\rangle \end{pmatrix} = m \begin{pmatrix} |\psi_N\rangle \\ |\psi_{N+\pi}\rangle \\ |\psi_{N+\pi+\pi}\rangle \end{pmatrix}. \tag{5.1}$$

We first attempt to reduce the three coupled equations to calculate the dressed mass of the N corresponding to the state $|\psi_N\rangle$. From the third equation

$$K^\dagger|\psi_{N+\pi}\rangle + M_{\widetilde{N}+\pi+\pi}|\psi_{N+\pi+\pi}\rangle = m|\psi_{N+\pi+\pi}\rangle \tag{5.2}$$

we obtain

$$|\psi_{N+\pi+\pi}\rangle = (m - M_{\widetilde{N}+\pi+\pi})^{-1} K^\dagger|\psi_{N+\pi}\rangle. \tag{5.3}$$

Inserting the latter into the second equation following from Eq. (5.1) we end up with

$$\begin{aligned} K^\dagger|\psi_N\rangle + M_{\widetilde{N}+\pi}|\psi_{N+\pi}\rangle + K|\psi_{N+\pi+\pi}\rangle &= m|\psi_{N+\pi}\rangle \\ \rightarrow |\psi_{N+\pi}\rangle = (m - M_{\widetilde{N}+\pi} - K(m - M_{\widetilde{N}+\pi+\pi})^{-1} K^\dagger)^{-1} K^\dagger|\psi_N\rangle. \end{aligned} \tag{5.4}$$

Finally we insert this into the first equation following from Eq. (5.1) to obtain

$$M_{\widetilde{N}}|\psi_N\rangle + K \underbrace{(m - M_{\widetilde{N}+\pi} - K(m - M_{\widetilde{N}+\pi+\pi})^{-1} K^\dagger)^{-1}}\, K^\dagger|\psi_N\rangle = m|\psi_N\rangle. \tag{5.5}$$

Assuming the expression marked by the brace to represent only a minor contribution we may expand it in the following way

$$\begin{aligned} &(m - M_{\widetilde{N}+\pi} - K(m - M_{\widetilde{N}+\pi+\pi})^{-1} K^\dagger)^{-1} \\ \approx &(m - M_{\widetilde{N}+\pi})^{-1} \\ + &(m - M_{\widetilde{N}+\pi})^{-1} \underbrace{K(m - M_{\widetilde{N}+\pi+\pi})^{-1} K^\dagger}(m - M_{\widetilde{N}+\pi})^{-1} + \ldots \end{aligned} \tag{5.6}$$

In order to obtain the latter result we have used the operator expansion

$$(A+\epsilon B)^{-1} = A^{-1} - \epsilon A^{-1} B A^{-1} + \mathcal{O}(\epsilon^2) \tag{5.7}$$

for small $\epsilon > 0$. Finally we have the following eigenvalue equation

$$\Bigg[M_{\widetilde{N}} + K(m - M_{\widetilde{N}+\pi})^{-1} K^\dagger + \underbrace{K(m - M_{\widetilde{N}+\pi})^{-1} K (m - M_{\widetilde{N}+\pi+\pi})^{-1} K^\dagger (m - M_{\widetilde{N}+\pi})^{-1} K^\dagger}\Bigg] |\psi_N\rangle = m|\psi_N\rangle. \tag{5.8}$$

As compared to Eq. (4.17) the optical potential now contains an additional term, which we have marked by the brace. Its first-order contribution is pictorially shown in Fig. 5.1. The corresponding dynamics is usually viewed as stemming from so-called crossed two-π loops.

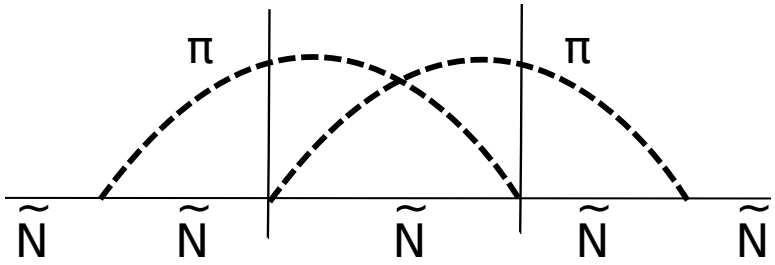

Figure 5.1.: Pictorial representation of the first-order term of the crossed two-π loop contributions.

Among others corresponding contributions have already been considered in the literature by [GS93], [PT00], and [KNLS13].

In order to solve Eq. (5.8), one-, two- or three-particle velocity state completeness relations have to be inserted at appropriate places. In addition to the one- and two-particle ones defined in the previous chapter we need the velocity states corresponding to the interaction-free $\pi\pi\widetilde{N}$ mass operator

$$M_{\widetilde{N}+\pi+\pi}|\widetilde{N},\pi_1,\pi_2 : v,\vec{k}_{\pi_1},\vec{k}_{\pi_2}\rangle = \left(m_{\widetilde{N}} + m_{\pi_1} + m_{\pi_2}\right)|\widetilde{N},\pi_1,\pi_2 : v,\vec{k}_{\pi_1},\vec{k}_{\pi_2}\rangle. \tag{5.9}$$

Their completeness and orthogonality relations read

$$\mathbb{1}_{\widetilde{N}+\pi_1+\pi_2} = \int \frac{d^3v}{(2\pi)^3 v_0} \int \frac{d^3k_{\pi_1}}{(2\pi)^3 2\omega_{\pi_1}} \int \frac{d^3k_{\pi_2}}{(2\pi)^3 2\omega_{\pi_2}} \frac{(\omega_{\pi_1}+\omega_{\pi_2}+\omega_{\widetilde{N}})^3}{2\omega_{\widetilde{N}}} \times |\widetilde{N},\pi_1,\pi_2 : v,\vec{k}_{\pi_1},\vec{k}_{\pi_2}\rangle\langle\widetilde{N},\pi_1,\pi_2 : v,\vec{k}_{\pi_1},\vec{k}_{\pi_2}| \tag{5.10}$$

and

$$\begin{aligned}&\langle\widetilde{N},\pi_1,\pi_2 : v',\vec{k}'_{\pi_1},\vec{k}'_{\pi_2}|\widetilde{N},\pi_1,\pi_2 : v,\vec{k}_{\pi_1},\vec{k}_{\pi_2}\rangle \\ &= (2\pi)^3 v'_0 \delta^3(\vec{v}'-\vec{v}) \frac{2\omega_{\widetilde{N}} 2\omega_{\pi_1} 2\omega_{\pi_2}}{(\omega_{\widetilde{N}}+\omega_{\pi_1}+\omega_{\pi_2})^3} (2\pi)^3 \delta^3(\vec{k}'_{\pi_1}-\vec{k}_{\pi_1})(2\pi)^3\delta^3(\vec{k}'_{\pi_2}-\vec{k}_{\pi_2}),\end{aligned} \tag{5.11}$$

where now $\vec{k}_{\widetilde{N}} + \vec{k}_{\pi_1} + \vec{k}_{\pi_2} = 0$.

By considering the second term in Eq. (5.8) and extracting the matrix element

$$\langle \widetilde{N}, \pi : v, \vec{k}_{\pi_1} | K(m - M_{\widetilde{N}+\pi+\pi})^{-1} K^\dagger | \widetilde{N}, \pi : v', \vec{k}'_{\pi_2} \rangle \tag{5.12}$$

we now have to use Eq. (5.10) to end up with two vertex matrix elements:

$$\begin{aligned}
&\langle \widetilde{N}, \pi : v, \vec{k}_{\pi_1} | K(m - M_{\widetilde{N}+\pi+\pi})^{-1} \mathbb{1}''_{\widetilde{N}+\pi_1+\pi_2} K^\dagger | \widetilde{N}, \pi : v', \vec{k}'_{\pi_2} \rangle \\
&= \int \frac{d^3 v''}{(2\pi)^3 v''_0} \int \frac{d^3 k''_{\pi_1}}{(2\pi)^3 2\omega''_{\pi_1}} \int \frac{d^3 k''_{\pi_2}}{(2\pi)^3 2\omega''_{\pi_2}} \frac{(\omega''_{\pi_1} + \omega''_{\pi_2} + \omega_{\widetilde{N}})^3}{2\omega_{\widetilde{N}}} \\
&\times \langle \widetilde{N}, \pi : \vec{k}_{\pi_1} | K | \widetilde{N}, \pi_1, \pi_2 : \vec{k}''_{\pi_1}, \vec{k}''_{\pi_2} \rangle (m - M_{\widetilde{N}+\pi+\pi})^{-1} \\
&\times \langle \widetilde{N}, \pi_1, \pi_2 : \vec{k}''_{\pi_1}, \vec{k}''_{\pi_2} | K^\dagger | \widetilde{N}, \pi : \vec{k}'_{\pi_2} \rangle .
\end{aligned} \tag{5.13}$$

The vertex matrix-element of the type $\langle \widetilde{N}, \pi : \vec{k}'_{\pi_1} | K | \widetilde{N}, \pi_1, \pi_2 : \vec{k}_{\pi_1}, \vec{k}_{\pi_2} \rangle$ and the complex conjugated one are obtained by following the procedure described in Sec. 4.2.1.

The final expressions are given here

- $$\begin{aligned}
&\langle \widetilde{N}, \pi : \vec{k}'_{\pi_1} | \mathcal{L}^{PV}_{\pi_2}(0) | \widetilde{N}, \pi_1, \pi_2 : \vec{k}_{\pi_1}, \vec{k}_{\pi_2} \rangle \\
&= -i \frac{f}{m_\pi} \bar{u}(k_{\widetilde{N}}, \sigma) \gamma^\mu \gamma_5 I(\tau_{\widetilde{N}}, \tau'_{\widetilde{N}}, \tau_{\pi_2}) u(k'_{\widetilde{N}}, \sigma') \left(k_{\pi_2}\right)_\mu 2\omega'_{k_{\pi_1}} \delta^3(\vec{k}'_{\pi_1} - \vec{k}_{\pi_1}),
\end{aligned} \tag{5.14}$$

- $$\begin{aligned}
&\langle \widetilde{N}, \pi_1, \pi_2 : \vec{k}_{\pi_1}, \vec{k}_{\pi_2} | \mathcal{L}^{PV\dagger}_{\pi_1}(0) | \widetilde{N}, \pi : \vec{k}'_{\pi_2} \rangle \\
&= i \frac{f}{m_\pi} \bar{u}(\vec{k}'_{\widetilde{N}}, \sigma') \gamma^\mu \gamma_5 I(\tau'_{\widetilde{N}}, \tau_{\widetilde{N}}, \tau_{\pi_1}) u(\vec{k}_{\widetilde{N}}, \sigma) \left(k_{\pi_1}\right)_\mu 2\omega'_{k_{\pi_2}} \delta^3(\vec{k}'_{\pi_2} - \vec{k}_{\pi_2})
\end{aligned} \tag{5.15},$$

where in each matrix element there appears an additional delta function for the spectator π. For further information about the Dirac spinors see App. A.2.

Isospin Considerations

We exemplify the case of an incoming and outgoing proton and consequently three different πN transitions. The numbers at the vertices in Fig. 5.2 denote the isospin contributions that are obtained by calculating $I(\tau'_{\widetilde{N}}, \tau_{\widetilde{N}}, \tau_\pi)$ at each vertex. The calculation has been done as described in Sec. 4.2.3 and consequently the final overall isospin factor is -3.

5.1.1. Solution and Results

The eigenvalue Eq. (5.8) has again the property that the searched eigenvalue m occurs also on the l.h.s. and so it can be solved in the same way as described in Sec. 4.3.

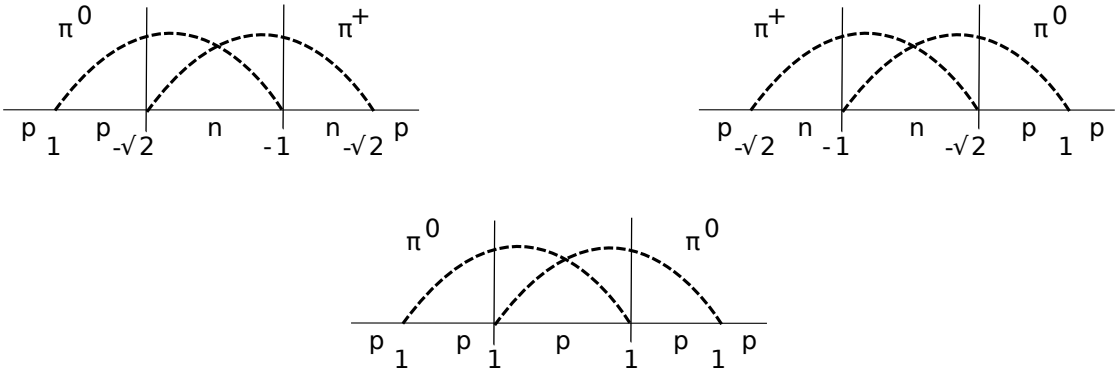

Figure 5.2.: Different possible πN transitions for the case of an incoming and outgoing p.

Kinematics

We may again assume that the incoming and outgoing $\widetilde{N}$ is at rest, so its four-momentum is given by

$$k_{\widetilde{N}} = \begin{pmatrix} m_{\widetilde{N}} \\ 0 \\ 0 \\ 0 \end{pmatrix}. \tag{5.16}$$

In the region where there is a $\widetilde{N}$ and a π, due to momentum conservation, we have

$$k'_\pi = \begin{pmatrix} \omega'_\pi \\ k'_\pi \sin\theta' \cos\phi' \\ k'_\pi \sin\theta' \sin\phi' \\ k'_\pi \cos\theta' \end{pmatrix}, \qquad k'_{\widetilde{N}} = \begin{pmatrix} \omega'_{\widetilde{N}} \\ -k'_\pi \sin\theta' \cos\phi' \\ -k'_\pi \sin\theta' \sin\phi' \\ -k'_\pi \cos\theta' \end{pmatrix} \tag{5.17}$$

and

$$k''_\pi = \begin{pmatrix} \omega''_\pi \\ k''_\pi \sin\theta'' \cos\phi'' \\ k''_\pi \sin\theta'' \sin\phi'' \\ k''_\pi \cos\theta'' \end{pmatrix}, \qquad k''_{\widetilde{N}} = \begin{pmatrix} \omega''_{\widetilde{N}} \\ -k''_\pi \sin\theta'' \cos\phi'' \\ -k''_\pi \sin\theta'' \sin\phi'' \\ -k''_\pi \cos\theta'' \end{pmatrix}. \tag{5.18}$$

Further, due to momentum conservation, $\vec{k}_{\widetilde{N}} + \vec{k}'_\pi + \vec{k}''_\pi = 0$, in the crossed-terms region we end up with

$$k'_\pi = \begin{pmatrix} \omega'_\pi \\ k'_\pi \sin\theta' \cos\phi' \\ k'_\pi \sin\theta' \sin\phi' \\ k'_\pi \cos\theta' \end{pmatrix}, \qquad k''_\pi = \begin{pmatrix} \omega''_\pi \\ k''_\pi \sin\theta'' \cos\phi'' \\ k''_\pi \sin\theta'' \sin\phi'' \\ k''_\pi \cos\theta'' \end{pmatrix},$$

$$k_{\widetilde{N}} = \begin{pmatrix} \omega_{\widetilde{N}} \\ -(k'_\pi \sin\theta' \cos\phi' + k''_\pi \sin\theta'' \cos\phi'') \\ -(k'_\pi \sin\theta' \sin\phi' + k''_\pi \sin\theta'' \sin\phi'') \\ -(k'_\pi \cos\theta' + k''_\pi \cos\theta'') \end{pmatrix}. \tag{5.19}$$

These are all definitions of energies and momenta that are needed. Detailed information on how to treat the products of spinors appearing in Eqs. (5.14) and (5.15) can be found in App. A.2.

In analogy to Sec. 4.3 at the vertices various input form factors have been used to solve the nonlinear eigenvalue Eq. (5.8). The particular form factors used are the same as discussed in Sec. 4.3 and shown in Fig. 4.3 while the associated parameters are presented in Tab. 4.1.

Results

By using the inputs as specified above we find that the contribution of the crossed two-π loops in Eq. (5.8) is very small, namely, only of the order of $\sim$1 MeV in the dressed N mass. Therefore the effects of this kind of two-π contributions are practically negligible.

We may think of even other two-π effects, namely, by including an interaction among the two pions. This is considered in the following section.

5.2. Interactions in the $\pi\widetilde{N}$ Channel

In this section an additional $\pi\widetilde{N}$ interaction potential is added to the free $\pi\widetilde{N}$ mass operator. The starting point is Eq. (4.14), but we assume the mass operator $M_{\widetilde{N}+\pi}$ to be an interacting one composed of $M^{free}_{\widetilde{N}+\pi} + V_{\pi\widetilde{N}}$. Thus we obtain for the state $|\psi_N\rangle$

$$\begin{aligned} m_{\widetilde{N}}\langle\widetilde{N}:v|\psi_N\rangle + \underbrace{\langle\widetilde{N}:v|K(m-M_{\widetilde{N}+\pi})^{-1}K^\dagger|\psi_N\rangle}_{} &= m\langle\widetilde{N}:v|\psi_N\rangle, \\ \rightarrow \langle\widetilde{N}:v|K(m-M^{free}_{\widetilde{N}+\pi}-V_{\pi\widetilde{N}})^{-1}K^\dagger|\psi_N\rangle. & \end{aligned} \tag{5.20}$$

which is formally equivalent to the eigenvalue Eq. (4.14). Only the optical potential contains a $\pi\widetilde{N}$ interaction, which can be diagrammatically depicted as in Fig. 5.3. Including the $\pi\widetilde{N}$ interaction only to the first order, we can expand the propagator term

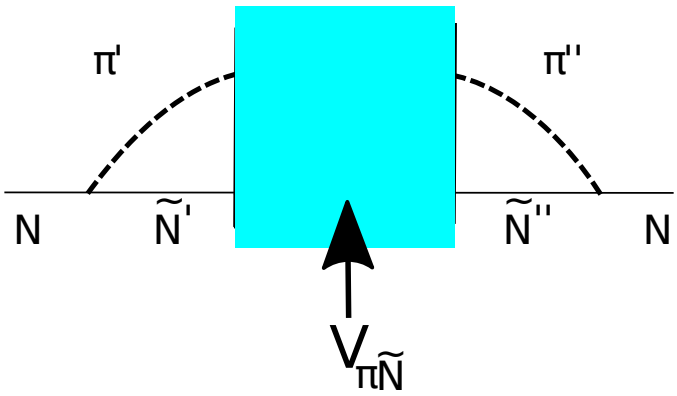

Figure 5.3.: Pictorial representation of the first-order term of the optical potential according to Eq. (5.20).

in Eq. (5.20) as

$$\left(m - M^{free}_{\widetilde{N}+\pi} - V_{\pi\widetilde{N}}\right)^{-1} \approx \left(m - M^{free}_{\widetilde{N}+\pi}\right)^{-1} + \left(m - M^{free}_{\widetilde{N}+\pi}\right)^{-1} V_{\pi\widetilde{N}} \left(m - M^{free}_{\widetilde{N}+\pi}\right)^{-1}, \tag{5.21}$$

where we have again used the operator expansion in Eq. (5.7).

The final eigenvalue equation then reads:

$$\begin{aligned}
&m_{\widetilde{N}}\langle\widetilde{N}:v|\psi_N\rangle + \langle\widetilde{N}:v|K(m - M^{free}_{\widetilde{N}+\pi} - V_{\pi\widetilde{N}})^{-1}K^\dagger|\psi_N\rangle \\
&\quad \approx m_{\widetilde{N}}\langle\widetilde{N}:v|\psi_N\rangle + \langle\widetilde{N}:v|K \\
&\quad \times \Big(\quad (m - M^{free}_{\widetilde{N}+\pi})^{-1} + \epsilon(m - M^{free}_{\widetilde{N}+\pi})^{-1} V_{\pi\widetilde{N}} (m - M^{free}_{\widetilde{N}+\pi})^{-1} \quad \Big) \\
&\quad \times K^\dagger|\psi_N\rangle = m\langle\widetilde{N}:v|\psi_N\rangle \\
&\quad \Rightarrow m_{\widetilde{N}}\langle\widetilde{N}:v|\psi_N\rangle + \langle\widetilde{N}:v|K(m - M^{free}_{\widetilde{N}+\pi})^{-1}K^\dagger|\psi_N\rangle \\
&\quad \underbrace{+ \langle\widetilde{N}:v|K(m - M^{free}_{\widetilde{N}+\pi})^{-1} V_{\pi\widetilde{N}} (m - M^{free}_{\widetilde{N}+\pi})^{-1}K^\dagger|\psi_N\rangle}_{} = m\langle\widetilde{N}:v|\psi_N\rangle.
\end{aligned} \tag{5.22}$$

In the following we discuss possible choices for the interaction potential $V_{\pi\widetilde{N}}$.

Eq. (5.22) is formally equivalent to Eq. (5.8), if we choose

$$V_{\pi\widetilde{N}} = K\left(m - M_{\widetilde{N}+\pi+\pi}\right)^{-1} K^\dagger, \tag{5.23}$$

where in the first case a third (interaction-free) $\pi\pi\widetilde{N}$ channel was considered, whereas in the second case a specific $\pi\widetilde{N}$ interaction is foreseen. In the following we discuss the so-called contact interactions in $\pi\widetilde{N}$ s-wave.

5.2.1. Contact Interaction in $\pi\widetilde{N}$ S-Wave

The contact interactions are represented by σ and ρ terms in s-wave, respectively.

Thus

$$V_{\pi\widetilde{N}} = \underbrace{-4\pi\frac{\lambda_I(\vec{k}'_\pi,\vec{k}_\pi)}{m_\pi^2}\bar{\psi}\gamma^\mu\vec{\tau}\psi\cdot[\vec{\phi}\times\partial_\mu\vec{\phi}]}_{V_{\rho\pi\widetilde{N}}} \underbrace{-4\pi\frac{\lambda_0(\vec{k}'_\pi,\vec{k}_\pi)}{m_\pi}\bar{\psi}\psi[\vec{\phi}\cdot\vec{\phi}]}_{V_{\sigma\pi\widetilde{N}}}, \tag{5.24}$$

which is taken from Ref. [CS00]. The first term denotes the coupling to the isovector nucleonic current and the second is the $\pi\widetilde{N}$ coupling in the isoscalar channel.

Pictorially the additional term in Eq. (5.22) is shown in Fig. 5.4 with the individual σ and ρ contact terms depicted in Fig. 5.5.

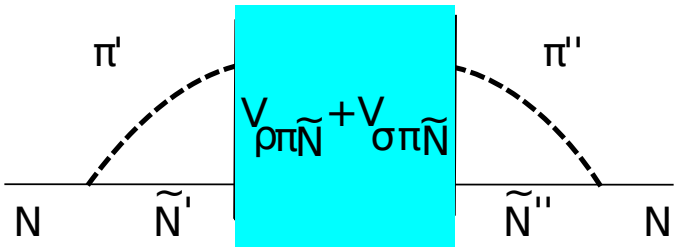

Figure 5.4.: Pictorial representation of the first-order term in the optical potential according to the contact interactions in s- and p-waves.

Figure 5.5.: Pictorial representation of the first-order term in the optical potential according to $\rho\pi\widetilde{N}$ and $\sigma\pi\widetilde{N}$ contact terms

The $\rho\pi\widetilde{N}$ Contact Term

Let us first examine the $\rho\pi\widetilde{N}$ contact-term contribution shown on the l.h.s. of Fig. 5.5:

$$\begin{aligned}&\langle\widetilde{N},\pi:\vec{k}'_{\pi_1}|V_{\rho\pi\widetilde{N}}|\widetilde{N},\pi:\vec{k}_{\pi_2}\rangle\\&=\langle\widetilde{N},\pi:\vec{k}'_{\pi_1}|-4\pi\frac{\lambda_I(\vec{k}'_\pi,\vec{k}_\pi)}{m_\pi^2}\bar{\psi}\gamma^\mu\vec{T}\psi\cdot[\vec{\phi}\times\partial_\mu\vec{\phi}]|\widetilde{N},\pi:\vec{k}_{\pi_2}\rangle.\end{aligned}\tag{5.25}$$

Using the field expansions given in Eqs. (4.22)-(4.25) one ends up with

$$\langle\widetilde{N},\pi:\vec{k}'_{\pi_1}|V_{\rho\pi\widetilde{N}}|\widetilde{N},\pi:\vec{k}_{\pi_2}\rangle=i4\pi\frac{\lambda_I}{m_\pi^2}\bar{u}(k_{\widetilde{N}},\sigma)\gamma^\mu u(k'_{\widetilde{N}},\sigma')k_{\pi_\mu}.\tag{5.26}$$

Isospin Considerations

The isospin part of the $\rho\pi\widetilde{N}$ potential is given by

$$V_{\rho\pi\widetilde{N}}^{isospin}=\vec{T}\cdot[\vec{\phi}\times\dot{\vec{\phi}}]\tag{5.27}$$

with

$$\vec{T}=\begin{pmatrix}\tau_1\\\tau_2\\\tau_3\end{pmatrix},\quad\vec{\phi}=\begin{pmatrix}\pi_1\\\pi_2\\\pi_3\end{pmatrix}\text{ and }\dot{\vec{\phi}}=\begin{pmatrix}\dot{\pi}_1\\\dot{\pi}_2\\\dot{\pi}_3\end{pmatrix}\tag{5.28}$$

given in Cartesian representation. The relation between Cartesian and spherical representations is given in Eq. (4.2.3) and it has to be applied two times such that one ends up with the vector product $[\vec{\phi}\times\vec{\phi}']$ in spherical coordinates [Car71]

$$(\vec{\phi}\times\dot{\vec{\phi}})=\begin{pmatrix}(\vec{\phi}\times\dot{\vec{\phi}})^+\\(\vec{\phi}\times\dot{\vec{\phi}})^-\\(\vec{\phi}\times\dot{\vec{\phi}})^0\end{pmatrix}=i\begin{pmatrix}\pi^0\dot{\pi}^+-\pi^+\dot{\pi}^0\\\pi^-\dot{\pi}^0-\pi^0\dot{\pi}^-\\\pi^-\dot{\pi}^+-\pi^+\dot{\pi}^-\end{pmatrix}.\tag{5.29}$$

After using the definition of the scalar product in spherical representation, the final result for $V_{\rho\pi N}^{isospin}$ reads

$$V_{\rho\pi N}^{isospin}=-\tau^+(\vec{\phi}\times\dot{\vec{\phi}})^--\tau^-(\vec{\phi}\times\dot{\vec{\phi}})^++\tau^0(\vec{\phi}\times\dot{\vec{\phi}})^0.\tag{5.30}$$

As in the previous descussions, we assume a proton to be the incoming and outgoing particle and so the only possible process is given in Fig. 5.6. We have to multiply with 2 since this process can also happen the other way around.

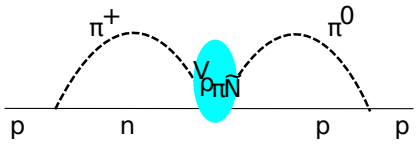

Figure 5.6.: ρ contact term in isospin space.

To calculate the isospin contribution at the $\rho\pi\widetilde{N}$ vertex, the matrix element

$$\langle n|V^{isospin}_{\rho\pi\widetilde{N}}|p\rangle \tag{5.31}$$

has to be considered. Looking at the definitions in Eq. (4.41), the only term surviving in this matrix element is $-\tau^-(\vec{\phi}\times\dot{\vec{\phi}})^+$. Taking a closer look at

$$\langle n|-\tau^-(\vec{\phi}\times\dot{\vec{\phi}})^+|p\rangle = -i\langle n|\tau^-|p\rangle\pi^0\dot{\pi}^+ + i\langle n|\tau^-|p\rangle\pi^+\dot{\pi}^0, \tag{5.32}$$

we observe that only the second part is contributing, since the first one would describe a neutron together with a π^0 and the proton with a π^+, which is not possible. The isospin matrix element $i\langle n|\tau^-|p\rangle\pi^+\dot{\pi}^0$ gives $i\sqrt{2}$ multiplied with $-\sqrt{2}$ coming from the $p\pi^+n$ vertex.

The form factor $\lambda_I(\vec{k}''_\pi,\vec{k}'''_\pi)$ is given as stated in Ref. [CS00] by

$$\lambda_I(\vec{k}''_\pi,\vec{k}'''_\pi) = \frac{m_\rho^2}{m_\rho^2-(k''_\pi-k'''_\pi)^2} \tag{5.33}$$

and the corresponding coupling constant has a value of

$$\frac{\lambda_I}{m_\pi^2} = \frac{f_\rho^2}{8\pi m_\rho^2} = 0.045, \tag{5.34}$$

where the mass of the ρ is

$$m_\rho = 775\ \text{MeV}. \tag{5.35}$$

The $\sigma\pi\widetilde{N}$ Contact Term

The $\sigma\pi\widetilde{N}$ contact term contribution shown on the r.h.s. of Fig. 5.5 is expressed as

$$\begin{aligned}&\langle\widetilde{N},\pi:\vec{k}'_\pi|V_{\sigma\pi\widetilde{N}}|\widetilde{N},\pi:\vec{k}_\pi\rangle\\ &=\langle\widetilde{N},\pi:\vec{k}'_\pi|-4\pi\frac{\lambda_0}{m_\pi}\bar{\psi}\psi[\vec{\phi}\cdot\vec{\phi}]|\widetilde{N},\pi:\vec{k}_\pi\rangle.\end{aligned} \tag{5.36}$$

First the scalar product of the π field expansion, Eq. (4.22), will be treated separately

$$\vec{\phi}(0)\cdot\vec{\phi}(0) = \sum_\lambda(-)^\lambda\phi(0)^\lambda\phi(0)^{-\lambda}, \tag{5.37}$$

λ denoting the three possible isospinstates of the π. Multiplying creation and annihilation operators

$$\int \frac{d^3k}{(2\pi)^3 2\omega_k} \int \frac{d^3k'}{(2\pi)^3 \omega'_k} \sum_\lambda (-)^\lambda \left[c^{-\lambda}(\vec{k}') + c^{\lambda\dagger}(\vec{k}')\right]\left[c^{\lambda}(\vec{k}) + c^{-\lambda\dagger}(\vec{k})\right] \tag{5.38}$$

one ends up with one surviving term

$$\int \frac{d^3k}{(2\pi)^3 2\omega_k} \int \frac{d^3k'}{(2\pi)^3 \omega'_k} \sum_\lambda (-)^\lambda c^{\lambda\dagger}(\vec{k}') c^{\lambda}(\vec{k}). \tag{5.39}$$

By inserting the nucleon field expansions, Eqs. (4.24) and (4.25) by only considering the particle terms, Eq. (5.36) becomes

$$\begin{aligned}
&\langle \widetilde{N}, \pi : \vec{k}'_\pi | V_{\sigma\pi\widetilde{N}} | \widetilde{N}, \pi : \vec{k}_\pi \rangle = -4\pi \frac{\lambda_0}{m_\pi} \langle 0 | a(\vec{k}'_{\widetilde{N}}, \sigma') c^\alpha(\vec{k}'_\pi) : \\
&\int \frac{d^3p'}{(2\pi)^3 3\omega'_p} \sum_{s'=\pm\frac{1}{2}} \bar{u}(p', s') a^\dagger(\vec{p}', s') \int \frac{d^3p}{(2\pi)^3} \sum_{s=\pm\frac{1}{2}} u(p, s) a(\vec{p}, s) \\
&\int \frac{d^3k}{(2\pi)^3 2\omega_k} \int \frac{d^3k'}{(2\pi)^3 \omega'_k} \sum_\lambda (-)^\lambda c^{\lambda\dagger}(\vec{k}') c^{\lambda}(\vec{k}) \\
&: a^\dagger(\vec{k}_{\widetilde{N}}, \sigma) c^{\dagger\beta}(\vec{k}_\pi) | 0 \rangle
\end{aligned} \tag{5.40}$$

and for the final result we obtain

$$-4\pi \frac{\lambda_0(k'_\pi, k_\pi)}{m_\pi} \bar{u}(k'_{\widetilde{N}}, \sigma') u(k_{\widetilde{N}}, \sigma) \delta^{\alpha\beta}. \tag{5.41}$$

The $\delta^{\alpha\beta}$ tells us that the isospin component of the π outgoing and incoming is the same although the momenta may be different. So two different processes have to be taken into account, these are shown in Fig. 5.7. In the end we obtain an overall isospin factor

Figure 5.7.: σ contact term in isospin space.

of 3.

The function $\lambda_0(k'_\pi, k_\pi)$ is given by

$$\lambda_0(k'_\pi, k_\pi) = -\frac{1}{2}(1+\epsilon) m_\pi \left(a_{SR} + a_\sigma \frac{m_\sigma^2}{m_\sigma^2 - (k'_\pi - k_\pi)^2} \right) \tag{5.42}$$

with

- m_σ=550 MeV,
- a_σ=0.22 m_π^{-1},
- a_{SR}=-0.233 m_π^{-1},
- $\epsilon = \frac{m_\pi}{m_{\widetilde{N}}}$.

The input parameters are again the ones proposed in Ref. [CS00].

5.2.2. Solution and Results

Kinematics and Solution Method

It is assumed that the incoming and outgoing N is at rest, so its four-momentum is given as

$$k_{\widetilde{N}} = \begin{pmatrix} m_{\widetilde{N}} \\ 0 \\ 0 \\ 0 \end{pmatrix}. \tag{5.43}$$

In the region where there is a N and a π, due to momentum conservation, we have

$$k'_\pi = \begin{pmatrix} \omega'_\pi \\ k'_\pi \sin\theta' \cos\phi' \\ k'_\pi \sin\theta' \sin\phi' \\ k'_\pi \cos\theta' \end{pmatrix}, \qquad k'_{\widetilde{N}} = \begin{pmatrix} \omega'_{\widetilde{N}} \\ -k'_\pi \sin\theta' \cos\phi' \\ -k'_\pi \sin\theta' \sin\phi' \\ -k'_\pi \cos\theta' \end{pmatrix} \tag{5.44}$$

and

$$k''_\pi = \begin{pmatrix} \omega''_\pi \\ k''_\pi \sin\theta'' \cos\phi'' \\ k''_\pi \sin\theta'' \sin\phi'' \\ k''_\pi \cos\theta'' \end{pmatrix}, \qquad k''_{\widetilde{N}} = \begin{pmatrix} \omega''_{\widetilde{N}} \\ -k''_\pi \sin\theta'' \cos\phi'' \\ -k''_\pi \sin\theta'' \sin\phi'' \\ -k''_\pi \cos\theta'' \end{pmatrix}. \tag{5.45}$$

These are all definitions of energies and momenta that are needed while, detailed information how to treat the products of spinors appearing in Eqs. (5.14) and (5.15) can be found in App. A.2.

In analogy to Sec. 4.3 various input form factors have been used to solve the nonlinear eigenvalue Eq. (5.22) together with the input Eq. (5.26) for the ρ and Eq. (5.41) for the σ. The used $\pi\widetilde{N}\widetilde{N}$ vertex form factors are shown in Fig. 4.3 and the associated parameters are given in Tab. 4.1. We emphasize that thereby the model is completely fixed with regard to the vertex form factors, the coupling constants and the πN interaction employed.

Results

With the $V_{\pi N}$ interaction as specified above we find again only a minor contribution to the mass of the dressed N, according to two-π contact forces. At most an effect of a few MeV, e. g. , ∼1 MeV in case of the RCQM is obtained.

5.3. Summary

In this chapter we have investigated the contributions of different variants of an additional $\pi\pi N$ channel on top of coupling the bare N to the πN channel. We found that both crossed-term as well as contact-term two-π contributions produce only small effects in the mass of the dressed N. In practice both of them are negligible in the CC approach followed here. Of course, one could alter some input parameters, such as vertex form factors, coupling constants or specifically the πN potential. However, here we content ourselves with the insight gained so far into the π dressing effects on the N mass. Later on in Part. IV we shall anyway focus on a microscopic description of the vertex form factors and dressed masses of the N and Δ, where both of these properties can be dealt with consistently.

6. The Δ Coupled to the πN Channel

6.1. Eigenvalue Equation

In this section, the CC framework is used to describe the one-π effects in the Δ and also the $\Delta \to \pi N$ decay. To this aim we start with the following CC eigenvalue equation

$$\begin{pmatrix} M_{\widetilde{\Delta}} & K \\ K^\dagger & M_{\widetilde{N}+\pi} \end{pmatrix} \begin{pmatrix} |\psi_\Delta\rangle \\ |\psi_{N+\pi}\rangle \end{pmatrix} = m \begin{pmatrix} |\psi_\Delta\rangle \\ |\psi_{N+\pi}\rangle \end{pmatrix}, \tag{6.1}$$

where $M_{\widetilde{\Delta}}$ is representing the mass operator of the bare $\widetilde{\Delta}$ and $M_{\widetilde{N}+\pi}$ the mass operator of the interaction-free $\pi\widetilde{N}$ system, as already considered in Sec. 4.1, Eq. (4.8). m is the Δ mass eigenvalue we are interested in.

In order to go on, we first consider the eigenstates of $M_{\widetilde{\Delta}}$ and their completeness and orthonormality relations:

$$M_{\widetilde{\Delta}}|\widetilde{\Delta}:v\rangle = m_{\widetilde{\Delta}}|\widetilde{\Delta}:v\rangle, \tag{6.2}$$

$$\langle\widetilde{\Delta}:v'|\widetilde{\Delta}:v\rangle = (2\pi)^3 v_0 \delta^3(\vec{v}'-\vec{v})\frac{2}{m^2_{\widetilde{\Delta}}}, \tag{6.3}$$

$$\mathbb{1}_{\widetilde{\Delta}} = \int \frac{d^3v}{(2\pi)^3 v_0}\frac{m^2_{\widetilde{\Delta}}}{2}|\widetilde{\Delta}:v\rangle\langle\widetilde{\Delta}:v|. \tag{6.4}$$

The calculation is done along the same lines as in Ch. 4. Finally one obtains a similar eigenvalue equation as in Eq. (4.14), namely:

$$m_{\widetilde{\Delta}}\langle\widetilde{\Delta}:v|\psi_\Delta\rangle + \langle\widetilde{\Delta}:v|K\left(m-M_{\widetilde{N}+\pi}\right)^{-1}\mathbb{1}''_{\widetilde{N}+\pi}K^\dagger\mathbb{1}'_{\widetilde{\Delta}}|\psi_\Delta\rangle = m\langle\widetilde{\Delta}:v|\psi_\Delta\rangle \tag{6.5}$$

$$\begin{aligned}
&\Rightarrow m_{\widetilde{\Delta}}\langle\widetilde{\Delta}:v\mid\psi_\Delta\rangle + \int\frac{d^3v'}{(2\pi)^3 v'_0}\int\frac{d^3v''}{(2\pi)^3 v''_0}\int\frac{d^3k''_\pi}{(2\pi)^3 2\omega''_\pi}\frac{\left(\omega''_\pi+\omega''_{\widetilde{N}}\right)^3}{2\omega''_{\widetilde{N}}}\frac{m'^2_{\widetilde{\Delta}}}{2} \\
&\times\langle\widetilde{\Delta}:v\mid K\mid\widetilde{N},\pi:v'',\vec{k}''_\pi\rangle\frac{1}{m-\omega''_{\widetilde{N}}-\omega''_\pi}\langle\widetilde{N},\pi:v'',\vec{k}''_\pi\mid K^\dagger\mid\widetilde{\Delta}:v'\rangle\langle\widetilde{\Delta}:v'\mid\psi_N\rangle \\
&= m\langle\widetilde{\Delta}:v\mid\psi_\Delta\rangle.
\end{aligned} \tag{6.6}$$

Again the eigenvalue m is appearing on the l.h.s. and on the r.h.s. of the equation, and it will now adopt complex values, if the eigenvalue becomes larger than the threshold mass $m_{\widetilde{N}}+m_\pi$. The real part is describing the resonance position and two times the imaginary part gives the Δ decay width.

In short, Eq. (6.5) reads

$$m_{\widetilde{\Delta}}\langle\widetilde{\Delta}:v\mid\psi_\Delta\rangle+\int\frac{d^3v'}{(2\pi)^3\,v_0'}\langle\widetilde{\Delta}:v\mid V_{opt}(m)\mid\widetilde{\Delta}:v'\rangle\langle\widetilde{\Delta}:v'\mid\psi_\Delta\rangle=m\langle\widetilde{\Delta}:v\mid\psi_\Delta\rangle \tag{6.7}$$

where the matrix element of the so-called optical potential $V_{opt}(m)$ is given as

$$\begin{aligned}\langle\widetilde{\Delta}:v\mid V_{opt}(m)\mid\widetilde{\Delta}:v'\rangle=&\int\frac{d^3v''}{(2\pi)^3\,v_0''}\int\frac{d^3k_\pi''}{(2\pi)^3\,2\omega_\pi''}\frac{\left(\omega_\pi''+\omega_{\widetilde{N}}''\right)^3}{2\omega_{\widetilde{N}}''}\frac{m_{\widetilde{\Delta}}^{'2}}{2}\\&\times\langle\widetilde{\Delta}:v\mid K\mid\widetilde{N},\pi:v'',\vec{k}_\pi''\rangle\frac{1}{m-\omega_{\widetilde{N}}''-\omega_\pi''}\langle\widetilde{N},\pi:v'',\vec{k}_\pi''\mid K^\dagger\mid\widetilde{\Delta}:v'\rangle.\end{aligned} \tag{6.8}$$

It is diagrammatically represented in Fig.6.1.

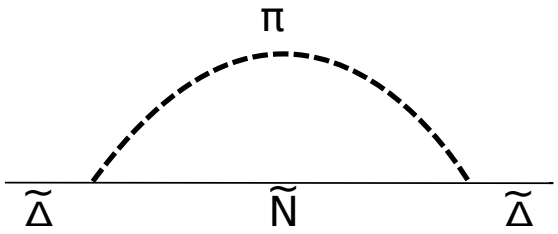

Figure 6.1.: Pictorial representation of the first-order term of the optical potential according to Eq. (6.8).

6.2. Vertex Matrix Elements

We now evaluate the two vertex matrix elements

$$\langle\widetilde{\Delta}:v|K|\widetilde{N},\pi:v',\vec{k}_\pi'\rangle,\quad\langle\widetilde{N},\pi:v',\vec{k}_\pi'|K^\dagger|\widetilde{\Delta}:v\rangle. \tag{6.9}$$

They are obtained by following the same procedure as in Sec. 4.2.

In using Eq. (3.7), the matrix elements containing the Lagrangian densities have to be considered. The latter is taken as suggested in Ref. [BD64]

$$\mathcal{L}_{\pi\widetilde{N}\widetilde{\Delta}}(x)=-\frac{f_{\pi\widetilde{N}\widetilde{\Delta}}}{m_\pi}\bar{\psi}(x)\vec{T}\psi^\mu(x)\cdot\partial_\mu\vec{\phi}(x)+h.c., \tag{6.10}$$

where $\vec{\phi}(x)$ is the π field operator given in Eq. (4.22) and $\psi(x)$ is the Dirac field operator for the spin-$\frac{1}{2}$ $\widetilde{N}$ given in Eq. (4.24). $\psi^\mu(x)$ is the Rarita-Schwinger field operator for the spin-$\frac{3}{2}$ $\widetilde{\Delta}$. Details about the $\widetilde{\Delta}$ Rarita-Schwinger spinors and the $\widetilde{N}$ Dirac spinors can be found in App. A.2.

The final results are

$$\langle\widetilde{\Delta}|\mathcal{L}_{\pi\widetilde{N}\widetilde{\Delta}}(0)|\widetilde{N},\pi:\vec{k}_\pi\rangle = -i\sum\frac{f_{\pi\widetilde{N}\widetilde{\Delta}}}{m_\pi}\bar{u}^\mu(k_{\widetilde{\Delta}},\sigma_{\widetilde{\Delta}})I\left(\tau_{\widetilde{\Delta}},\tau'_{\widetilde{N}},\tau_\pi\right)u(k'_{\widetilde{N}},\sigma'_{\widetilde{N}})(k_\pi)_\mu,$$

$$\langle\widetilde{N},\pi:\vec{k}_\pi|\mathcal{L}^\dagger_{\pi\widetilde{N}\widetilde{\Delta}}(0)|\widetilde{\Delta}\rangle = i\sum\frac{f_{\pi\widetilde{N}\widetilde{\Delta}}}{m_\pi}\bar{u}'(k_{\widetilde{N}},\sigma'_{\widetilde{N}})I\left(\tau'_{\widetilde{N}},\tau_{\widetilde{\Delta}},\tau_\pi\right)u^\mu(k_{\widetilde{\Delta}},\sigma_{\widetilde{\Delta}})(k_\pi)_\mu. \quad (6.11)$$

However, the Lagrangian given in Eq. (6.10) is not the only possibility to describe the $\pi\widetilde{N}\widetilde{\Delta}$ coupling at the vertex. Additionally we checked the Lagrangian density proposed by Pascalutsa and Tjon in Ref. [PT00]

$$\mathcal{L}^{GI}_{\pi\widetilde{N}\widetilde{\Delta}}(x) = \frac{f_{\pi\widetilde{N}\widetilde{\Delta}}}{m_\pi m_{\widetilde{\Delta}}}\epsilon^{\mu\nu\alpha\beta}\left(\partial_\mu\bar{\psi}_\nu(x)\right)\gamma_5\gamma_\alpha T_a\psi(x)\partial_\beta\phi^a(x) + h.c., \quad (6.12)$$

where the (GI) refers to a gauge-invariant $\pi\widetilde{N}\widetilde{\Delta}$ coupling. It is invariant under the Rarita-Schwinger gauge transformation:

$$\psi_\mu(x) \to \psi_\mu(x) + \partial_\mu\epsilon(x) \quad (6.13)$$

with $\epsilon(x)$ being a spinor field. The advantage of this coupling is that the spin-$\frac{1}{2}$ components of the Δ field do not appear, thus the spin-$\frac{1}{2}$ background is totally absent from the corresponding Δ-exchange amplitudes.

The calculation has been repeated in using the gauge invariant Lagrangian density and although the analytical structure is different, the final numerical result is the same.

6.2.1. Spin and Isospin Considerations

As in Sec. 4.2, we have to fix the incoming and outgoing particle properties and sum over all intermediate possibilities. In the process actually under investigation we have four different possibilities for the spin projection of the incoming $\widetilde{\Delta}$. The result must be the same for all of them and must not depend on a particular choice.

Considering the isospin degrees of freedom it can easily be verified that the isospin contribution is the same for either the Δ^{++}, Δ^+, Δ^0 or the Δ^- to be the incoming and outgoing particle. All the different possibilities are shown in Fig. 6.2 and each choice gives an isospin factor of 1.

6.3. Solution of the Eigenvalue Equation

We now turn to the solution of the eigenvalue Eq. (6.7) with the optical potential written in Eq. (6.8) and pictorially shown in Fig.6.1.

Again, it is assumed that the incoming particle, the $\widetilde{\Delta}$ is at rest and so its four-momentum is given as

$$k_{\widetilde{\Delta}} = \begin{pmatrix} m_{\widetilde{\Delta}} \\ 0 \\ 0 \\ 0 \end{pmatrix}. \quad (6.14)$$

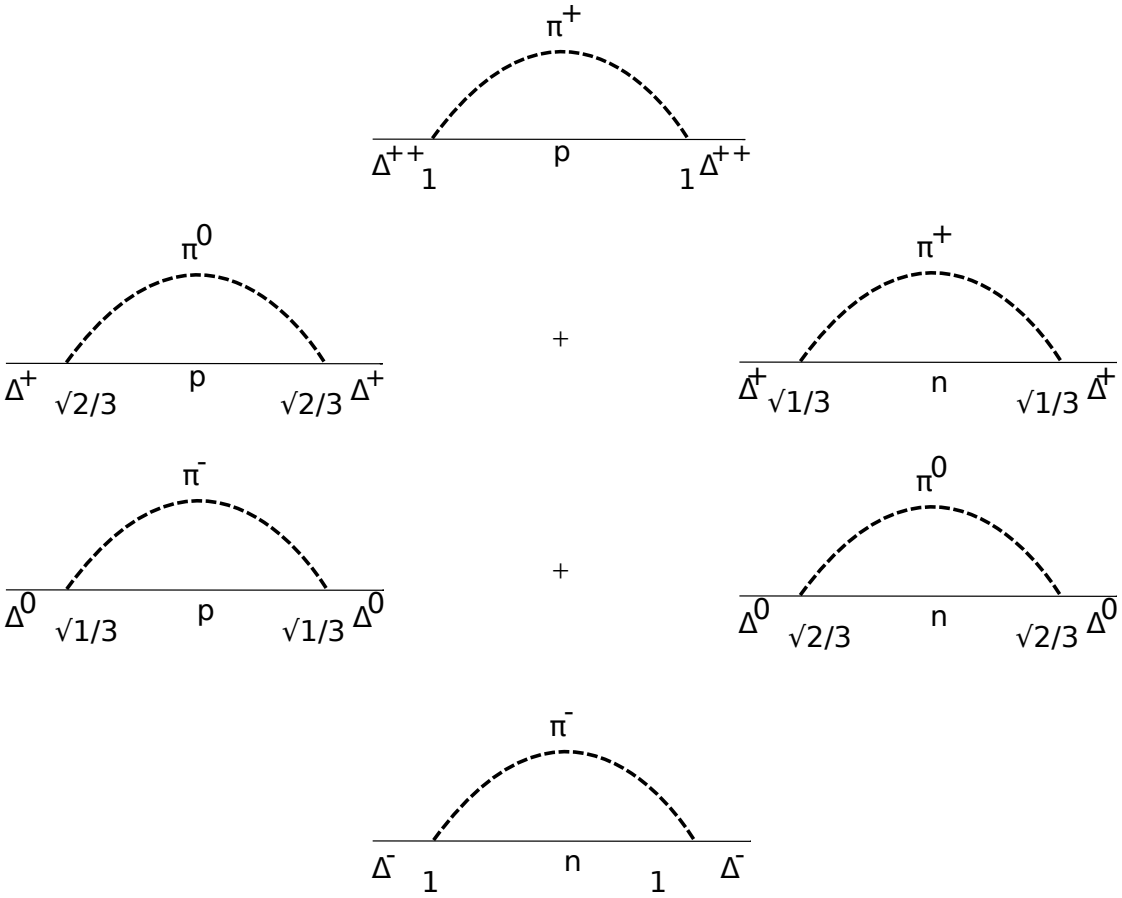

Figure 6.2.: Different possibilities of incoming and outgoing $\widetilde{\Delta}$ states in isospin space.

In the intermediate region where there is a $\widetilde{N}$ and a π, due to momentum conservation, we have

$$k'_\pi = \begin{pmatrix} \omega'_\pi \\ k'_\pi \sin\theta' \cos\phi' \\ k'_\pi \sin\theta' \sin\phi' \\ k'_\pi \cos\theta' \end{pmatrix} \qquad \text{and} \qquad k'_{\widetilde{N}} = \begin{pmatrix} \omega'_{\widetilde{N}} \\ -k'_\pi \sin\theta' \cos\phi' \\ -k'_\pi \sin\theta' \sin\phi' \\ -k'_\pi \cos\theta' \end{pmatrix}. \tag{6.15}$$

6.3.1. Input Vertex Form Factors

As stated before, in solving Eq. (6.7), eventually we obtain a complex eigenvalue. Taking a closer look at the propagator in Eq. (6.8) we notice that the integrand has a pole for some $\vec{k}''_\pi > 0$, namely, if m becomes larger than the $\pi\widetilde{N}$ threshold $m_{\widetilde{N}} + m_\pi$. As in the preceding chapter, the eigenvalue equation will be solved via iteration, only now we start with an arbitrary complex eigenvalue in the optical potential Eq. (6.8).

To account for the extended structure at the $\pi\widetilde{N}\widetilde{\Delta}$ vertices, again form factors from different models are employed, namely from Refs. [MCP09], [PR05b], and [KNLS13] which come with the following parametrizations:

$$\mathcal{F}_{\pi\widetilde{N}\widetilde{\Delta}}\left(\vec{k}_\pi^2\right) = \frac{1}{1+\left(\frac{\vec{k}_\pi}{\Lambda_1}\right)^2+\left(\frac{\vec{k}_\pi}{\Lambda_2}\right)^4} \qquad \text{(RCQM, SL and PR Multipole)}, \tag{6.16}$$

$$\mathcal{F}_{\pi\widetilde{N}\widetilde{\Delta}}\left(\vec{k}_\pi^2\right) = \left(\frac{\Lambda^2}{\vec{k}_\pi^2+\Lambda^2}\right)^2 \qquad \text{(KNLS)}, \tag{6.17}$$

and

$$\mathcal{F}_{\pi\widetilde{N}\widetilde{\Delta}}\left(\vec{k}_\pi^2\right) = \exp^{-\vec{k}_\pi^2/\Lambda^2} \qquad \text{(PR Gauss)}. \tag{6.18}$$

The different form factors are shown in Fig. 6.3 and the associated parameters occurring in the form-factor parametrizations are given in Tab. 6.1 together with the $\pi\widetilde{N}\widetilde{\Delta}$ coupling constants.

	RCQM	SL	KNLS	PR Gauss	PR Multipole
$\frac{f^2_{\pi\widetilde{N}\widetilde{\Delta}}}{4\pi}$	0.188	0.334	0.126	0.167	0.167
λ_1	0.594	0.458			0.853
λ_2	0.998	0.648			1.014
Λ			0.709	0.603	

Table 6.1.: Coupling constants and parameters for the $\pi\widetilde{N}\widetilde{\Delta}$ vertex form factors.

6.4. Results and Discussion

We now give the results for the one-π loop effects on the Δ mass from our CC theory using the $\pi\widetilde{N}\widetilde{\Delta}$ vertex form factor models discussed above.

In Tab. 6.2 we have collected the results for the π dressing of the $\widetilde{\Delta}$ by coupling to an explicit $\pi\widetilde{N}$ channel. The effects on the real part of the Δ mass scatter between 27 MeV and 103 MeV, depending on the model employed for the $\pi\widetilde{N}\widetilde{\Delta}$ vertex. The smallest value is obtained in case of the KNLS form factor, whose dependence on $\vec{k}_\pi^2$ is similar to the one of SL (see Fig. 6.3), but it comes with a much weaker $\pi\widetilde{N}\widetilde{\Delta}$ coupling constant (see Tab. 6.2). Although SL and KNLS start out with the same model, the latter one is more advanced in the sense that more channels were taken into account and so the coupling constant was reduced to less than half of its original value. $\frac{f^2_{\pi\widetilde{N}\widetilde{\Delta}}}{4\pi}$ given by KNLS compares well with the couplings given by the other models but the effect on the mass is in comparison to the others much smaller due to the different $\vec{k}_\pi^2$ dependence of the form factor. The two parametrizations of the PR model reveal the largest effects

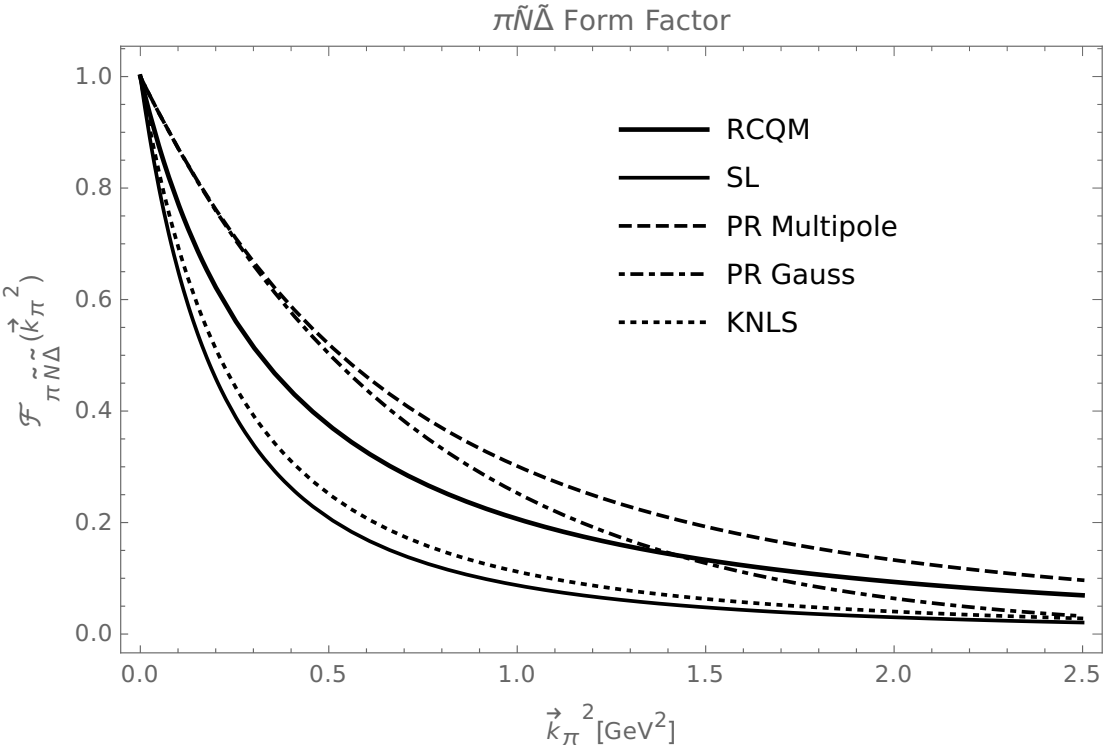

Figure 6.3.: $\pi\widetilde{N}\widetilde{\Delta}$ form factor parametrizations as functions of the three-momentum squared from various models in the literature.

	RCQM	SL	KNLS	PR Gauss	PR Multipole
$m_{\widetilde{N}}$	1067	1031	1037	1025	1051
$Re[m_\Delta]$	1232	1232	1232	1232	1232
$m_{\widetilde{\Delta}}$	1300	1290	1259	1321	1335
$Re[m_\Delta] - m_{\widetilde{\Delta}}$	-68	-58	-27	-89	-103
$2\,Im[m_\Delta] = \Gamma$	4	23	7	16	8
$\Gamma_{exp}(\Delta \to \pi N)$			~ 117		

Table 6.2.: π loop effects on the Δ mass m_Δ from coupling to the πN channel. $m_{\widetilde{\Delta}}$ and $m_{\widetilde{N}}$ are the bare $\widetilde{\Delta}$ and $\widetilde{N}$ masses, respectively. The latter is the same as in the π dressing of the $\widetilde{N}$ in Ch. 4, cf. Tab. 4.2. All values given in MeV. The π mass is assumed to be $m_\pi = 139$ MeV.

on the real part of the Δ mass. The coupling is similar as in the other models but the

PR form factors differ among each other and in comparison to the others.

With regard to the Δ, the most interesting result concerns the resonance decay widths Γ given in Tab. 6.2. As mentioned before, in solving the eigenvalue Eq. (6.7) for a resonance above the decay threshold the mass eigenvalue m becomes complex. Two times the imaginary part of the complex mass eigenvalue m yields the resonance decay width, $\Gamma = 2\,\mathrm{Im}\,m$. The different values for Γ vary between 4 MeV and 23 MeV. They are much smaller than the experimentally measured value of $\Gamma_{exp}(\Delta \to \pi N) \sim 117$ MeV. In the CC approach the magnitude of the obtained resonance decay width depends on the coupling strength to the decay channel and of course on the phase space. In calculating the Γ values given in Tab. 6.2 we used as input the bare $\widetilde{N}$ masses calculated in Ch. 4 and presented in Tab. 4.2 and again quoted in Tab. 6.2. The values $m_{\widetilde{N}} + m_\pi$ now determine the thresholds, which vary between 1206 MeV for the RCQM and 1164 MeV for the PR Gauss parametrization. The RCQM threshold is thus very close to the physical Δ mass $m_\Delta = 1232$ MeV and so the decay width results in $\Gamma = 4$ MeV because of the small phase space. Due to the comparatively large phase space in the PR Gauss model, Γ assumes a value four times larger than the RCQM. The SL model comes along with a similar threshold as the PR Gauss parametrization but its coupling to the decay channel appears to be larger which obviously leads to a bigger decay width of $\Gamma = 23$ MeV.

Improvement

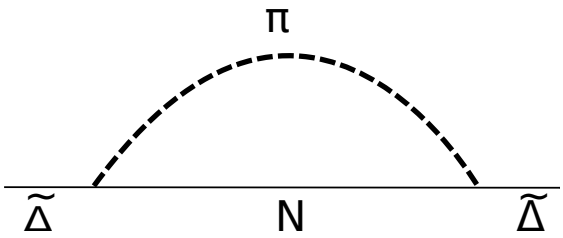

Figure 6.4.: Pictorial representation of the first-order term of the optical potential with assuming a physical N in the intermediate state.

As already mentioned above, within the CC approach the resulting decay widths are depending essentially on two ingredients: the strength of the coupling to the decay channel (due to the vertex form factors and corresponding coupling constants) and the size of the phase space allowed by the decay threshold. For the results given in Tab. 6.2 the Δ decay goes to a bare N and a π. Consequently the decay threshold lies too high and there is no chance to produce a realistic decay width. We may now assume a physical N of $m_N = 939$ MeV as a decay product. This situation then corresponds to an optical potential as shown in Fig. 6.4. In this case we obtain the results quoted in Tab. 6.3. We observe that the effects of the coupling to the πN channel on the real part of the Δ mass vary between 29 MeV and 114 MeV. This is not so much different from the values given in Tab. 6.2. Since the decay threshold $m_N + m_\pi$ is now much lower in all cases, namely 1078 MeV, the resulting resonance decay widths are considerably

	RCQM	SL	KNLS	PR Gauss	PR Multipole
m_N	939	939	939	939	939
$Re[m_\Delta]$	1232	1232	1232	1232	1232
$m_{\widetilde{\Delta}}$	1309	1288	1261	1328	1347
$Re[m_\Delta] - m_{\widetilde{\Delta}}$	-77	-56	-29	-96	-114
$2\,Im[m_\Delta] = \Gamma$	47	64	27	51	52
$\Gamma_{exp}(\Delta \to \pi N)$			~ 117		

Table 6.3.: One-loop effects on the Δ mass m from coupling to the πN channel, where now a physical N is assumed in the intermediate state, according to Fig. 6.4. All values are given in MeV. The π mass is assumed to be $m_\pi = 139$ MeV.

larger and vary between 27 MeV and 63 MeV. At least in the SL model, due to the large coupling constant and the enlarged phase space half of the experimentally measured resonance decay width has already been obtained.

Summary

In this chapter we have treated the Δ resonance in our relativistic CC approach foreseeing a coupling to a πN channel. In this way we have produced the dressing effect by one-π loops on the Δ resonance energy and the strong Δ decay width. We have considered two variants of this type of calculation, where the decay products are either a $\pi\widetilde{N}$ or a πN. The dressing effects on the real part of the Δ mass are not much affected by the position of the decay threshold, they turn out to range between 27 MeV and 114 MeV depending on the vertex form factor model employed. However, the sizes of the decay widths are much enhanced in case of the lower threshold dictated by the πN exit channel. Still the experimental value of $\Gamma \sim 117$ MeV is not reached. This may appear surprising as the Δ width is to more than 99% governed by the πN decay. Obviously the approach followed so far is either deficient and/or requires further ingredients. In the following we shall first consider additional pionic contributions.

7. The Δ with Additional Pionic Contributions

As stated above, the particular version of the CC approach considered in the previous chapter is only the simplest way of including explicit π degrees of freedom into the $\pi N\Delta$ system. Here we investigate the possible role of further π effects.

7.1. Additional $\pi\pi\widetilde{N}$ Channel

In analogy to Sec 5.1, we are interested, if an additional interaction-free $\pi\pi\widetilde{N}$ channel will help to improve the results obtained in the previous chapter. Therefore we assume a CC mass operator eigenvalue equation of the form:

$$\begin{pmatrix} M_{\widetilde{\Delta}} & K & 0 \\ K^\dagger & M_{\widetilde{N}+\pi} & K \\ 0 & K^\dagger & M_{\widetilde{N}+\pi+\pi} \end{pmatrix} \begin{pmatrix} |\psi_\Delta\rangle \\ |\psi_{N+\pi}\rangle \\ |\psi_{N+\pi+\pi}\rangle \end{pmatrix} = m \begin{pmatrix} |\psi_\Delta\rangle \\ |\psi_{N+\pi}\rangle \\ |\psi_{N+\pi+\pi}\rangle \end{pmatrix}. \tag{7.1}$$

It results in an equation analogous to Eq. (5.8) with only the incoming and outgoing $\widetilde{N}$ replaced by $\widetilde{\Delta}$:

$$\Big[M_{\widetilde{\Delta}} + K(m - M_{\widetilde{N}+\pi})^{-1} K^\dagger + \underbrace{K(m - M_{\widetilde{N}+\pi})^{-1} K (m - M_{\widetilde{N}+\pi+\pi})^{-1} K^\dagger (m - M_{\widetilde{N}+\pi})^{-1} K^\dagger}_{} \Big] |\psi_\Delta\rangle = m|\psi_\Delta\rangle. \tag{7.2}$$

The optical-potential term marked by the brace is pictorially shown in first order in Fig. 7.1. To solve Eq. (7.2) we proceed in the same iterative way as explained in Sec. 5.1.

7.1.1. Solution and Results

Kinematics

For the kinematics, beyond what is already specified in Ch. 5, Eq. (5.17)-(5.19), we need in addition the four-momentum of the bare incoming and outgoing Δ as rest:

$$k_{\widetilde{\Delta}} = \begin{pmatrix} m_{\widetilde{\Delta}} \\ 0 \\ 0 \\ 0 \end{pmatrix}. \tag{7.3}$$

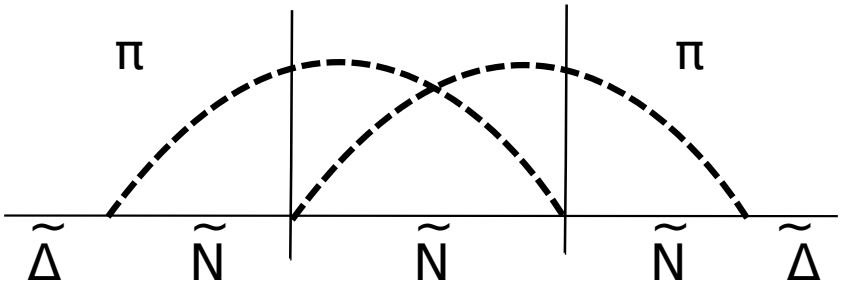

Figure 7.1.: Pictorial representation of the first-order term in the optical potential of two-π loop contributions according to Eq. (7.2)

The occurring vertex form factors and coupling constants are used as specified in the previous chapters 4 and 6.

For the additional $\pi\pi\widetilde{N}$ channel now included, we arrive at the Δ results given in Tab. 7.1. It is immediately seen that the crossed-term two-π loops do not alter much neither the dressed Δ mass nor the decay width shown in Tab. 6.2. In practice the corresponding effects are negligible. This result parallels the one for the N case obtained in Ch. 5.

	RCQM	SL	KNLS	PR Gauss	PR Multipole
$m_{\widetilde{N}}$	1067	1031	1037	1025	1051
$Re[m_\Delta]$	1232	1232	1232	1232	1232
$m_{\widetilde{\Delta}}$	1302	1291	1260	1323	1337
$Re[m_\Delta] - m_{\widetilde{\Delta}}$	-70	-59	-28	-91	-105
$2\,Im[m_\Delta] = \Gamma$	5	26	8	17	8
$\Gamma_{exp}(\Delta \to \pi N)$			~ 117		

Table 7.1.: Effects on the Δ mass m from taking an additional $\pi\pi\widetilde{N}$ channel into account. The assumed masses for the bare $\widetilde{N}$ in the intermediate state are the same as in Tab. 4.2 and Tab. 6.2. All values are given in MeV. The π mass is assumed to be $m_\pi = 139$ MeV.

7.2. Summary

In this chapter we have investigated dressing of the Δ resonance in its most obvious manner, namely, by coupling to the πN as well as $\pi\pi N$ channels. Considering the fact

that the Δ decays almost exclusively (with a probability of $> 99\%$) into πN already coupling to a πN channel should have turned out as sufficient. This expectation is obviously not met with a theory on the macroscopic level, if one employs form factor inputs as existing in the literature.

In the next part we shall therefore develop a CC approach on the microscopic quark level. It will allow us to produce the vertex form factors as well as the dressing effects on the N and Δ masses in a consistent manner.

Part IV.

Coupled-Channels Theory on the Quark Level

8. {QQQ} System Coupled to π Channels

In the previous chapters we have considered π dressing of the N and Δ, where we have used $\pi\widetilde{N}N$ and $\pi\widetilde{N}\Delta$ vertex form factors from models in the literature. In particular we calculated the effects due to π loop diagrams of the types shown in Figs. 4.2, 5.1, 5.5, 6.1 and 6.4.

In this part of the thesis we put the same kind of investigation on the quark level. Thereby we shall construct a relativistic constituent-quark model with explicit coupling to one-π channels. It will allow us to develop in a consistent manner both the vertex form factors, including coupling constants, and the dressing effects on masses of ground and excited states, here in particular of the N and the Δ. There will be no longer a need to resort to form factor models foreign to our π dressing procedures.

8.1. Microscopic Mass Eigenvalue Equation

In order to study explicit π degrees of freedom in a microscopic model we consider an eigenvalue equation coupling a bare cluster of three confined quarks to a channel with an additional π:

$$\begin{pmatrix} M_{\widetilde{cl}} & K \\ K^\dagger & M_{\widetilde{cl}+\pi} \end{pmatrix} \begin{pmatrix} |\psi_{cl}\rangle \\ |\psi_{cl+\pi}\rangle \end{pmatrix} = m \begin{pmatrix} |\psi_{cl}\rangle \\ |\psi_{cl+\pi}\rangle \end{pmatrix}. \tag{8.1}$$

Here $M_{\widetilde{cl}}$ is the mass operator of the bare three-quark cluster, whereas $M_{\widetilde{cl}+\pi}$ is the mass operator of the channel with the bare cluster plus one π without (final-state) π interaction. K and $K^\dagger$ are the operators that account for the πQQ coupling; they will be identified with a proper Lagrangian density. Both $|\psi_{cl}\rangle$ and $|\psi_{cl+\pi}\rangle$ contain effects from the π coupling.

Here we emphasize that in our model the π couples directly to the constituent quarks, as it is considered as the Goldstone boson resulting from the spontaneous breaking of chiral symmetry in low-energy QCD, like the constituent quarks acquire their dynamical mass. This is completely in line with so-called chiral models in the literature and in particular with the GBE RCQM. The πQQ vertex is considered as pointlike.

After a Feshbach reduction eliminating the $(\widetilde{cl}+\pi)$-channel we end up with the eigenvalue equation

$$M_{\widetilde{cl}}|\psi_{cl}\rangle + K(m - M_{\widetilde{cl}+\pi})^{-1}K^\dagger|\psi_{cl}\rangle = m|\psi_{cl}\rangle \tag{8.2}$$

for the π-dressed QQQ cluster.

Mass Operators and Eigenstates

For the practical solution of Eq. (8.2), we need eigenstates of the bare-cluster mass operator $M_{\widetilde{cl}}$ as well as $M_{\widetilde{cl}+\pi}$. The former is defined as the sum of the mass operators of three free quarks and a confinement potential

$$M_{\widetilde{cl}} = M_{QQQ} + V_{conf}, \tag{8.3}$$

where V_{conf} will be of harmonic oscillator (h.o.) type; it is specified in detail in Sec. 8.2.1 below. Eigenstates and eigenvalues corresponding to $M_{\widetilde{cl}}$ are defined as

$$M_{\widetilde{cl}}|v; nJ\Sigma\rangle = m_{\widetilde{cl}}|v; nJ\Sigma\rangle \tag{8.4}$$

with n denoting the principal quantum number of the system, J the spin (total angular momentum) and Σ its z-projection.

The mass operator of the second channel contains an additional (interaction-free) π and is defined as

$$M_{\widetilde{cl}+\pi} = M_{\widetilde{cl}} + M_\pi \tag{8.5}$$

with corresponding eigenstates and eigenvalues from the equation

$$M_{\widetilde{cl}+\pi}|v; nJ\Sigma; \vec{k}_\pi\rangle = \left(\omega_{\widetilde{cl}} + \omega_\pi\right)|v; nJ\Sigma; \vec{k}_\pi\rangle \tag{8.6}$$

with $\omega_{\widetilde{cl}} = \sqrt{m_{\widetilde{cl}}^2 + \vec{k}_\pi^2}$ the energy of the cluster and $\omega_\pi = \sqrt{m_\pi^2 + \vec{k}_\pi^2}$ the π energy.

The completeness relations and normalization conditions for velocity states according to the two mass operators in Eq. (8.3) and (8.5) are

$$\mathbb{1}_{\widetilde{cl}} = \sum_n \int \frac{d^3v}{(2\pi)^3 v^0} \frac{{m_{\widetilde{cl}}}^2}{2} |v; nJ\Sigma\rangle\langle v; nJ\Sigma|, \tag{8.7}$$

$$\langle v'; n'J'\Sigma'|v; nJ\Sigma\rangle = (2\pi)^3 v^0 \delta^3(\vec{v}' - \vec{v}) \frac{2}{m_{\widetilde{cl}}^2} \delta_{n'n}\delta_{J'J}\delta_{\Sigma'\Sigma}, \tag{8.8}$$

$$\mathbb{1}_{\widetilde{cl}+\pi} = \sum_n \int \frac{d^3v}{(2\pi)^3 v^0} \int \frac{d^3k_\pi}{(2\pi)^3 2\omega_\pi} \frac{(\omega_{\widetilde{cl}} + \omega_\pi)^3}{2\omega_{\widetilde{cl}}} |v; nJ\Sigma; \vec{k}_\pi\rangle\langle v; nJ\Sigma; \vec{k}_\pi|, \tag{8.9}$$

$$\begin{aligned}\langle v'; n'J'\Sigma'; \vec{k}'_\pi|v; nJ\Sigma; \vec{k}_\pi\rangle \\ = (2\pi)^3 v^0 \delta^3(\vec{v}' - \vec{v}) \frac{2\omega_{\widetilde{cl}} 2\omega_\pi}{(\omega_{\widetilde{cl}} + \omega_\pi)^3} (2\pi)^3 \delta^3(\vec{k}'_\pi - \vec{k}_\pi) \delta_{n'n}\delta_{J'J}\delta_{\Sigma'\Sigma}.\end{aligned} \tag{8.10}$$

In treating of the eigenvalue Eq. (8.2) we additionally need free QQQ and $QQQ+\pi$ velocity states with orthonormality relations as follows

$$\begin{aligned}\mathbb{1}_{QQQ} = &\sum_{\substack{\mu_1\mu_2\mu_3\\ \tau_1\tau_2\tau_3}} \int \frac{d^3v}{(2\pi)^3 v^0} \int \frac{d^3k_1}{(2\pi)^3 2\omega_1} \int \frac{d^3k_2}{(2\pi)^3 2\omega_2} \frac{(\omega_1+\omega_2+\omega_3)^3}{2\omega_3}\\ &\times|v;\vec{k}_1\mu_1\tau_1,\vec{k}_2\mu_2\tau_2,\vec{k}_3\mu_3\tau_3\rangle\langle v;\vec{k}_1\mu_1\tau_1,\vec{k}_2\mu_2\tau_2,\vec{k}_3\mu_3\tau_3|, \end{aligned} \tag{8.11}$$

$$\begin{aligned}&\langle v';\vec{k}'_1\mu'_1\tau'_1,\vec{k}'_2\mu'_2\tau'_2,\vec{k}'_3\mu'_3\tau'_3|v;\vec{k}_1\mu_1\tau_1,\vec{k}_2\mu_2\tau_2,\vec{k}_3\mu_3\tau_3\rangle\\ &\quad=(2\pi)^3 v^0\delta^3(\vec{v}'-\vec{v})\frac{2\omega_1 2\omega_2 2\omega_3}{(\omega_1+\omega_2+\omega_3)^3}(2\pi)^3\delta^3(\vec{k}'_1-\vec{k}_1)(2\pi)^3\delta^3(\vec{k}'_2-\vec{k}_2)\\ &\quad\times\delta_{\mu'_1\mu_1}\delta_{\mu'_2\mu_2}\delta_{\mu'_3\mu_3}\delta_{\tau'_1\tau_1}\delta_{\tau'_2\tau_2}\delta_{\tau'_3\tau_3}, \end{aligned} \tag{8.12}$$

where 1, 2, 3 indicate the three quarks and the sum of their three-momenta fulfill the relation $\vec{k}_1+\vec{k}_2+\vec{k}_3=0$.

The states of the free QQQ plus the π system fulfill the following orthonormality relations

$$\begin{aligned}\mathbb{1}_{QQQ+\pi} = &\sum_{\substack{\mu_1\mu_2\mu_3\\ \tau_1\tau_2\tau_3}} \int \frac{d^3v}{(2\pi)^3 v^0} \int \frac{d^3k_1}{(2\pi)^3 2\omega_1} \int \frac{d^3k_2}{(2\pi)^3 2\omega_2} \int \frac{d^3k_\pi}{(2\pi^3) 2\omega_\pi}\\ &\times\frac{(\omega_1+\omega_2+\omega_3+\omega_\pi)^3}{2\omega_3}\\ &\times|v;\vec{k}_1\mu_1\tau_1,\vec{k}_2\mu_2\tau_2,\vec{k}_3\mu_3\tau_3;\vec{k}_\pi\rangle\langle v;\vec{k}_1\mu_1\tau_1,\vec{k}_2\mu_2\tau_2,\vec{k}_3\mu_3\tau_3;\vec{k}_\pi|, \end{aligned} \tag{8.13}$$

$$\begin{aligned}&\langle v';\vec{k}'_1\mu'_1\tau'_1,\vec{k}'_2\mu'_2\tau'_2,\vec{k}'_3\mu'_3\tau'_3;\vec{k}'_\pi|v;\vec{k}_1\mu_1\tau_1,\vec{k}_2\mu_2\tau_2,\vec{k}_3\mu_3\tau_3;\vec{k}_\pi\rangle\\ &\quad=(2\pi)^3 v^0\delta^3(\vec{v}'-\vec{v})\frac{2\omega_1 2\omega_2 2\omega_3 2\omega_\pi}{(\omega_1+\omega_2+\omega_3+\omega_\pi)^3}\\ &\quad\times(2\pi)^3\delta^3(\vec{k}'_1-\vec{k}_1)(2\pi)^3\delta^3(\vec{k}'_2-\vec{k}_2)(2\pi)^3\delta^3(\vec{k}'_\pi-\vec{k}_\pi)\\ &\quad\times\delta_{\mu'_1\mu_1}\delta_{\mu'_2\mu_2}\delta_{\mu'_3\mu_3}\delta_{\tau'_1\tau_1}\delta_{\tau'_2\tau_2}\delta_{\tau'_3\tau_3}, \end{aligned} \tag{8.14}$$

where now $\vec{k}_1+\vec{k}_2+\vec{k}_3+\vec{k}_\pi=0$.

Now Eq. (8.2) can be represented with $\langle v;nJ\Sigma|$, and inserting $\mathbb{1}_{\widetilde{cl}}$ one obtains

$$\langle v;nJ\Sigma|M_{\widetilde{cl}}|\psi_{cl}\rangle + \langle v;nJ\Sigma|K(m-M_{\widetilde{cl}+\pi})^{-1}K^\dagger\mathbb{1}_{\widetilde{cl}}|\psi_{cl}\rangle = \langle v;nJ\Sigma|m|\psi_{cl}\rangle, \tag{8.15}$$

which finally leads to an eigenvalue equation of the form

$$\begin{aligned}&\langle v;nJ\Sigma|M_{\widetilde{cl}}|\psi_{cl}\rangle\\ &\quad+\sum_n\int\frac{d^3v}{(2\pi)^3v^0}\frac{{m_{\widetilde{cl}}}^2}{2}\langle v;nJ\Sigma|\underbrace{K(m-M_{\widetilde{cl}+\pi})^{-1}K^\dagger}_{V_{opt}}|v;nJ\Sigma\rangle\\ &\quad\times\langle v;nJ\Sigma|\psi_{cl}\rangle = \langle v;nJ\Sigma|m|\psi_{cl}\rangle, \end{aligned} \tag{8.16}$$

where we have marked the optical potential with the brace.

In dealing with Eq. (8.16) we expand $|\psi_{cl}\rangle$ in h.o. eigenstates of $M_{\widetilde{cl}}$ as

$$|\psi_{cl}\rangle = \sum_n |v;nJ\Sigma\rangle\langle v;nJ\Sigma|\psi_{cl}\rangle = \sum_n A_{nJ\Sigma}|v;nJ\Sigma\rangle. \tag{8.17}$$

8.2. Quark Wave Function

Next we discuss the N and Δ wave functions Ψ_{XSTC} where X is taken for spatial, S for the spin, T for the isospin and C for the color degrees of freedom. In general, baryon wave functions are totally antisymmetric and the mentioned parts have to be combined in a proper way.

All baryons are color singlets, i. e. the color part is totally antisymmetric, and therefore Ψ_{XST} has to be totally symmetric. In the following two subsections we will specify the spatial and the spin-isospin parts of this totally symmetric three-quark wave function.

8.2.1. Harmonic-Oscillator Wave Function

Quarks have not been observed as free particles. They always appear confined. For confinement we assume a h.o. potential between the quarks. Furthermore we restrict ourselves to states with total orbital angular momentum $L = 0$.

With this assumptions the spatial $O(3)$ part is symmetric. Therefore also the $SU(6)$ spin-isospin part must be symmetric. Its representaion is a 56plet. This 56plet contains Δ with $S = \frac{3}{2}$ and N with $S = \frac{1}{2}$. For the ground state with $L = 0$ and positive parity T we find for the lowest mass states in the spectrum a decuplet and an octet:

$$10, J^P = \frac{3}{2}^+; \quad 8, J^P = \frac{1}{2}^+. \tag{8.18}$$

In the following we will choose for the spatial part of the ground state wave function with $L^P = 0^+$

$$\psi_X = \exp[-\frac{1}{2}\alpha^2(\vec{k}_1^2 + \vec{k}_2^2 + \vec{k}_3^2)]. \tag{8.19}$$

8.2.2. Spin-Isospin Wave Function

Here we specify the spin-isospin part of Ψ_{XST} for the N and the Δ. Both consist of u and d quarks only and their isospin functions are given in Tab. 8.1.

The N is a $T = \frac{1}{2}$ particle, while the Δ has isospin $T = \frac{3}{2}$. The isospin projections τ run in unity steps from $-T$ to T. T and τ are quoted in the third column of Tab. 8.1.

For the spin S and its z-projection μ an analogous table can be given, and the coupling scheme is the same for quark spins and isospins. First the isospin (spin) of quark one and two are coupled to an intermediate isospin (spin) s, which can assume the values 0 or 1, with corresponding projection τ_s (μ_s). Then the third quark is added to end up with the total isospin (spin) T and corresponding z-projections τ.

Baryon	Ψ_F	T, τ	S/A
p	$\frac{1}{\sqrt{2}}(uud - udu)$	$\frac{1}{2}, \frac{1}{2}$	A
p	$-\frac{1}{\sqrt{6}}(uud + udu - 2duu)$	$\frac{1}{2}, \frac{1}{2}$	S
n	$\frac{1}{\sqrt{2}}(dud - ddu)$	$\frac{1}{2}, -\frac{1}{2}$	A
n	$\frac{1}{\sqrt{6}}(dud + ddu - 2udd)$	$\frac{1}{2}, -\frac{1}{2}$	S
Δ^{++}	uuu	$\frac{3}{2}, \frac{3}{2}$	S
Δ^{+}	$\frac{1}{\sqrt{3}}(uud + udu + duu)$	$\frac{3}{2}, \frac{1}{2}$	S
Δ^{0}	$\frac{1}{\sqrt{3}}(udd + dud + ddu)$	$\frac{3}{2}, -\frac{1}{2}$	S
Δ^{-}	ddd	$\frac{3}{2}, -\frac{3}{2}$	S

Table 8.1.: Isospin functions for N and Δ corresponding to total isospin T and z-projection τ with inherent symmetries.

As can be seen from Tab. 8.1 the isospin (spin) part for the N can either be symmetric (S) or antisymmetric (A). In order to obtain a totally symmetric N spin-isospin wave function we have to treat spin and isospin in the same manner. That is the reason why in each one of the intermediate Clebsch-Gordan coefficients there appears the same s, respectively. The symmetric and antisymmetric parts have to be combined in the following way

$$\frac{1}{\sqrt{2}} \sum_{s} \sum_{\substack{\mu_1,\mu_2,\mu_3,\mu_s \\ \tau_1,\tau_2,\tau_3,\tau_s}} C^{s\mu_s}_{\frac{1}{2}\mu_1\frac{1}{2}\mu_2} C^{\frac{1}{2}\mu_N}_{\frac{1}{2}\mu_3 s\mu_s} C^{s\tau_s}_{\frac{1}{2}\tau_1\frac{1}{2}\tau_2} C^{\frac{1}{2}\tau_N}_{\frac{1}{2}\tau_3 s\tau_s}, \tag{8.20}$$

where the factor $\frac{1}{\sqrt{2}}$ is the normalization due to summing over the intermediate s from 0 to 1.

To define the totally symmetric Δ spin-isospin wave function the intermediate isospin (spin) quantum number s has to be 1 to finally end up with the total isospin (spin) of $\frac{3}{2}$ as is described by the following product of Clebsch-Gordan coefficients

$$\sum_{\substack{\mu_1,\mu_2,\mu_3,\mu_s \\ \tau_1,\tau_2,\tau_3,\tau_s}} C^{s\mu_s}_{\frac{1}{2}\mu_1\frac{1}{2}\mu_2} C^{\frac{3}{2}\mu_\Delta}_{\frac{1}{2}\mu_3 s\mu_s} C^{s\tau_s}_{\frac{1}{2}\tau_1\frac{1}{2}\tau_2} C^{\frac{3}{2}\tau_\Delta}_{\frac{1}{2}\tau_3 s\tau_s}. \tag{8.21}$$

8.3. Microscopic Optical Potential

Inserting the completeness relations Eq. (8.11) and Eq. (8.13) into the optical potential V_{opt} defined in the eigenvalue equation (8.16) one obtains

$$\langle v; nJ\Sigma|\bar{\mathbb{1}}_{QQQ} K \mathbb{1}^{iv}_{QQQ+\pi} (m - M_{\widetilde{cl}+\pi})^{-1} \mathbb{1}''_{\widetilde{cl}+\pi} \mathbb{1}'''_{QQQ+\pi} K^{\dagger} \bar{\mathbb{1}}'_{QQQ} |v'; n'J'\Sigma'\rangle, \tag{8.22}$$

whose first-order terms can pictorially be represented as shown in Fig. 8.1.

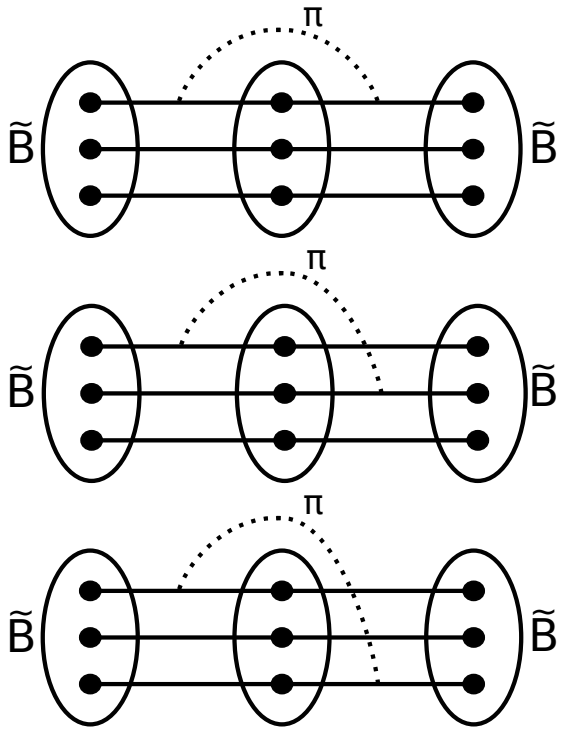

Figure 8.1.: Pictorial representation of the first-order term of the optical potential at the quark level. The possibilities how the first Q on the l. h. s. can couple to the ones on the r. h. s. are shown. Incoming and outgoing is a bare baryon $\widetilde{B}$ taken as a confined QQQ cluster. In the intermediate region a confined QQQ cluster and a free π are propagating.

In treating this optical potential we have to deal with individual quark and π momenta as well as their spins in different reference frames. The quantities referring to the QQQ system are marked with a bar, the ones belonging to the $QQQ+\pi$ system not. The corresponding momenta and spins are related by Lorentz transformations. They result in changes of the momentum dependencies and rotations of the spins. We work in the point form of RQM, which allows to operate the latter in a simpler and more transparent way as the angular-momentum operators are not affected by iterations (see also Sec. 2.2 and references given there).

We now continue by inserting the full expressions for the completeness relations

$$
\begin{aligned}
&\langle v; nJ\Sigma|\bar{\mathbb{1}}_{QQQ} K \mathbb{1}^{iv}_{QQQ+\pi}(m - M_{\widetilde{cl}+\pi})^{-1}\mathbb{1}''_{\widetilde{cl}+\pi}\mathbb{1}'''_{QQQ+\pi}K^{\dagger}\bar{\mathbb{1}}'_{QQQ}|v'; n'J'\Sigma'\rangle \\
&\quad= \sum_{\substack{\bar{\mu}_1\bar{\mu}_2\bar{\mu}_3 \\ \bar{\tau}_{q1}\bar{\tau}_{q2}\bar{\tau}_{q3}}} \int \frac{d^3\bar{v}}{(2\pi)^3\bar{v}^0}\int \frac{d^3\bar{k}_1}{(2\pi)^3 2\bar{\omega}_1}\int \frac{d^3\bar{k}_2}{(2\pi)^3 2\bar{\omega}_2}\frac{(\bar{\omega}_1+\bar{\omega}_2+\bar{\omega}_3)^3}{2\bar{\omega}_3} \\
&\quad\times\langle v; nJ\Sigma|\bar{v}; \bar{\vec{k}}_1\bar{\mu}_1\bar{\tau}_1, \bar{\vec{k}}_2\bar{\mu}_2\bar{\tau}_2, \bar{\vec{k}}_3\bar{\mu}_3\bar{\tau}_3\rangle \\
&\quad\times\sum_{\substack{\mu_1^{iv}\mu_2^{iv}\mu_3^{iv} \\ \tau_1^{iv}\tau_2^{iv}\tau_3^{iv}}}\int\frac{d^3v^{iv}}{(2\pi)^3 v_0^{iv}}\int\frac{d^3k_1^{iv}}{(2\pi)^3 2\omega_1^{iv}}\int\frac{d^3k_2^{iv}}{(2\pi)^3 2\omega_2^{iv}}\int\frac{d^3k_\pi^{iv}}{(2\pi^3)2\omega_\pi^{iv}} \\
&\quad\times\frac{(\omega_1^{iv}+\omega_2^{iv}+\omega_3^{iv}+\omega_\pi^{iv})^3}{2\omega_3^{iv}} \\
&\quad\times\langle\bar{v}; \bar{\vec{k}}_1\bar{\mu}_1\bar{\tau}_1, \bar{\vec{k}}_2\bar{\mu}_2\bar{\tau}_2, \bar{\vec{k}}_3\bar{\mu}_3\bar{\tau}_3|K|v^{iv}; \vec{k}^{iv}_{q1}\mu_1^{iv}\tau_1^{iv}, \vec{k}_2^{iv}\mu_2^{iv}\tau_2^{iv}, \vec{k}_3^{iv}\mu_3^{iv}\tau_3^{iv}; \vec{k}_\pi^{iv}\rangle \\
&\quad\times\sum_{n''}\int\frac{d^3v''}{(2\pi)^3 v_0''}\int\frac{d^3k_\pi''}{(2\pi)^3 2\omega_\pi''}\frac{(\omega''_{\widetilde{cl}}+\omega''_\pi)^3}{2\omega''_{\widetilde{cl}}} \\
&\quad\times\langle v^{iv}; \vec{k}^{iv}_{q1}\mu_1^{iv}\tau_1^{iv}, \vec{k}_2^{iv}\mu_2^{iv}\tau_2^{iv}, \vec{k}_3^{iv}\mu_3^{iv}\tau_3^{iv}; \vec{k}_\pi^{iv}|(m - M_{\widetilde{cl},\pi})^{-1}|v''; n''J''\Sigma''; k_\pi''\rangle \\
&\quad\times\sum_{\substack{\mu_1'''\mu_2'''\mu_3''' \\ \tau_1'''\tau_2'''\tau_3'''}}\int\frac{d^3v'''}{(2\pi)^3 v_0'''}\int\frac{d^3k_1'''}{(2\pi)^3 2\omega_1'''}\int\frac{d^3k_2'''}{(2\pi)^3 2\omega_2'''}\int\frac{d^3k_\pi'''}{(2\pi^3)2\omega_\pi'''} \\
&\quad\times\frac{(\omega_1'''+\omega_2'''+\omega_3'''+\omega_\pi''')^3}{2\omega_3'''} \\
&\quad\times\langle v''; n''J''\Sigma''; k_\pi''|v'''; \vec{k}_1'''\mu_1'''\tau_1''', \vec{k}_2'''\mu_2'''\tau_2''', \vec{k}_3'''\mu_3'''\tau_3'''; \vec{k}_\pi'''\rangle \\
&\quad\times\sum_{\substack{\bar{\mu}_1'\bar{\mu}_2'\bar{\mu}_3' \\ \bar{\tau}_1'\bar{\tau}_2'\bar{\tau}_3'}}\int\frac{d^3\bar{v}'}{(2\pi)^3\bar{v}_0'}\int\frac{d^3\bar{k}_1'}{(2\pi)^3 2\bar{\omega}_1'}\int\frac{d^3\bar{k}_2'}{(2\pi)^3 2\bar{\omega}_2'}\frac{(\bar{\omega}_1'+\bar{\omega}_2'+\bar{\omega}_3')^3}{2\bar{\omega}_3'} \\
&\quad\times\langle v'''; \vec{k}_1'''\mu_1'''\tau_1''', \vec{k}_2'''\mu_2'''\tau_2''', \vec{k}_3'''\mu_3'''\tau_3'''; \vec{k}_\pi'''|K^{\dagger}|\bar{v}'; \bar{\vec{k}}_1'\bar{\mu}_1'\bar{\tau}_1', \bar{\vec{k}}_2'\bar{\mu}_2'\bar{\tau}_2', \bar{\vec{k}}_3'\bar{\mu}_3'\bar{\tau}_3'\rangle \\
&\quad\times\langle\bar{v}'; \bar{\vec{k}}_1'\bar{\mu}_1'\bar{\tau}_1', \bar{\vec{k}}_2'\bar{\mu}_2'\bar{\tau}_2', \bar{\vec{k}}_3'\bar{\mu}_3'\bar{\tau}_3'|v'; n'J'\Sigma'\rangle. \qquad (8.23)
\end{aligned}
$$

8.3.1. Matrix Elements

In this section we will take a closer look at all different kinds of matrix elements appearing in Eq. (8.23).

Vertex Matrix Elements:

The vertex matrix elements

- $\langle \bar{v}; \bar{\vec{k}}_1 \bar{\mu}_1 \bar{\tau}_1, \bar{\vec{k}}_2 \bar{\mu}_2 \bar{\tau}_2, \bar{\vec{k}}_3 \bar{\mu}_3 \bar{\tau}_3 | K | v^{iv}; \vec{k}^{iv}_{q1} \mu^{iv}_1 \tau^{iv}_1, \vec{k}^{iv}_2 \mu^{iv}_2 \tau^{iv}_2, \vec{k}^{iv}_3 \mu^{iv}_3 \tau^{iv}_3; \vec{k}^{iv}_\pi \rangle,$ (8.24)

- $\langle v'''; \vec{k}'''_1 \mu'''_1 \tau'''_1, \vec{k}'''_2 \mu'''_2 \tau'''_2, \vec{k}'''_3 \mu'''_3 \tau'''_3; \vec{k}'''_\pi | K^\dagger | \bar{v}'; \bar{\vec{k}}'_1 \bar{\mu}'_1 \bar{\tau}'_1, \bar{\vec{k}}'_2 \bar{\mu}'_2 \bar{\tau}'_2, \bar{\vec{k}}'_3 \bar{\mu}'_3 \bar{\tau}'_3 \rangle,$ (8.25)

describe the coupling of the π to one of the quarks, while the other two quarks are left as spectators, i. e. we assume a spectator approximation.

As in the previous chapters, the matrix elements containing the vertex operators K and $K^\dagger$ can be identified with matrix elements resulting from PV or PS Lagrangian densities as given in Eq. (3.7), and so we have

$$\begin{aligned}
&\langle \bar{v}; \bar{\vec{k}}_1 \bar{\mu}_1 \bar{\tau}_1, \bar{\vec{k}}_2 \bar{\mu}_2 \bar{\tau}_2, \bar{\vec{k}}_3 \bar{\mu}_3 \bar{\tau}_3 | K | v^{iv}; \vec{k}^{iv}_{q1} \mu^{iv}_1 \tau^{iv}_1, \vec{k}^{iv}_2 \mu^{iv}_2 \tau^{iv}_2, \vec{k}^{iv}_3 \mu^{iv}_3 \tau^{iv}_3; \vec{k}^{iv}_\pi \rangle \\
&= \bar{v}^{0iv} \delta^3(\vec{v}^{iv} - \bar{\vec{v}}) \frac{(2\pi)^3}{\sqrt{(\omega^{iv}_1 + \omega^{iv}_2 + \omega^{iv}_3 + \omega^{iv}_\pi)^3 (\bar{\omega}_1 + \bar{\omega}_2 + \bar{\omega}_3)^3}} \\
&\times \langle \bar{\vec{k}}_1 \bar{\mu}_1 \bar{\tau}_1, \bar{\vec{k}}_2 \bar{\mu}_2 \bar{\tau}_2, \bar{\vec{k}}_3 \bar{\mu}_3 \bar{\tau}_3 | \mathcal{L}^{PV}_{\pi QQ}(0) | \vec{k}^{iv}_1 \mu^{iv}_1 \tau^{iv}_1, \vec{k}^{iv}_2 \mu^{iv}_2 \tau^{iv}_2, \vec{k}^{iv}_3 \mu^{iv}_3 \tau^{iv}_3; \vec{k}^{iv}_\pi \rangle .
\end{aligned} \tag{8.26}$$

The PV Lagrangian density at the quark level is given as

$$\mathcal{L}^{PV}_{\pi QQ} = -\frac{f_{\pi QQ}}{2m_Q} \bar{\psi}(x) \gamma^\mu \gamma_5 \vec{T} \psi(x) \partial_\mu \cdot \vec{\phi}(x) \tag{8.27}$$

with $f_{\pi QQ}$ the PV πQQ coupling constant, $\bar{\psi}(x)$ and $\psi(x)$ the quark fields and $\vec{\phi}(x)$ the π field. $\vec{T}$ denotes the isospin operator, which is responsible for the correct isospin treatment at the vertices. In the following we write instead of the product $\langle Q | \vec{T} \cdot \vec{\phi}(x) | Q \rangle$ the abbreviation $I(\tau_i, \tau'_i, \tau'_\pi)$. The appearing field expansions in the Lagrangian density are given in Eqs. (4.22), (4.24) and (4.25), with the Dirac fields for the N replaced by the ones for the quarks.

Following the procedure given in Sec. 4.2 the final expressions for the vertex matrix elements read

$$\begin{aligned}
&\langle \bar{\vec{k}}_1 \bar{\mu}_1 \bar{\tau}_1, \bar{\vec{k}}_2 \bar{\mu}_2 \bar{\tau}_2, \bar{\vec{k}}_3 \bar{\mu}_3 \bar{\tau}_3 | \mathcal{L}^{PV}_{\pi QQ}(0) | \vec{k}^{iv}_1 \mu^{iv}_1 \tau^{iv}_1, \vec{k}^{iv}_2 \mu^{iv}_2 \tau^{iv}_2, \vec{k}^{iv}_3 \mu^{iv}_3 \tau^{iv}_3; \vec{k}^{iv}_\pi \rangle \\
&= \frac{f_{\pi QQ}}{2m_Q} \bar{u}(\bar{\vec{k}}_1, \bar{\mu}_1) \gamma^\mu \gamma_5 I(\bar{\tau}_1, \tau^{iv}_1, \tau^{iv}_\pi) u(\vec{k}^{iv}_1, \mu^{iv}_1) \cdot k^{iv}_{\pi_\mu} \\
&\times (2\pi)^3 2\omega^{iv}_2 \delta^3(\vec{k}^{iv}_2 - \bar{\vec{k}}_2) \delta_{\mu^{iv}_2 \bar{\mu}_2} \delta_{\tau^{iv}_2 \bar{\tau}_2} (2\pi)^3 2\omega^{iv}_3 \delta^3(\vec{k}^{iv}_3 - \bar{\vec{k}}_3) \delta_{\mu^{iv}_3 \bar{\mu}_3} \delta_{\tau^{iv}_3 \bar{\tau}_3}
\end{aligned} \tag{8.28}$$

and

$$\begin{aligned}
&\langle \vec{k}'''_1 \mu'''_1 \tau'''_1, \vec{k}'''_2 \mu'''_2 \tau'''_2, \vec{k}'''_3 \mu'''_3 \tau'''_3; \vec{k}'''_\pi | \mathcal{L}^{PV\dagger}_{\pi QQ}(0) | \bar{\vec{k}}'_1 \bar{\mu}'_1, \bar{\tau}'_1 \bar{\vec{k}}'_2 \bar{\mu}'_2 \bar{\tau}'_2, \bar{\vec{k}}'_3 \bar{\mu}'_3 \bar{\tau}'_3 \rangle \\
&= \frac{f_{\pi QQ}}{2m_Q} k^{'''\dagger}_{\pi_\mu} \bar{u}(\vec{k}'''_1 \mu'''_1) \gamma^\mu \gamma_5 I(\bar{\tau}'_1, \tau'''_1, \tau'''_\pi) u(\bar{\vec{k}}'_1, \bar{\mu}'_1) \\
&\times (2\pi)^3 2\bar{\omega}'_2 \delta^3(\bar{\vec{k}}'_2 - \vec{k}'''_2) \delta_{\bar{\mu}'_2 \mu'''_2} \delta_{\bar{\tau}'_2 \tau'''_2} (2\pi)^3 2\bar{\omega}'_3 \delta^3(\bar{\vec{k}}'_3 - \vec{k}'''_3) \delta_{\bar{\mu}'_3 \mu'''_3} \delta_{\bar{\tau}'_3 \tau'''_3},
\end{aligned} \tag{8.29}$$

where it is assumed that the π is coupling only to quark 1, while quarks 2 and 3 are left as spectators. Since the πQQ interaction is taken as pointlike, we foresee no vertex form factors.

8.3.2. Overlaps of States

Overlaps of Cluster States and Free Three-Particle States:

To obtain the final expressions for the overlaps of cluster states (of the confined QQQ system) and free three-particle states

- $\langle v; nJ\Sigma | \bar{v}; \bar{\vec{k}}_1 \bar{\mu}_1 \bar{\tau}_1, \bar{\vec{k}}_2 \bar{\mu}_2 \bar{\tau}_2, \bar{\vec{k}}_3 \bar{\mu}_3 \bar{\tau}_3 \rangle$,

(8.30)

- $\langle \bar{v}; \bar{\vec{k}}'_1 \bar{\mu}'_1 \bar{\tau}'_1, \bar{\vec{k}}'_2 \bar{\mu}'_2 \bar{\tau}'_2, \bar{\vec{k}}'_3 \bar{\mu}'_3 \bar{\tau}'_3 | v'; n'J'\Sigma' \rangle$,

(8.31)

we make use of the h.o. wave functions $\psi_{nJ\Sigma}(|\bar{\vec{k}}_1|, |\bar{\vec{k}}_2|)$,

$$\begin{aligned} &\langle v; nJ\Sigma | \bar{v}; \bar{\vec{k}}_1 \bar{\mu}_1 \bar{\tau}_1, \bar{\vec{k}}_2 \bar{\mu}_2 \bar{\tau}_2, \bar{\vec{k}}_3 \bar{\mu}_3 \bar{\tau}_3 \rangle \\ &\quad = \mathcal{N} v^0 \delta^3(\vec{v} - \bar{\vec{v}}) \psi_{nJ\Sigma}(|\bar{\vec{k}}_1|, |\bar{\vec{k}}_2|) \\ &\quad \times C^{J\Sigma}_{lm_l S\mu_S} C^{S\mu_S}_{s\mu_s \frac{1}{2}\bar{\mu}_3} C^{T\tau_S}_{s\tau_s \frac{1}{2}\bar{\tau}_3} C^{s\mu_s}_{\frac{1}{2}\bar{\mu}_1 \frac{1}{2}\bar{\mu}_2} C^{s\tau_s}_{\frac{1}{2}\bar{\tau}_1 \frac{1}{2}\bar{\tau}_2} \end{aligned} \tag{8.32}$$

and determine the normalization factor $\mathcal{N}$. The appearing Clebsch-Gordan coefficients are coupling the three individual quark spin and isospin components to total ones. Depending on the considered process an additional normalization factor has to be added. This is due to the fact that the spin-isospin part of the wave function has to be fully symmetric which has been discussed in detail in Sec. 8.2.2.

To obtain $\mathcal{N}$, we start with the normalization condition for the cluster states

$$\langle v'; n'J'\Sigma' | v; nJ\Sigma \rangle = 2v^0 \delta^3(\vec{v} - \vec{v}') \frac{(2\pi)^3}{m^2_{\widetilde{cl}}} \delta_{nn'} \delta_{JJ'} \delta_{\Sigma\Sigma'} \tag{8.33}$$

and insert the completeness relation for the QQQ state

$$\begin{aligned} \bar{\mathbb{1}}_{QQQ} = \sum_{\substack{\bar{\mu}_1 \bar{\mu}_2 \bar{\mu}_3 \\ \bar{\tau}_1 \bar{\tau}_2 \bar{\tau}_3}} \int \frac{d^3\bar{v}}{(2\pi)^3 \bar{v}^0} \int \frac{d^3\bar{k}_1}{(2\pi)^3 2\bar{\omega}_1} \int \frac{d^3\bar{k}_2}{(2\pi)^3 2\bar{\omega}_2} \frac{(\bar{\omega}_1 + \bar{\omega}_2 + \bar{\omega}_3)^3}{2\bar{\omega}_3} \\ \times |\bar{v}; \bar{\vec{k}}_1 \bar{\mu}_1 \bar{\tau}_1, \bar{\vec{k}}_2 \bar{\mu}_2 \bar{\tau}_2, \bar{\vec{k}}_3 \bar{\mu}_3 \bar{\tau}_3 \rangle \langle \bar{v}; \bar{\vec{k}}_1 \bar{\mu}_1 \bar{\tau}_1, \bar{\vec{k}}_2 \bar{\mu}_2 \bar{\tau}_2, \bar{\vec{k}}_3 \bar{\mu}_3 \bar{\tau}_3 | \end{aligned} \tag{8.34}$$

leading to

$$\langle v'; n'J'\Sigma' | \bar{\mathbb{1}}_{QQQ} | v; nJ\Sigma \rangle. \tag{8.35}$$

After some calculation the result for $\mathcal{N}$ reads

$$\mathcal{N} = \frac{(2\pi)^6}{m_{\widetilde{cl}}}\sqrt{2}\sqrt{\frac{2\bar{\omega}_1 2\bar{\omega}_2 2\bar{\omega}_3}{(\bar{\omega}_1+\bar{\omega}_2+\bar{\omega}_3)^3}} \tag{8.36}$$

and so the final expressions for the two overlaps are

$$\begin{aligned}\langle v; nJ\Sigma|\bar{v}; \bar{\vec{k}}_1\bar{\mu}_1\bar{\tau}_1, \bar{\vec{k}}_2\bar{\mu}_2\bar{\tau}_2, \bar{\vec{k}}_3\bar{\mu}_3\bar{\tau}_3\rangle &= (2\pi)^6\frac{\sqrt{2}}{m_{\widetilde{cl}}}\sqrt{\frac{2\bar{\omega}_1 2\bar{\omega}_2 2\bar{\omega}_3}{(\bar{\omega}_1+\bar{\omega}_2+\bar{\omega}_3)^3}} \\ \times v^0\delta^3(\vec{v}-\bar{\vec{v}})\psi^*_{nJ\Sigma}(|\bar{\vec{k}}_1|,|\bar{\vec{k}}_2|)&\frac{1}{\sqrt{2}}C^{J,\Sigma *}_{lm_l Sm_S}C^{Sm_S *}_{sm_s\frac{1}{2}\bar{\mu}_3}C^{S\tau_S *}_{s\tau_s\frac{1}{2}\bar{\tau}_3}C^{sm_s *}_{\frac{1}{2}\bar{\mu}_1\frac{1}{2}\bar{\mu}_2}C^{s\tau_s *}_{\frac{1}{2}\bar{\tau}_1\frac{1}{2}\bar{\tau}_2},\end{aligned} \tag{8.37}$$

$$\begin{aligned}\langle \bar{v}; \bar{\vec{k}}'_1\bar{\mu}'_1\bar{\tau}'_1, \bar{\vec{k}}'_2\bar{\mu}'_2\bar{\tau}'_2, \bar{\vec{k}}'_3\bar{\mu}'_3\bar{\tau}'_3|v'; n'J'\Sigma'\rangle &= (2\pi)^6\frac{\sqrt{2}}{m'_{\widetilde{cl}}}\sqrt{\frac{2\bar{\omega}'_1 2\bar{\omega}'_2 2\bar{\omega}'_3}{(\bar{\omega}'_1+\bar{\omega}'_2+\bar{\omega}'_3)^3}} \\ \times v'_0\delta^3(\vec{v}'-\bar{\vec{v}}')\psi_{n'J'\Sigma'}(|\bar{\vec{k}}'_1|,|\bar{\vec{k}}'_2|)&\frac{1}{\sqrt{2}}C^{J',\Sigma'}_{l'm'_l S'm'_S}C^{S'm'_S}_{s'm'_s\frac{1}{2}\bar{\mu}'_3}C^{S'\tau'_S}_{s'\tau'_s\frac{1}{2}\bar{\tau}'_3}C^{s'm'_s}_{\frac{1}{2}\bar{\mu}'_1\frac{1}{2}\bar{\mu}'_2}C^{s'\tau'_s}_{\frac{1}{2}\bar{\tau}'_1\frac{1}{2}\bar{\tau}'_2}.\end{aligned} \tag{8.38}$$

Overlaps of States with an Additional π:

To obtain the final expressions for the overlaps of cluster states and free three-particle states with an additional π

- $\langle v^{iv}; \vec{k}^{iv}_1\mu^{iv}_1\tau^{iv}_1, \vec{k}^{iv}_2\mu^{iv}_2\tau^{iv}_2, \vec{k}^{iv}_3\mu^{iv}_3\tau^{iv}_3; \vec{k}^{iv}_\pi|v''; n''J''\Sigma''; \vec{k}''_\pi\rangle,$ (8.39)
- $\langle v''; n''J''\Sigma''; \vec{k}''_\pi|v'''; \vec{k}'''_1\mu'''_1\tau'''_1, \vec{k}'''_2\mu'''_2\tau'''_2, \vec{k}'''_3\mu'''_3\tau'''_3; \vec{k}'''_\pi\rangle$ (8.40)

we again make use of the h.o. wave functions $\psi_{nJ\Sigma}(|\bar{\vec{k}}_1|,|\bar{\vec{k}}_2|)$ and determine the normalization $\mathcal{N}'$

$$\begin{aligned}&\langle v^{iv}; \vec{k}^{iv}_1\mu^{iv}_1\tau^{iv}_1, \vec{k}^{iv}_2\mu^{iv}_2\tau^{iv}_2, \vec{k}^{iv}_3\mu^{iv}_3\tau^{iv}_3; \vec{k}^{iv}_\pi|v''; n''J''\Sigma''; \vec{k}''_\pi\rangle \\ &= \mathcal{N}'\sum_{\substack{\bar{\mu}_1\bar{\mu}_2\bar{\mu}_3\\ \bar{\tau}_1\bar{\tau}_2\bar{\tau}_3}}(2\pi)^6\frac{\sqrt{2}}{m''_{cl}}\sqrt{\frac{2\omega^{iv}_1 2\omega^{iv}_2 2\omega^{iv}_3}{(\omega^{iv}_1+\omega^{iv}_2+\omega^{iv}_3)^3}}v^{0iv}\delta^3(\vec{v}''-\vec{v}^{iv}) \\ &\times(2\pi)^3 2\omega^{iv}_\pi\delta^3(\vec{k}^{iv}_\pi-\vec{k}''_\pi)\frac{1}{\sqrt{2}}C^{J''\Sigma''}_{l''m''_l S''m''_S}C^{Sm_S}_{s''m''_s\frac{1}{2}\bar{\mu}^{iv}_3}C^{s''m''_s}_{\frac{1}{2}\bar{\mu}^{iv}_1\frac{1}{2}\bar{\mu}^{iv}_2} \\ &\times C^{S\tau_S}_{s''\tau''_s\frac{1}{2}\bar{\tau}^{iv}_3}C^{s''\tau''_s}_{\frac{1}{2}\bar{\tau}^{iv}_1\frac{1}{2}\bar{\tau}^{iv}_2}D^{\frac{1}{2}}_{\mu^{iv}_1\bar{\mu}^{iv}_1}D^{\frac{1}{2}}_{\mu^{iv}_2\bar{\mu}^{iv}_2}D^{\frac{1}{2}}_{\mu^{iv}_3\bar{\mu}^{iv}_3}\psi_{n''J''\Sigma''}(|\bar{\vec{k}}^{iv}_1|,|\bar{\vec{k}}^{iv}_2|).\end{aligned} \tag{8.41}$$

Contrary to Eq. (8.32) there appear Wigner D-functions rotating the spin projections given in the $QQQ+\pi$ frame into the QQQ frame. Here it is important to notice that

the appearing wave functions and the corresponding bared momenta $\vec{\bar{k}}_i$ refer to the reference frame of the QQQ state, whereas the momenta $\vec{k}_i$ belong to the $QQQ + \pi$ system. It is therefore nessesary to know the transformation of the momenta k_i to $\bar{k}_i$. In Ref. [Kra01] this transformation procedure is given for an arbitrary number of particles. For our case the transformation reads

$$d^3k_i = d^3\bar{k}_i \frac{2\omega_1 2\omega_2 2\omega_3}{2\bar{\omega}_1 2\bar{\omega}_2 2\bar{\omega}_3} \frac{(2\bar{\omega}_1 + 2\bar{\omega}_2 + 2\bar{\omega}_3)}{(2\omega_1 + 2\omega_2 + 2\omega_3)}. \tag{8.42}$$

In analogy to the previous discussion we start with the normalization condition of eigenstates of $M_{cl+\pi}$

$$\begin{aligned}\langle v''; n''J''\Sigma''; \vec{k}''_\pi | v'''; n'''J'''\Sigma'''; \vec{k}'''_\pi \rangle \\ = (2\pi)^6 \frac{2\omega''_\pi 2\omega''_{\widetilde{cl}}}{(\omega''_\pi + \omega''_{\widetilde{cl}})^3} v^{0''} \delta^3(\vec{v}'' - \vec{v}''')\delta^3(\vec{k}''_\pi - \vec{k}'''_\pi)\delta_{n''n'''}\delta_{J''J'''}\delta_{\Sigma''\Sigma'''},\end{aligned} \tag{8.43}$$

where the completeness relation of the eigenstates of the free mass operator $M_{QQQ+\pi}$, Eq. (8.13), has to be inserted

$$\langle v''; n''J''\Sigma''; \vec{k}''_\pi | \mathbb{1}_{QQQ+\pi} | v'''; n'''J'''\Sigma'''; \vec{k}'''_\pi \rangle. \tag{8.44}$$

This leads to the final expression

$$\begin{aligned}\mathcal{N}' = &\frac{m''_{cl}}{\sqrt{2}} \sqrt{\frac{2\bar{\omega}''_{\widetilde{cl}}}{(\omega''_\pi + \bar{\omega}''_{\widetilde{cl}})^3}} \sqrt{\frac{(\omega_1^{iv} + \omega_2^{iv} + \omega_3^{iv})^3}{(\omega_1^{iv} + \omega_2^{iv} + \omega_3^{iv} + \omega_\pi^{iv})^3}} \sqrt{\frac{2\bar{\omega}_1^{iv} 2\bar{\omega}_2^{iv} 2\bar{\omega}_3^{iv}}{\bar{\omega}_1^{iv} + \bar{\omega}_2^{iv} + \bar{\omega}_3^{iv}}} \\ &\times \sqrt{\frac{\omega_1^{iv} + \omega_2^{iv} + \omega_3^{iv}}{2\omega_1^{iv} 2\omega_2^{iv} 2\omega_3^{iv}}}.\end{aligned} \tag{8.45}$$

Using the latter, we finally express the overlaps as

$$\begin{aligned}&\langle v^{iv}; \vec{k}_1^{iv} \mu_1^{iv} \tau_1^{iv}, \vec{k}_2^{iv} \mu_2^{iv} \tau_{q2}^{iv}, \vec{k}_3^{iv} \mu_3^{iv} \tau_3^{iv}; \vec{k}_\pi^{iv} | v''; n''J''\Sigma''; \vec{k}''_\pi \rangle \\ &= \sum_{\substack{\bar{\mu}_1^{iv} \bar{\mu}_2^{iv} \bar{\mu}_3^{iv} \\ \tau_1^{iv} \bar{\tau}_2^{iv} \bar{\tau}_3^{iv}}} \sqrt{\frac{2\bar{\omega}''_{\widetilde{cl}}}{(\omega''_\pi + \omega''_{\widetilde{cl}})^3}} \sqrt{\frac{\omega_1^{iv} + \omega_2^{iv} + \omega_3^{iv}}{(\omega_1^{iv} + \omega_2^{iv} + \omega_3^{iv} + \omega_\pi^{iv})^3}} \sqrt{\frac{2\bar{\omega}_1^{iv} 2\bar{\omega}_2^{iv} 2\bar{\omega}_3^{iv}}{(\bar{\omega}_1^{iv} + \bar{\omega}_2^{iv} + \bar{\omega}_3^{iv})}} \\ &\times (2\pi)^6 v^{0iv} \delta^3(\vec{v}'' - \vec{v}^{iv})(2\pi)^3 2\omega_\pi^{iv} \delta^3(\vec{k}_\pi^{iv} - \vec{k}''_\pi) \\ &\times \frac{1}{\sqrt{2}} C^{J''\Sigma''}_{l''m''_l S''m''_S} C^{S''m''_S}_{s''m''_s \frac{1}{2}\bar{\mu}_3^{iv}} C^{s''m''_s}_{\frac{1}{2}\bar{\mu}_1^{iv}\frac{1}{2}\bar{\mu}_2^{iv}} C^{S''\tau''_S}_{s''\tau''_s \frac{1}{2}\bar{\tau}_3^{iv}} C^{s''\tau''_s}_{\frac{1}{2}\bar{\tau}_1^{iv}\frac{1}{2}\bar{\tau}_2^{iv}} \\ &\times D^{\frac{1}{2}}_{\mu_1^{iv}\bar{\mu}_1^{iv}} D^{\frac{1}{2}}_{\mu_2^{iv}\bar{\mu}_2^{iv}} D^{\frac{1}{2}}_{\mu_3^{iv}\bar{\mu}_3^{iv}} \psi_{n''J''\Sigma''}(|\vec{\bar{k}}_1^{iv}|, |\vec{\bar{k}}_2^{iv}|)\end{aligned} \tag{8.46}$$

and

$$
\begin{aligned}
&\langle v''; n''J''\Sigma''; \vec{k}''_\pi | v'''; \vec{k}'''_1 \mu'''_1 \tau'''_1, \vec{k}'''_2 \mu'''_2 \tau'''_2, \vec{k}'''_3 \mu'''_3 \tau'''_3; \vec{k}'''_\pi \rangle \\
&\quad = \sum_{\bar{\mu}'''_1, \bar{\mu}'''_2, \bar{\mu}'''_3} \sqrt{\frac{2\bar{\omega}''_{\widetilde{cl}}}{(\omega''_\pi + \omega''_{\widetilde{cl}})^3}} \sqrt{\frac{\omega'''_1 + \omega'''_2 + \omega'''_3}{(\omega'''_1 + \omega'''_2 + \omega'''_3 + \omega'''_\pi)^3}} \sqrt{\frac{2\bar{\omega}'''_1 2\bar{\omega}'''_2 2\bar{\omega}'''_3}{(\bar{\omega}'''_1 + \bar{\omega}'''_2 + \bar{\omega}'''_3)}} \\
&\quad \times (2\pi)^6 v^{0'''} \delta^3(\vec{v}'' - \vec{v}''') (2\pi)^3 2\omega'''_\pi \delta^3(\vec{k}'''_\pi - \vec{k}''_\pi) \\
&\quad \times \frac{1}{\sqrt{2}} C^{J''\Sigma''*}_{l''m''_l S''m''_S} C^{S''m''_S*}_{s''m''_s \frac{1}{2}\bar{\mu}'''_3} C^{s''m''_s*}_{\frac{1}{2}\bar{\mu}'''_1 \frac{1}{2}\bar{\mu}'''_2} C^{S''\tau''_S*}_{s''\tau''_s \frac{1}{2}\bar{\tau}'''_3} C^{s''\tau''_s*}_{\frac{1}{2}\bar{\tau}'''_1 \frac{1}{2}\bar{\tau}'''_2} \\
&\quad \times D^{\frac{1}{2}*}_{\mu'''_1 \bar{\mu}'''_1} D^{\frac{1}{2}*}_{\mu'''_2 \bar{\mu}'''_2} D^{\frac{1}{2}*}_{\mu'''_3 \bar{\mu}'''_3} \psi^*_{n''J''\Sigma''}(|\vec{\bar{k}}'''_1|, |\vec{\bar{k}}'''_2|).
\end{aligned} \tag{8.47}
$$

8.4. Final Optical Potential

Inserting all the detailed expressions obtained above into Eq. (8.23) the optical potential at the quark level finally reads

$$
\begin{aligned}
&\langle v; nJ\Sigma | K(m - M^{-1}_{\widetilde{cl}+\pi}) K^\dagger | v'; n'J'\Sigma' \rangle \\
&\quad = 6 \sum_{\substack{\bar{\mu}_1 \bar{\mu}_2 \bar{\mu}_3 \\ \bar{\tau}_1 \bar{\tau}_2 \bar{\tau}_3}} \sum_{\mu^{iv}_1} \sum_{\substack{\bar{\mu}^{iv}_1 \bar{\mu}^{iv}_2 \bar{\mu}^{iv}_3 \\ \bar{\tau}^{iv}_1 \bar{\tau}^{iv}_2 \bar{\tau}^{iv}_3}} \sum_{n'' M''_n J''\Sigma''} \sum_{\mu'''_1} \sum_{\substack{\bar{\mu}'''_1 \bar{\mu}'''_2 \bar{\mu}'''_3 \\ \bar{\tau}'''_1 \bar{\tau}'''_2 \bar{\tau}'''_3}} \sum_{\substack{\bar{\mu}'_1 \bar{\mu}'_2 \bar{\mu}'_3 \\ \bar{\tau}'_1 \bar{\tau}'_2 \bar{\tau}'_3}} \\
&\quad \times \int d^3\bar{k}_2 \int d^3\bar{k}_3 \int \frac{d^3 k''_\pi}{(2\pi)^3 2\omega''_\pi} \int d^3\bar{k}'_2 \int d^3\bar{k}'_3 \\
&\quad \times \frac{\sqrt{2}}{m_{\widetilde{cl}} 2\omega^{iv}_1} \sqrt{\frac{(\omega^{iv}_1 + \bar{\omega}_2 + \bar{\omega}_3)}{2\bar{\omega}_1 2\bar{\omega}_2 2\bar{\omega}_3}} \sqrt{\frac{2\bar{\omega}^{iv}_1 2\bar{\omega}^{iv}_2 2\bar{\omega}^{iv}_3}{(\bar{\omega}^{iv}_1 + \bar{\omega}^{iv}_2 + \bar{\omega}^{iv}_3)}} \psi^*_{nJ\Sigma}(|\vec{\bar{k}}_2|, |\vec{\bar{k}}_3|) \\
&\quad \times \frac{1}{\sqrt{2}} C^{J\Sigma*}_{lm_l S m_S} C^{Sm_S*}_{sm_s \frac{1}{2}\bar{\mu}_3} C^{sm_s*}_{\frac{1}{2}\bar{\mu}_1 \frac{1}{2}\bar{\mu}_2} C^{T\tau_S*}_{s\tau_s \frac{1}{2}\bar{\tau}_3} C^{s\tau_s*}_{\frac{1}{2}\bar{\tau}_1 \frac{1}{2}\bar{\tau}_2} \\
&\quad \times \frac{f_{qq\pi}}{2m_q} \bar{u}(\vec{\bar{k}}_1 \bar{\mu}_1) \gamma^\mu \gamma_5 I(\tau^{iv}_q, \bar{\tau}_q, \tau''_\pi) u(\vec{\bar{k}}^{iv}_1 \mu^{iv}_1) k''_{\pi_\mu} \\
&\quad \times (m - \omega''_{\widetilde{cl}} - \omega''_\pi)^{-1} \psi_{n''J''\Sigma''}(|\vec{\bar{k}}^{iv}_2|, |\vec{\bar{k}}^{iv}_3|) \\
&\quad \times \frac{1}{\sqrt{2}} C^{J''\Sigma''}_{l''m''_l S''m''_S} C^{S''m''_S}_{s''m''_s \frac{1}{2}\bar{\mu}^{iv}_3} C^{s''m''_s}_{\frac{1}{2}\bar{\mu}^{iv}_1 \frac{1}{2}\bar{\mu}^{iv}_2} C^{T''\tau''_S}_{s''\tau''_s \frac{1}{2}\bar{\tau}^{iv}_3} C^{s''\tau''_s}_{\frac{1}{2}\bar{\tau}^{iv}_1 \frac{1}{2}\bar{\tau}^{iv}_2} \\
&\quad \times D^{\frac{1}{2}}_{\mu^{iv}_1 \bar{\mu}^{iv}_1} D^{\frac{1}{2}}_{\bar{\mu}_2 \bar{\mu}^{iv}_2} D^{\frac{1}{2}}_{\bar{\mu}_3 \bar{\mu}^{iv}_3}
\end{aligned}
$$

$$
\begin{aligned}
&\times \frac{\sqrt{2}}{M'_n 2\omega'''_1}\sqrt{\frac{2\bar{\omega}'''_1 2\bar{\omega}'''_2 2\bar{\omega}'''_3}{2\bar{\omega}'_1 2\bar{\omega}'_2 2\bar{\omega}'_3}}\sqrt{\frac{(\omega'''_1+\bar{\omega}_2+\bar{\omega}_3)}{(\bar{\omega}'''_1+\bar{\omega}''_2+\bar{\omega}'''_3)}}\psi^*_{n''J''\Sigma''}(|\vec{\bar{k}}'''_2|,|\vec{\bar{k}}'''_3|)\\
&\times \frac{1}{\sqrt{2}}C^{J''\Sigma''*}_{l''m''_l S''m''_S}C^{S''m''_S*}_{s''m''_s \frac{1}{2}\bar{\mu}'''_3}C^{s''m''_s}_{\frac{1}{2}\bar{\mu}'''_1 \frac{1}{2}\bar{\mu}'''_2}C^{T''\tau''_S*}_{s''\tau''_s \frac{1}{2}\bar{\tau}'''_3}C^{s''\tau''_s}_{\frac{1}{2}\bar{\tau}'''_1 \frac{1}{2}\bar{\tau}'''_2}\\
&\times D^{\frac{1}{2}*}_{\mu'''_1\bar{\mu}'''_1}D^{\frac{1}{2}*}_{\bar{\mu}'''_2\bar{\mu}'_2}D^{\frac{1}{2}*}_{\bar{\mu}'''_3\bar{\mu}'_3}\\
&\times \frac{f_{qq\pi}}{2m_q}k''^{\dagger}_{\pi\mu}\bar{u}(\vec{k}'''_1,\mu'''_1)\gamma^\mu\gamma_5 I(\tau'''_q,\bar{\tau}'_q,\tau''_\pi)u(\vec{\bar{k}}'_1,\bar{\mu}'_1)\psi_{n'J'\Sigma'}(|\vec{\bar{k}}'_2|,|\vec{\bar{k}}'_3|)\\
&\times \frac{1}{\sqrt{2}}C^{J'\Sigma'}_{l'm'_l S'm'_S}C^{S'm'_S}_{S'm'_S \frac{1}{2}\bar{\mu}'_3}C^{s'm'_s}_{\frac{1}{2}\bar{\mu}'_1 \frac{1}{2}\bar{\mu}'_2}C^{T'\tau'_S}_{S'\tau'_S \frac{1}{2}\bar{\tau}'_3}C^{s'\tau'_s}_{\frac{1}{2}\bar{\tau}'_1 \frac{1}{2}\bar{\tau}'_2}v^0\delta^3(\vec{v}-\vec{v}'). \qquad (8.48)
\end{aligned}
$$

We note again that the calculation was done within the point-form spectator model (PFSM). Within this model it is assumed that the π couples to one quark, while the others are left as spectators. For symmetry reasons we have to multiply each vertex with a factor 3 according to the three possibilities of the π exchange in Fig. 8.1. This leads to the factor 6 in Eq. (8.48) above.

8.5. Strong Vertex Form Factors

The optical potential in Eq. (8.48) derived along the microscopic CC approach allows us to access various $\pi\widetilde{B}\widetilde{B}$ vertex form factors, if we compare it with the corresponding expression on the macroscopic level:

$$
\begin{aligned}
\langle\widetilde{B}|V_{opt}|\widetilde{B}'\rangle = &\frac{f^2_{\pi\widetilde{B}\widetilde{B}}}{4\pi}\int\frac{d^3k''_\pi}{2\omega''_\pi 2\omega''_{\widetilde{B}}2m_{\widetilde{B}}}\\
&\times\mathcal{F}_{\pi\widetilde{B}\widetilde{B}''}(|\vec{k}''_\pi|)\langle\widetilde{B}\,|\,\mathcal{L}_{\pi\widetilde{B}\widetilde{B}}(0)\,|\,\widetilde{B}'',\pi:\vec{k}''_\pi\rangle\\
&\times(m-\omega''_{\widetilde{B}}-\omega''_\pi)^{-1}\mathcal{F}_{\pi\widetilde{B}'\widetilde{B}''}(|\vec{k}''_\pi|)\langle\widetilde{B}'',\pi:\vec{k}''_\pi\,|\,\mathcal{L}^\dagger_{\pi\widetilde{B}\widetilde{B}}(0)\,|\,\widetilde{B}'\rangle. \qquad (8.49)
\end{aligned}
$$

This expression is just a generalization of the optical potential as in Eq. (4.17), where now the vertex operator K has already been identified with the ones from the Lagrangian density, Eq. (3.7), and the coupling constants as well as vertex form factors have been written out explicitly.

Assuming $\widetilde{N}$, $\widetilde{\Delta}$ and π degrees of freedom we can specifically deduce from a microscopic theory the vertex form factors $\mathcal{F}_{\pi\widetilde{N}\widetilde{N}}$ and $\mathcal{F}_{\pi\widetilde{N}\widetilde{\Delta}}$ as employed in Part III in investigating the N and Δ with explicit pions on the hadronic level. However, in addition we have now access to the vertex form factors $\mathcal{F}_{\pi\widetilde{\Delta}\widetilde{N}}$ as well as $\mathcal{F}_{\pi\widetilde{\Delta}\widetilde{\Delta}}$. In the following we give their explicit expressions by comparing Eqs. (8.49) and (8.48).

8.5.1. Strong $\pi\widetilde{N}\widetilde{N}$ Vertex Form Factor

We start with the expression of the $\pi\widetilde{N}\widetilde{N}$ vertex form factor $\mathcal{F}_{\pi\widetilde{N}\widetilde{N}}$ according to Fig. 8.2

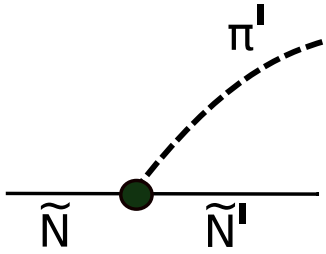

Figure 8.2.: Pictorial representation of the $\pi\widetilde{N}\widetilde{N}$ vertex.

The vertex form factor $\mathcal{F}_{\pi\widetilde{N}\widetilde{N}}$ follows from comparing the expression (8.48) for an incoming and outgoing $\widetilde{N}$ with Eq. (8.49):

$$
\begin{aligned}
\mathcal{F}_{\pi\widetilde{N}\widetilde{N}}(|\vec{k}'_\pi|) = \frac{3}{2} & \sum_{\mu'_{q_1}\bar{\mu}'_{q_1}\bar{\mu}'_{q_2}\bar{\mu}'_{q_3}\bar{\mu}_{q_2}\bar{\mu}_{q_3}\bar{\mu}_{q_1}\bar{\tau}_{q_1}\bar{\tau}_{q_2}\bar{\tau}_{q_3}\bar{\tau}'_{q_1}ss'} \\
& \times \int d^3\bar{k}_{q_2} \int d^3\bar{k}_{q_3} \frac{\sqrt{(\omega'_{q_1}+\bar{\omega}_{q_2}+\bar{\omega}_{q_3})}}{\sqrt{2\bar{\omega}_{q_1}2\bar{\omega}_{q_2}2\bar{\omega}_{q_3}}} \frac{\sqrt{2m_{\widetilde{cl}}2\omega'_{cl}}}{2\omega'_{q_1}} \sqrt{\frac{2\bar{\omega}'_{q_1}2\bar{\omega}'_{q_2}2\bar{\omega}'_{q_3}}{(\bar{\omega}'_{q_1}+\bar{\omega}'_{q_2}+\bar{\omega}'_{q_3})}} \\
& \times \psi_{nJ\Sigma}(|\vec{\bar{k}}_{q_2}|,|\vec{\bar{k}}_{q_3}|) C^{\frac{1}{2}m_{\widetilde{N}}}_{sm_s\frac{1}{2}\bar{\mu}_{q_3}} C^{sm_s}_{\frac{1}{2}\bar{\mu}_{q_1}\frac{1}{2}\bar{\mu}_{q_2}} C^{\frac{1}{2}\tau_{\widetilde{N}}}_{s\tau_s\frac{1}{2}\bar{\tau}_{q_3}} C^{s\tau_s}_{\frac{1}{2}\bar{\tau}_{q_1}\frac{1}{2}\bar{\tau}_{q_2}} \\
& \times k'^{\dagger}_{\pi\mu}\bar{u}(\vec{k}'_{q_1}\mu'_{q_1})\gamma^\mu\gamma_5 I(\bar{\tau}_{q_1},\tau'_{q_1},\tau'_\pi)u(\vec{\bar{k}}_{q_1}\bar{\mu}_{q_1}) \\
& \times \psi^*_{n'J'\Sigma'}(|\vec{k}'_{q_2}|,|\vec{k}'_{q_3}|) C^{\frac{1}{2}m'^*_{\widetilde{N}}}_{s'm'_s\frac{1}{2}\bar{\mu}'_{q_3}} C^{s'm'^*_s}_{\frac{1}{2}\bar{\mu}'_{q_1}\frac{1}{2}\bar{\mu}'_{q_2}} C^{\frac{1}{2}\tau'^*_{\widetilde{N}}}_{s'\tau'_s\frac{1}{2}\bar{\tau}'_{q_3}} C^{s'\tau'^*_s}_{\frac{1}{2}\bar{\tau}'_{q_1}\frac{1}{2}\bar{\tau}'_{q_2}} \\
& \times D^{\frac{1}{2}}_{\mu'_{q_1}\bar{\mu}'_{q_1}}(B(-\bar{k}'_{q_1})B(v)B(k'_{q_1})) \\
& \times D^{\frac{1}{2}}_{\bar{\mu}'_{q_2}\bar{\mu}_{q_2}}(B(-\bar{k}'_{q_2})B(v)B(\bar{k}_{q_2})) \\
& \times D^{\frac{1}{2}}_{\bar{\mu}'_{q_3}\bar{\mu}_{q_3}}(B(-\bar{k}'_{q_3})B(v)B(\bar{k}_{q_3})) \\
& \times \frac{1}{(k'^{\dagger}_{\pi_\mu}\bar{u}(\vec{k}'_{\widetilde{N}}\Sigma'_{\widetilde{N}})\gamma^\mu\gamma_5 I(\tau_{\widetilde{N}},\tau'_{\widetilde{N}},\tau'_\pi)u(\vec{k}_{\widetilde{N}}\Sigma_{\widetilde{N}}))}.
\end{aligned}
\tag{8.50}
$$

The factor 3 in the beginning of Eq. (8.50) is due to our assumption of the PFSM. The factor 2 in the denominator appears due to the normalization of the Clebsch-Gordan coefficients, as in Eq. (8.20).

In Eq. (8.50) there occur two three-dimensional integrations over spectator-quark momenta in the kinematical factors, the three-quark wave functions, the spinor products, and Wigner-D functions. In the last line of Eq. (8.50) there appears the macro-

scopic spinor structure, which is left from the comparison of Eq. (8.48) with Eq. (8.49) for the $\widetilde{N}$ case. It stems from the Lagrangian density for the $\pi\widetilde{N}\widetilde{N}$ system on the hadronic level. We note that the same type of PV coupling is also used on the quark level as evident from Eq. (8.50).

8.5.2. Strong $\pi\widetilde{N}\widetilde{\Delta}$ Vertex Form Factor

In the same way we proceed with the strong form factor for the $\pi\widetilde{N}\widetilde{\Delta}$ vertex. Here a Δ is incoming and in the intermediate state the N is propagating together with the π and the dynamics is governed by the Lagrangian density given in Eq. (6.12).

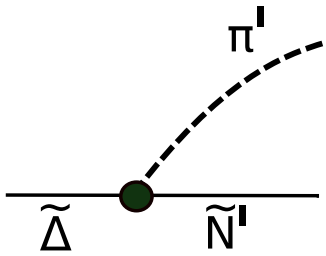

Figure 8.3.: Pictorial representation of the $\pi\widetilde{N}\widetilde{\Delta}$ vertex.

The final analytical function of the $\pi\widetilde{N}\widetilde{\Delta}$ vertex form factor according to the vertex shown in Fig. 8.3 reads:

$$
\begin{aligned}
\mathcal{F}_{\pi\widetilde{N}\widetilde{\Delta}}(|\vec{k}'_{\pi}|) = \frac{3}{\sqrt{2}} & \sum_{\mu'_{q_1}\bar{\mu}'_{\bar{q}_1}\bar{\mu}'_{\bar{q}_2}\bar{\mu}'_{\bar{q}_3}\bar{\mu}_{\bar{q}_2}\bar{\mu}_{\bar{q}_3}\bar{\mu}_{q_1}\tau_{q_1}\tau_{q_2}\tau_{q_3}\tau'_{q_1}ss'} \\
& \times \int d^3\bar{k}_{q_2} \int d^3\bar{k}_{q_3} \frac{\sqrt{(\omega'_{q_1}+\bar{\omega}_{q_2}+\bar{\omega}_{q_3})}}{\sqrt{2\bar{\omega}_{q_1}2\bar{\omega}_{q_2}2\bar{\omega}_{q_3}}} \frac{\sqrt{2m_{\widetilde{cl}}2\omega'_{cl}}}{2\omega'_{q_1}} \sqrt{\frac{2\bar{\omega}'_{q_1}2\bar{\omega}'_{q_2}2\bar{\omega}'_{q_3}}{(\bar{\omega}'_{q_1}+\bar{\omega}'_{q_2}+\bar{\omega}'_{q_3})}} \\
& \times \psi_{nJ\Sigma}(|\vec{\bar{k}}_{q_2}|,|\vec{\bar{k}}_{q_3}|) C^{\frac{3}{2}m_{\widetilde{\Delta}}}_{sm_s\frac{1}{2}\bar{\mu}_{q_3}} C^{sm_s}_{\frac{1}{2}\bar{\mu}_{q_1}\frac{1}{2}\bar{\mu}_{q_2}} C^{\frac{3}{2}\tau_{\widetilde{\Delta}}}_{s\tau_s\frac{1}{2}\bar{\tau}_{q_3}} C^{s\tau_s}_{\frac{1}{2}\bar{\tau}_{q_1}\frac{1}{2}\bar{\tau}_{q_2}} \\
& \times k'^{\dagger}_{\pi\mu}\bar{u}(\vec{k}'_{q_1}\mu'_{q_1})\gamma^{\mu}\gamma_5 I(\bar{\tau}_{q_1},\tau'_{q_1},\tau'_{\pi})u(\vec{\bar{k}}_{q_1}\bar{\mu}_{q_1}) \\
& \times \psi^{*}_{n'J'\Sigma'}(|\vec{k}'_{q_2}|,|\vec{k}'_{q_3}|) C^{\frac{1}{2}m'^{*}_{\widetilde{N}}}_{s'm'_s\frac{1}{2}\bar{\mu}'_{q_3}} C^{s'm'^{*}_s}_{\frac{1}{2}\bar{\mu}'_{q_1}\frac{1}{2}\bar{\mu}'_{q_2}} C^{\frac{1}{2}\tau'^{*}_{\widetilde{N}}}_{s'\tau'_s\frac{1}{2}\bar{\tau}'_{q_3}} C^{s'\tau'^{*}_s}_{\frac{1}{2}\bar{\tau}_{q_1}\frac{1}{2}\bar{\tau}_{q_2}} \\
& \times D^{\frac{1}{2}}_{\bar{\mu}'_{q_1}\mu'_{q_1}}(B(-\bar{k}'_{q_1})B(v)B(k'_{q_1})) \\
& \times D^{\frac{1}{2}}_{\bar{\mu}'_{q_2}\bar{\mu}_{q_2}}(B(-\bar{k}'_{q_2})B(v)B(\bar{k}_{q_2})) \\
& \times D^{\frac{1}{2}}_{\bar{\mu}'_{q_3}\bar{\mu}_{q_3}}(B(-\bar{k}'_{q_3})B(v)B(\bar{k}_{q_3})) \\
& \times \frac{1}{(\epsilon^{\mu\nu\alpha\beta}k^{\dagger'}_{\pi_\beta}\bar{u}(\vec{k}'_{\widetilde{N}}\Sigma'_{\widetilde{N}})I(\tau_{\widetilde{\Delta}},\tau'_{\widetilde{N}},\tau'_{\pi})\gamma_5\gamma_{\alpha}u_{\nu}(\vec{k}_{\widetilde{\Delta}}\Sigma_{\widetilde{\Delta}})k^{\dagger}_{\widetilde{\Delta}_{\mu}})}.
\end{aligned}
\tag{8.51}
$$

It is of similar form as the $\pi\widetilde{N}\widetilde{N}$ form factor given in Eq. (8.50). However, instead of the 2 in the denominator there appears a $\sqrt{2}$ due the normalization of the Clebsch-Gordan coefficients, Eq. (8.20). The term in the last line now remains from the $\pi\widetilde{N}\widetilde{\Delta}$ Lagrangian on the hadronic level, while the πQQ coupling is of PV type as in Eq. (8.50).

8.5.3. Strong $\pi\widetilde{\Delta}\widetilde{N}$ Vertex Form Factor

The strong form factor for the $\pi\widetilde{\Delta}\widetilde{N}$ vertex is extracted just in the same manner only an incoming $\widetilde{N}$ and an intermediate state $\widetilde{\Delta}$ appears together with the π. The dynamics is now governed by the Hermitian conjugate of the Lagrangian density in Eq. (6.12).

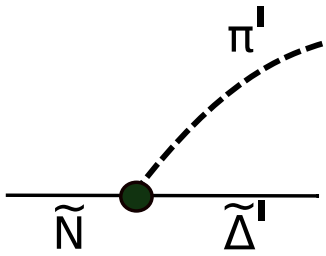

Figure 8.4.: Pictorial representation of the $\pi\widetilde{\Delta}\widetilde{N}$ vertex.

The final analytical expression for the strong $\pi\widetilde{\Delta}\widetilde{N}$ vertex form factor according to Fig. 8.4 reads

$$
\begin{aligned}
\mathcal{F}_{\pi\widetilde{\Delta}\widetilde{N}}(|\vec{k}'_{\pi}|) = \frac{3}{\sqrt{2}} & \sum_{\mu'_{q_1}\bar{\mu}'_{\bar{q}_1}\bar{\mu}'_{\bar{q}_2}\bar{\mu}'_{\bar{q}_3}\bar{\mu}_{\bar{q}_2}\bar{\mu}_{\bar{q}_3}\bar{\mu}_{\bar{q}_1}\bar{\tau}_{\bar{q}_1}\bar{\tau}_{\bar{q}_2}\bar{\tau}_{\bar{q}_3}\bar{\tau}'_{\bar{q}_1}ss'} \\
& \times \int d^3\bar{k}_{q_2} \int d^3\bar{k}_{q_3} \frac{\sqrt{(\omega'_{q_1}+\bar{\omega}_{q_2}+\bar{\omega}_{q_3})}}{\sqrt{2\bar{\omega}_{q_1}2\bar{\omega}_{q_2}2\bar{\omega}_{q_3}}} \frac{\sqrt{2m_{\widetilde{cl}}2\omega'_{cl}}}{2\omega'_{q_1}} \sqrt{\frac{2\bar{\omega}'_{q_1}2\bar{\omega}'_{q_2}2\bar{\omega}'_{q_3}}{(\bar{\omega}'_{q_1}+\bar{\omega}'_{q_2}+\bar{\omega}'_{q_3})}} \\
& \times \psi_{nJ\Sigma}(|\vec{\bar{k}}_{q_2}|,|\vec{\bar{k}}_{q_3}|) C^{\frac{3}{2}m_{\widetilde{N}}}_{sm_s\frac{1}{2}\bar{\mu}_{q_3}} C^{sm_s}_{\frac{1}{2}\bar{\mu}_{q_1}\frac{1}{2}\bar{\mu}_{q_2}} C^{\frac{3}{2}\tau_{\widetilde{N}}}_{s\tau_s\frac{1}{2}\bar{\tau}_{q_3}} C^{s\tau_s}_{\frac{1}{2}\bar{\tau}_{q_1}\frac{1}{2}\bar{\tau}_{q_2}} \\
& \times k'^{\dagger}_{\pi\mu}\bar{u}(\vec{k}'_{q_1}\mu'_{q_1})\gamma^{\mu}\gamma_5 I(\bar{\tau}_{q_1},\tau'_{q_1},\tau'_{\pi})u(\vec{\bar{k}}_{q_1}\bar{\mu}_{q_1}) \\
& \times \psi^*_{n'J'\Sigma'}(|\vec{k}'_{q_2}|,|\vec{k}'_{q_3}|) C^{\frac{1}{2}m'^*_{\widetilde{\Delta}}}_{s'm'_s\frac{1}{2}\bar{\mu}'_{q_3}} C^{s'm'^*_s}_{\frac{1}{2}\bar{\mu}'_{q_1}\frac{1}{2}\bar{\mu}'_{q_2}} C^{\frac{1}{2}\tau'^*_{\widetilde{\Delta}}}_{s'\tau'_s\frac{1}{2}\bar{\tau}'_{q_3}} C^{s'\tau'^*_s}_{\frac{1}{2}\bar{\tau}'_{q_1}\frac{1}{2}\bar{\tau}'_{q_2}} \\
& \times D^{\frac{1}{2}}_{\bar{\mu}'_{q_1}\mu'_{q_1}}(B(-\bar{k}'_{q_1})B(v)B(k'_{q_1})) \\
& \times D^{\frac{1}{2}}_{\bar{\mu}'_{q_2}\bar{\mu}_{q_2}}(B(-\bar{k}'_{q_2})B(v)B(\bar{k}_{q_2})) \\
& \times D^{\frac{1}{2}}_{\bar{\mu}'_{q_3}\bar{\mu}_{q_3}}(B(-\bar{k}'_{q_3})B(v)B(\bar{k}_{q_3})) \\
& \times \frac{1}{(\epsilon^{\mu\nu\alpha\beta}k'_{\widetilde{\Delta}_{\mu}}\bar{u}^{\nu}(\vec{k}'_{\widetilde{\Delta}}\Sigma'_{\widetilde{\Delta}})I(\tau'_{\widetilde{\Delta}},\tau_{\widetilde{N}},\tau'_{\pi})\gamma_5\gamma_{\alpha}u(\vec{k}_{\widetilde{N}}\Sigma_{\widetilde{N}})k'_{\pi_{\beta}})}.
\end{aligned}
\tag{8.52}
$$

Again, there appears the $\sqrt{2}$ in the denominator due to normalization of the Clebsch-Gordan coefficients. The term in the last line stems from the $\pi\widetilde{\Delta}\widetilde{N}$ coupling at hadronic level, while in the πQQ case PV type coupling has been used.

8.5.4. Strong $\pi\widetilde{\Delta}\,\widetilde{\Delta}$ Vertex Form Factor

To extract the strong form factor for the $\pi\widetilde{\Delta}\,\widetilde{\Delta}$ vertex, the Lagrangian density

$$\mathcal{L}_{\pi\widetilde{\Delta}\widetilde{\Delta}} = \frac{f_{\pi\widetilde{\Delta}\widetilde{\Delta}}}{m_{\widetilde{\Delta}}}\epsilon^{\mu\nu\alpha\lambda}\bar{\psi}_\mu \mathcal{T}^a (D_\alpha \psi_\nu) D^{ab}_\lambda \phi^b \tag{8.53}$$

proposed in Ref. [LMCPV12] is used. $f_{\pi\widetilde{\Delta}\widetilde{\Delta}}$ is the $\pi\widetilde{\Delta}\widetilde{\Delta}$ coupling constant, ϕ^b is denoting the π-field coupling to the two $\widetilde{\Delta}$ Rarita-Schwinger fields $\bar{\psi}_\mu$ and ψ_ν. The isospin operator $\mathcal{T}^a$ accounts for the correct isospin behavior at the vertex.

Using the general formula Eq. (8.49) for the $\pi\widetilde{\Delta}\,\widetilde{\Delta}$ optical potential

$$\begin{aligned}
\langle\widetilde{\Delta}|V_{opt}|\widetilde{\Delta}'\rangle = {} & \frac{f^2_{\pi\widetilde{\Delta}\,\widetilde{\Delta}}}{m^2_{\widetilde{\Delta}}}\int \frac{d^3k''_\pi}{2\omega''_\pi}\frac{1}{2\omega_{\widetilde{\Delta}''}}\frac{1}{\sqrt{m_{\widetilde{\Delta}^3}}}\frac{1}{\sqrt{m_{\widetilde{\Delta}'^3}}} \\
& \times \mathcal{F}_{\pi\widetilde{\Delta}\,\widetilde{\Delta}''}(|\vec{k}''_\pi|)\epsilon^{\mu\nu\alpha\lambda}\bar{u}_\mu(\vec{k}_{\widetilde{\Delta}},\Sigma_{\widetilde{\Delta}})I(\tau_{\widetilde{\Delta}},\tau''_{\widetilde{\Delta}},\tau''_\pi)k''_{\Delta_\alpha}u_\nu(\vec{k}''_{\widetilde{\Delta}},\Sigma''_{\widetilde{\Delta}})k''_{\pi_\mu}(m-\omega''_{\widetilde{\Delta}}-\omega''_\pi)^{-1} \\
& \times \left(\mathcal{F}_{\pi\widetilde{\Delta}'\,\widetilde{\Delta}''}(|\vec{k}''_\pi|)\epsilon^{\mu\nu\alpha\lambda}\bar{u}_\mu(\vec{k}'_{\widetilde{\Delta}},\Sigma'_{\widetilde{\Delta}})I(\tau'_{\widetilde{\Delta}},\tau''_{\widetilde{\Delta}},\tau''_\pi)k''_{\Delta_\alpha}u_\nu(\vec{k}''_{\widetilde{\Delta}},\Sigma''_{\widetilde{\Delta}})k''_{\pi_\mu}\right)^\dagger .
\end{aligned} \tag{8.54}$$

and comparing with the corresponding expression on the microscopic level (8.48) we arrive at the $\pi\widetilde{\Delta}\widetilde{\Delta}$ vertex form factors as diagrammatically represented in Fig. 8.5:

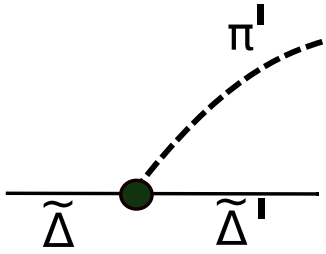

Figure 8.5.: Pictorial representation of the $\pi\widetilde{\Delta}\widetilde{\Delta}$ vertex.

$$
\begin{aligned}
\mathcal{F}_{\pi\widetilde{\Delta}\,\widetilde{\Delta}}(|\vec{k}'_{\pi}|) = 3 \sum_{\mu'_{q_1}\bar{\mu}'_{q_1}\bar{\mu}'_{q_2}\bar{\mu}'_{q_3}\bar{\mu}_{q_2}\bar{\mu}_{q_3}\bar{\mu}_{q_1}\bar{\tau}_{q_1}\bar{\tau}_{q_2}\bar{\tau}_{q_3}\tau'_{q_1}ss'} \\
\times \int d^3\bar{k}_{q_2} \int d^3\bar{k}_{q_3} \frac{\sqrt{(\omega'_{q_1}+\bar{\omega}_{q_2}+\bar{\omega}_{q_3})}}{\sqrt{2\bar{\omega}_{q_1}2\bar{\omega}_{q_2}2\bar{\omega}_{q_3}}} \frac{\sqrt{2m_{\widetilde{cl}}2\omega'_{cl}}}{2\omega'_{q_1}} \sqrt{\frac{2\bar{\omega}'_{q_1}2\bar{\omega}'_{q_2}2\bar{\omega}'_{q_3}}{(\bar{\omega}'_{q_1}+\bar{\omega}'_{q_2}+\bar{\omega}'_{q_3})}} \\
\times \psi_{nJ\Sigma}(|\vec{\bar{k}}_{q_2}|,|\vec{\bar{k}}_{q_3}|) C^{\frac{3}{2}m_{\widetilde{\Delta}}}_{sm_s\frac{1}{2}\bar{\mu}_{q_3}} C^{sm_s}_{\frac{1}{2}\bar{\mu}_{q_1}\frac{1}{2}\bar{\mu}_{q_2}} C^{\frac{3}{2}\tau_{\widetilde{\Delta}}}_{s\tau_s\frac{1}{2}\bar{\tau}_{q_3}} C^{s\tau_s}_{\frac{1}{2}\bar{\tau}_{q_1}\frac{1}{2}\bar{\tau}_{q_2}} \\
\times k'^{\dagger}_{\pi\mu} \bar{u}(\vec{k}'_{q_1}\mu'_{q_1}) \gamma'^{\mu}\gamma_5 I(\bar{\tau}_{q_1},\tau'_{q_1},\tau'_{\pi}) u(\vec{\bar{k}}_{q_1}\bar{\mu}_{q_1}) \\
\times \psi^*_{n'J'\Sigma'}(|\vec{k}'_{q_2}|,|\vec{k}'_{q_3}|) C^{\frac{3}{2}m'^{*}_{\widetilde{\Delta}}}_{s'm'_s\frac{1}{2}\bar{\mu}'_{q_3}} C^{s'm'^{*}_s}_{\frac{1}{2}\bar{\mu}'_{q_1}\frac{1}{2}\bar{\mu}'_{q_2}} C^{\frac{3}{2}\tau'^{*}_{\widetilde{\Delta}}}_{s'\tau'_s\frac{1}{2}\bar{\tau}'_{q_3}} C^{s'\tau'^{*}_s}_{\frac{1}{2}\bar{\tau}_{q_1}\frac{1}{2}\bar{\tau}_{q_2}} \\
\times D^{\frac{1}{2}}_{\bar{\mu}'_{q_1}\mu'_{q_1}}(B(-\bar{k}'_{q_1})B(v)B(k'_{q_1})) \\
\times D^{\frac{1}{2}}_{\bar{\mu}'_{q_2}\bar{\mu}_{q_2}}(B(-\bar{k}'_{q_2})B(v)B(\bar{k}_{q_2})) \\
\times D^{\frac{1}{2}}_{\bar{\mu}'_{q_3}\bar{\mu}_{q_3}}(B(-\bar{k}'_{q_3})B(v)B(\bar{k}_{q_3})) \\
\times \frac{1}{\left(\epsilon^{\mu\nu\alpha\lambda}\bar{u}_{\mu}(\vec{k}_{\widetilde{\Delta}},\Sigma_{\widetilde{\Delta}}) I(\tau_{\widetilde{\Delta}},\tau'_{\widetilde{\Delta}},\tau'_{\pi}) k'_{\widetilde{\Delta}_{\alpha}} u_{\nu}(\vec{k}'_{\widetilde{\Delta}},\Sigma'_{\widetilde{\Delta}}) k_{\pi_{\mu}}\right)^{\dagger}}.
\end{aligned}
\tag{8.55}
$$

The expression for the $\pi\widetilde{\Delta}\widetilde{\Delta}$ form factor is again very similar to the ones presented formerly, only that the normalization factor for the Clebsch- Gordan coefficients is now 1. A PV type coupling is used for the πQQ coupling and the $\pi\widetilde{\Delta}\widetilde{\Delta}$ one is given in Eq. (8.53).

8.6. Kinematical Considerations for the Vertex Form Factors on the Microscopic Level

The four-momentum of the two spectator quarks in spherical coordinates is written as

$$
\bar{k}_{q_i} = \begin{pmatrix} \sqrt{\vec{\bar{k}}^2_{q_i} + m^2_{q_i}} \\ \bar{k}_{q_i}\sin\theta_i\cos\phi_i \\ \bar{k}_{q_i}\sin\theta_i\sin\phi_i \\ \bar{k}_{q_i}\cos\theta_i \end{pmatrix}, \tag{8.56}
$$

where $i = 1, 2$. The bar denotes particles defined in the reference frame of the three-particle system shown in the outside boxes in Fig. 8.6. There the following relation holds

$$
\vec{\bar{k}}_{q_1} + \vec{\bar{k}}_{q_2} + \vec{\bar{k}}_{q_3} = 0. \tag{8.57}
$$

Particles defined in the four-particle reference frame corresponding to the inner box of Fig. 8.6 fulfill the following relation

$$
\vec{k}'_{q_1} + \vec{k}'_{q_2} + \vec{k}'_{q_3} + \vec{k}'_{\pi} = 0, \tag{8.58}
$$

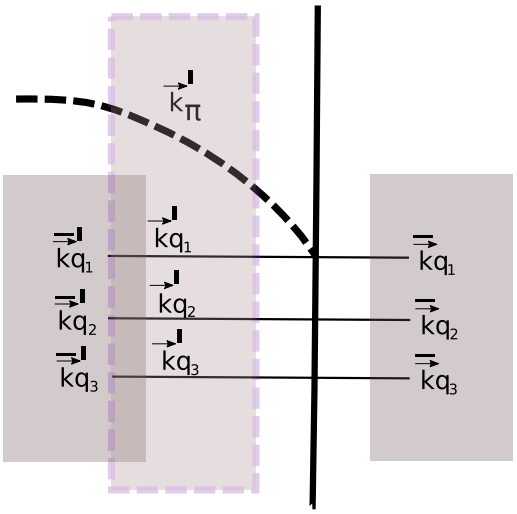

Figure 8.6.: Various three-momenta at an interaction vertex referring to different reference frames.

where k'_π is defined as

$$k'_\pi = \begin{pmatrix} \sqrt{\vec{k}'^2_\pi + m^2_\pi} \\ k'_\pi \sin\theta' \cos\phi' \\ k'_\pi \sin\theta' \sin\pi' \\ k'_\pi \cos\theta' \end{pmatrix}. \tag{8.59}$$

Assuming a spectator model for the interaction with the π the individual momenta of the spectator quarks are connected by

$$\bar{\vec{k}}_{q_2} = \vec{k}'_{q_2}, \qquad \text{and} \qquad \bar{\vec{k}}_{q_3} = \vec{k}'_{q_3} \tag{8.60}$$

Accordingly, k'_{q_2} and k'_{q_3} have to be boosted from the reference frame of four-particle system to the three-particle one via an inverse Lorentz boost, see Eq. (2.13)

$$\bar{k}'_{q_i} = B(-v')k'_{q_i} \tag{8.61}$$

with $i = 2, 3$. $\bar{\vec{k}}'_{q_1}$ can then be obtained via the relation:

$$\bar{\vec{k}}'_{q_1} + \bar{\vec{k}}'_{q_2} + \bar{\vec{k}}'_{q_3} = 0. \tag{8.62}$$

With these relations we have defined the kinematics.

9. Vertex From Factors and Masses from the Microscopic CC Approach

We are now ready to perform the calculation of the vertex form factors and π dressed masses on the microscopic quark level. We begin with specifying the input with regard to the πQ dynamics and then proceed with the treatment of the $QQQ+\pi$ system on the microscopic level.

9.1. πQ Dynamics

There are three ingredients in the optical potential Eq. (8.48) that have to be fixed, before we start with treating the eigenvalue equation (8.16). The first one is the constituent mass of the u and d quarks. In order to be consistent with the GBE RCQM of the Graz group [GPVW98, GPP$^+$98] we take it to be $m_Q = 340$ MeV, which may also be considered as a canonical value for the dynamical mass of the light quarks.

The second one is the parameter α in the h.o. wave function (8.19). It is determined by the strength of the confinement. We fix it to $\alpha = 3.66 \left(\frac{GeV}{c}\right)^{-2}$.

Finally the third ingredient is the strength of the πQQ coupling in the PV Lagrangian density as appearing in Eq. (8.49). Its value may be related to the phenomenological πNN coupling constant via the Goldberger Traiman relation (see, e. g., Ref. [GPP$^+$98]). It may thus vary in a range of $0.028 \leq \frac{f^2_{\pi QQ}}{4\pi} \leq 0.05$. In the calculation we took the value $\frac{f^2_{\pi QQ}}{4\pi} = 0.037$, which in our setting is consistent with a $\pi\widetilde{N}\widetilde{N}$ coupling constant $\frac{f^2_{\pi\widetilde{N}\widetilde{N}}}{4\pi} = 0.071$, i. e. close to the phenomenological value of 0.08 [EW88]. We note that the values of these three parameters follow from educated guesses. They are particularly chosen such that the size of the πQQ coupling together with the fall-off of the h.o. wave function leads to the correct splitting of the physical N and Δ masses and $\pi\widetilde{N}\widetilde{N}$ as well as $\pi\widetilde{N}\widetilde{\Delta}$ vertex form factors, whose momentum dependences resemble phenomenological ones.

9.2. Solution of the Microscopic CC Problem

For the solution of the microscopic $\{QQQ\}$ system coupled to pion channels we proceed in the way as described here below.

Nucleon

We start out form an arbitrary value for the bare N mass $m_{\widetilde{N}}$ (optimally of the size of ~ 1070 MeV, like in case of the GBE RCQM in Ch. 4, cf. Tab. 4.2) and calculate the vertex form factor $\mathcal{F}_{\pi\widetilde{N}\widetilde{N}}$ after Eq. (8.50). The resulting $\pi\widetilde{N}\widetilde{N}$ form factor is then employed in the eigenvalue equation (4.16) to obtain the physical N mass $m_N = 939$ MeV and a corresponding bare N mass $m^h_{\widetilde{N}}$ on the hadronic level. The latter value is then used to produce the next iteration to the vertex form factor $\mathcal{F}_{\pi\widetilde{N}\widetilde{N}}$. This process is continued until the bare N input mass $m_{\widetilde{N}}$ coincides with $m^h_{\widetilde{N}}$.

Δ

Once we have determined the bare N mass $m_{\widetilde{N}}$ and the physical N mass m_N, we may proceed to the Δ case. Again we start with an arbitrary bare Δ mass $m_{\widetilde{\Delta}}$ to calculate the vertex form factors $\mathcal{F}_{\pi\widetilde{N}\widetilde{\Delta}}$ after Eq. (8.52), where the bare N mass $m_{\widetilde{N}}$ is used as determined above. The resulting $\pi\widetilde{N}\widetilde{\Delta}$ form factor is then employed in the eigenvalue equation (6.7) to obtain the physical Δ mass m_Δ and the corresponding bare Δ mass $m^h_{\widetilde{\Delta}}$ on the hadronic level. The latter value is then used to produce the next iteration to the vertex form factor $\mathcal{F}_{\pi\widetilde{N}\widetilde{\Delta}}$. Again the process is continued until $m_{\widetilde{\Delta}}$ and $m^h_{\widetilde{\Delta}}$ coincide.

Up to now the vertex form factors $\mathcal{F}_{\pi\widetilde{N}\widetilde{N}}$ and $\mathcal{F}_{\widetilde{N}\widetilde{\Delta}}$ are fixed and the bare and dressed N and Δ masses are known.

$\mathcal{F}_{\pi\widetilde{\Delta}\widetilde{N}}$ and $\mathcal{F}_{\pi\widetilde{\Delta}\widetilde{\Delta}}$ Vertex From Factors

Now, when we have determined the $\pi\widetilde{N}\widetilde{N}$ and the $\pi\widetilde{N}\widetilde{\Delta}$ form factors as well as the N and Δ bare and physical masses, also the $\mathcal{F}_{\pi\widetilde{\Delta}\widetilde{N}}$ and $\mathcal{F}_{\pi\widetilde{\Delta}\widetilde{\Delta}}$ form factors according to the diagrams in Figs. 8.4 and 8.5 from Eqs. (8.52) and (8.55) can be obtained, respectively.

We emphasize that by following the procedure as described here, we have consistently obtained, starting from a microscopic CC theory, the various bare vertex form factors $\mathcal{F}_{\pi\widetilde{B}\widetilde{B}}$ for the N and the Δ as well as the dressing effects on their masses. The pertinent results are presented and discussed in the following sections.

9.3. Results for the N

This section contains the results for the bare vertex form factor $\mathcal{F}_{\pi\widetilde{N}\widetilde{N}}$, including the $\pi\widetilde{N}\widetilde{N}$ coupling constant, as well as the consistent evaluation of the bare and π-dressed N masses.

The vertex form factor as extracted via Eq. (8.50) depends on the three-momentum $|\vec{k}_\pi|$ and we obtain it numerically. The resulting data are shown in Fig. 9.1. In order to ease the practical use of this form factor we parametrize it according to the following multipole formula

$$\mathcal{F}_{\pi\widetilde{N}\widetilde{N}}\left(|\vec{k}_\pi|\right) = \frac{a}{1+\left(\frac{\vec{k}_\pi}{\Lambda_1}\right)^2+\left(\frac{\vec{k}_\pi}{\Lambda_2}\right)^4} \quad , \tag{9.1}$$

where a is a parameter reflecting its size at $|\vec{k}_\pi| = 0$ and Λ_1 as well as Λ_2 are so-called cut-off parameters. Normalizing the form factors to 1 at $|\vec{k}_\pi| = 0$ yields the bare $\pi\widetilde{N}\widetilde{N}$

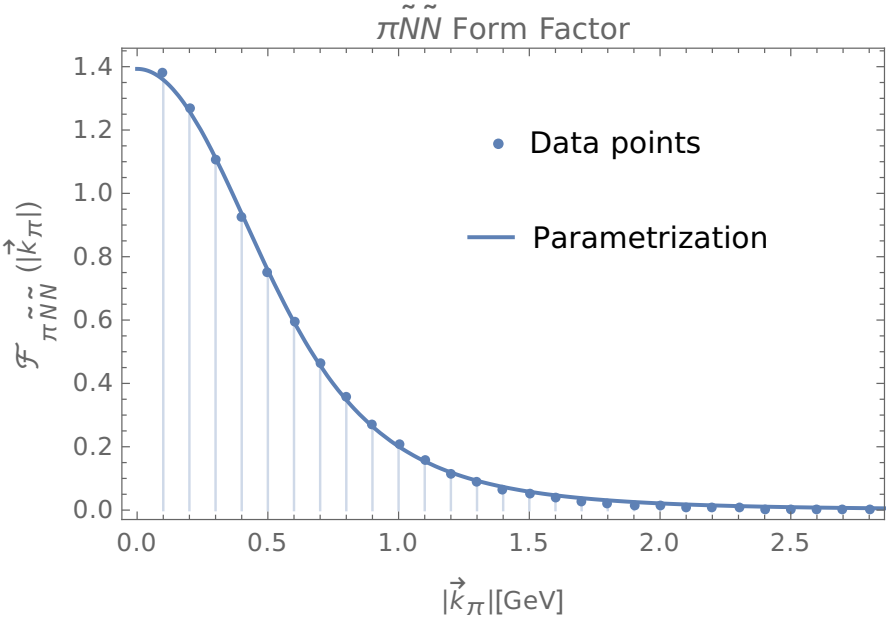

Figure 9.1.: Bare $\pi\widetilde{N}\widetilde{N}$ form factor resulting from the CC approach at the microscopic quark level together with its parametrization according to Eq. (9.1).

coupling constant. The pertinent parameters are listed in Tab. 9.1.

a	1.393
$\frac{f^2_{\pi\widetilde{N}\widetilde{N}}}{4\pi}$	0.071
λ_1	0.632
λ_2	0.735

Table 9.1.: Parameters of the bare $\pi\widetilde{N}\widetilde{N}$ form factor fitted with Eq. (9.1).

In Fig. 9.2 we compare our bare $\mathcal{F}_{\pi\widetilde{N}\widetilde{N}}$ with the form-factor models already considered in Ch. 4. They are now plotted as functions of $\vec{k}^2_\pi$. Apparently, the CC form factor as well as the corresponding coupling constant compare well with the RCQM, the SL and the KNLS ones. However, the form factor of both PR parametrizations are in comparison decreasing way too slowly and their coupling constant is almost 5 times smaller.

Finally, we show in Tab. 9.3 the effect on the N mass by taking the CC form factor into account. We obtain a reasonable bare mass that is only slightly higher than the other ones. Consequently the extracted CC form factor leads to a similar result in taking one-π loop effects into account.

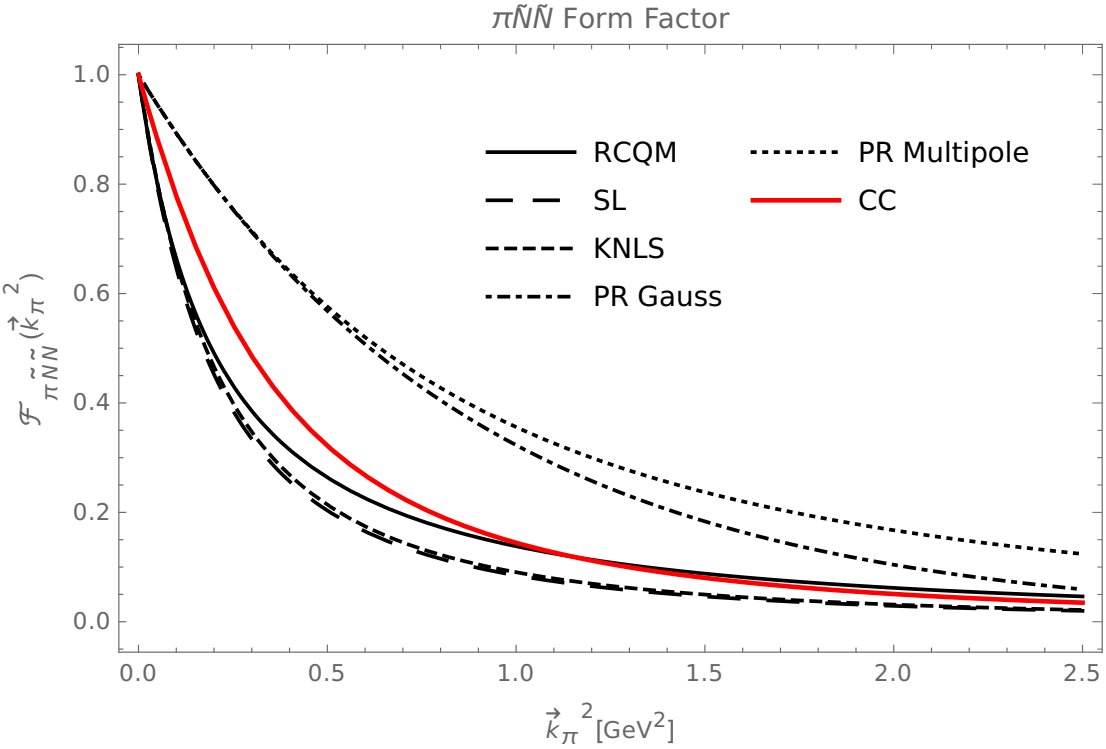

Figure 9.2.: CC $\pi\widetilde{N}\widetilde{N}$ form factor compared to other models used before.

	RCQM	SL	KNLS	PR Gauss	PR Multipole	CC
$\frac{f^2_{\pi\tilde{N}\tilde{N}}}{4\pi}$	0.0691	0.08	0.08	0.013	0.013	0.071
λ_1	0.451	0.453			0.945	0.632
λ_2	0.931	0.641			1.102	0.735
Λ			0.656	0.665		

Table 9.2.: Coupling constants and parameters for the $\pi\widetilde{N}\widetilde{N}$ vertex form factors according to different models in the literature compared to the CC one.

9.4. Results for the Δ

This section contains results for the bare $\pi\widetilde{N}\widetilde{\Delta}$ form factor, the $\pi\widetilde{N}\widetilde{\Delta}$ coupling constant as well as the bare and π-dressed Δ masses. We first show the numerical data of the bare $\pi\widetilde{N}\widetilde{\Delta}$ form factor in Fig. 9.3 together with its parametrization after Eq. (9.1), whose parameters are quoted in Tab. 9.4.

In Fig. 9.4 we compare our $\pi\widetilde{N}\widetilde{\Delta}$ form factor with the form factor models already considered in Ch. 6 .

We again observe that the CC form factor is quite similar to the RCQM one, where

	RCQM	SL	KNLS	PR Gauss	PR Multipole	CC
m_N	939	939	939	939	939	939
$m_{\widetilde{N}}$	1067	1031	1037	1025	1051	1096
$m_N - m_{\widetilde{N}}$	-128	-92	-98	-86	-112	-157

Table 9.3.: π loop effects on the nucleon mass m_N from coupling to the πN channel ($m_{\widetilde{N}}$ being the bare mass and m_N the dressed (physical) one). All values given in MeV. The π mass is always assumed to be m_π=139 MeV.

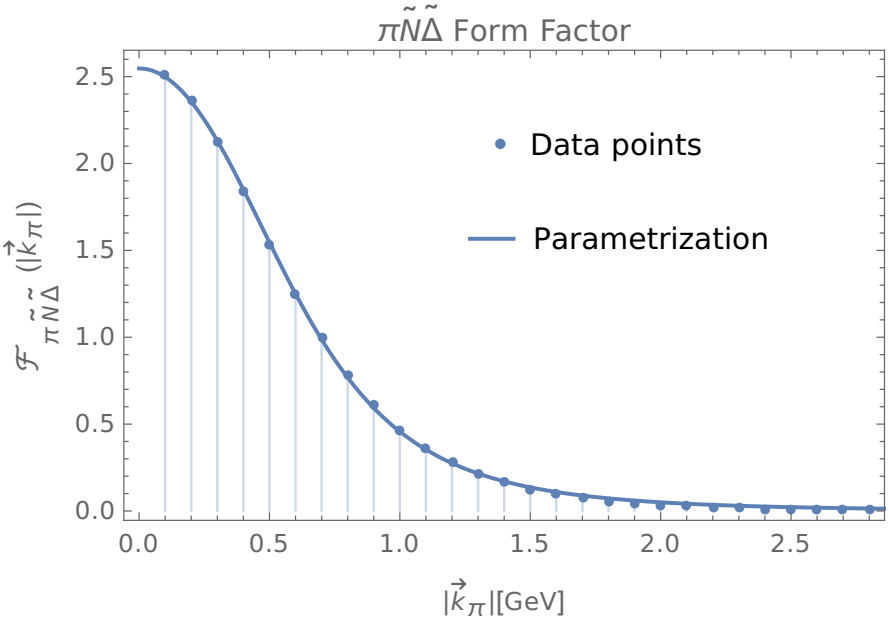

Figure 9.3.: Bare $\pi\widetilde{N}\widetilde{\Delta}$ form factor resulting from the CC approach at the microscopic quark level together with its parametrization according to Eq. (9.1).

a	2.547
$\frac{f^2_{\pi\widetilde{N}\widetilde{\Delta}}}{4\pi}$	0.239
λ_1	0.72
λ_2	0.784

Table 9.4.: Parameters of the bare $\pi\widetilde{N}\widetilde{\Delta}$ form factor fitted with Eq. (9.1).

the two fall more or less between the SL respectively KNLS and PR models.

Next we consider the π-dressing effect on the Δ mass, see Tab. 9.6, where also a comparison is given with the other models. Due to the relatively high bare N mass of 1096 MeV the threshold $m_\pi + m_{\widetilde{N}} = 1235$ MeV and thus lies above the real part of the

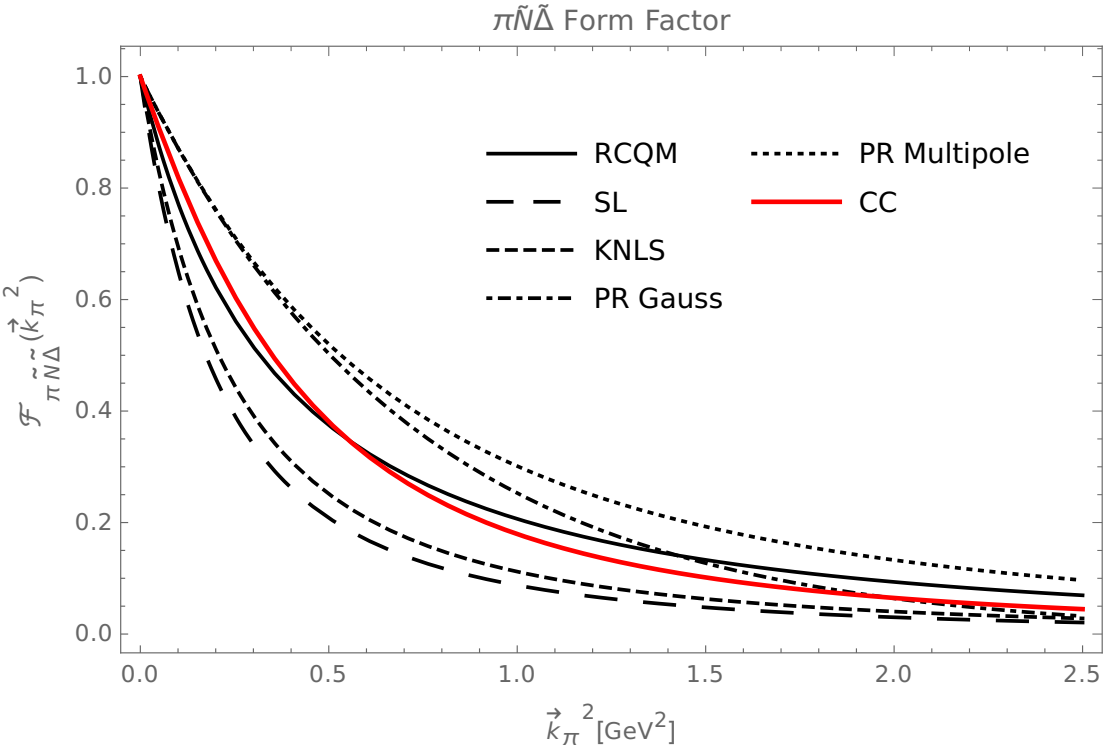

Figure 9.4.: CC $\pi\widetilde{N}\widetilde{\Delta}$ form factor compared to other models used before.

	RCQM	SL	KNLS	PR Gauss	PR Multipole	CC
$\frac{f^2_{\pi\widetilde{N}\widetilde{\Delta}}}{4\pi}$	0.188	0.334	0.126	0.167	0.167	0.239
λ_1	0.594	0.458			0.853	0.72
λ_2	0.998	0.648			1.014	0.784
Λ			0.709	0.603		

Table 9.5.: Coupling constants and parameters for the $\pi\widetilde{N}\widetilde{\Delta}$ vertex form factors according to different models in the literature compared to the CC one.

Δ mass, preventing its decay according to the diagram in Fig. 6.1.

The dressing effect on the N and Δ masses depends among others on the size of the πQQ coupling. Its influence is shown in Fig. 9.5. When the $\frac{f^2_{\pi QQ}}{4\pi}$ is turned on from 0 to the value of 0.037, marked by the vertical blue line, used in our practical calculation the N and Δ masses result as the physical ones. However, the threshold for the $\Delta \to \pi\widetilde{N}$ decay shown by the horizontal dashed line, happens to be above the Δ mass of 1232 MeV.

	RCQM	SL	KNLS	PR Gauss	PR Multipole	CC
$m_{\widetilde{N}}$	1067	1031	1037	1025	1051	1096
$Re[m_\Delta]$	1232	1232	1232	1232	1232	1232
$m_{\widetilde{\Delta}}$	1300	1290	1259	1321	1335	1309
$Re[m_\Delta] - m_{\widetilde{\Delta}}$	-68	-58	-27	-89	-103	-77
$2\,Im[m_\Delta] = \Gamma$	4	23	7	16	8	0
$\Gamma_{exp}(\Delta \to \pi N)$			~ 117			

Table 9.6.: π loop effects on the Δ mass m_Δ from coupling to the πN channel. $m_{\widetilde{\Delta}}$ and $m_{\widetilde{N}}$ are the bare $\widetilde{\Delta}$ and $\widetilde{N}$ masses, respectively. The latter is the same as in the π-dressing of the $\widetilde{N}$ in Ch. 4, cf. Tab. 4.2. All values given in MeV. The π mass is assumed to be $m_\pi = 139$ MeV.

9.4.1. Improved Description of the $\Delta \to \pi N$ Decay

A more realistic description of the $\Delta \to \pi N$ decay is achieved according to the diagram in Fig. 6.4, i. e. when the decay products are the π and a physical N. The corresponding results are given in Tab. 9.7.

	RCQM	SL	KNLS	PR Gauss	PR Multipole	CC
m_N	939	939	939	939	939	939
$Re[m_\Delta]$	1232	1232	1232	1232	1232	1232
$m_{\widetilde{\Delta}}$	1309	1288	1261	1329	1347	1327
$Re[m_\Delta] - m_{\widetilde{\Delta}}$	-77	-56	-29	-96	-115	-95
$2\,Im[m_\Delta] = \Gamma$	47	64	27	52	52	67
$\Gamma_{exp}(\Delta \to \pi N)$			~ 117			

Table 9.7.: π loop effects on the Δ mass m_Δ from coupling to the πN channel. $m_{\widetilde{\Delta}}$ and m_N are the bare $\widetilde{\Delta}$ and the physical N masses, respectively. All values given in MeV. The π mass is assumed to be $m_\pi = 139$ MeV.

If one now compares Tab. 9.6 to Tab. 9.7 one can immediately see the consequences on the decay width by lowering the decay threshold to $(m_\pi + m_N)$. Now the obtained decay width is also finite for the CC case, in fact it is already half of the experimentally measured value. In Tab. 9.6 the dressing effect on the bare Δ masses was between 27 MeV for the KNLS parametrization and 103 MeV for the PR multipole parametriza-

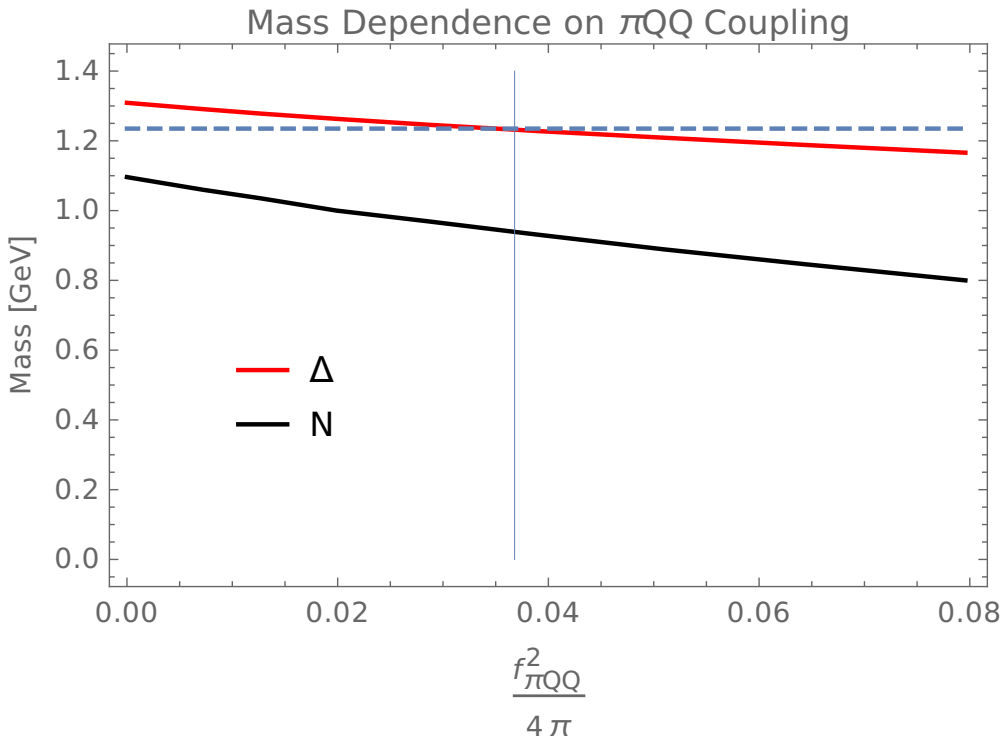

Figure 9.5.: Dependence of the N and Δ masses on πQQ coupling constant using the CC input. The horizontal dashed (blue) line marks the decay threshold. The vertical (blue) line indicates the size of the πQQ coupling constant used in our model.

tion, respectively. Now from Tab. 9.7 we observe that this range remains practically unaltered, namely between 29 MeV for the KNLS parametrization and 115 MeV for the PR multipole parametrisation. Therefore lowering the threshold seems to mostly affect the imaginary part of the eigenvalue and its real part is barely changed.

As in the previous discussion, the mass eigenvalues can again be plotted against the πQQ coupling, see Fig. 9.6. Now the decay threshold is lowered to 1078 MeV indicated by the horizontal dashed line. Thus the $\Delta(1232)$ can decay into πN and the obtained decay width for the process $\Delta(1232) \to \pi N$ is indicated by the band between the highest and lowest red line, the line in the middle specifying the Δ mass. If the πQQ coupling is zero, the decay width is zero and as the coupling is turned on, the decay width becomes larger until the coupling becomes too large and finally, when the decay threshold is reached, the decay width is vanishing again.

Further Improvement in Describing the $\Delta \to \pi N$ Decay

Now one can argue that in addition to using the dressed (physical) N mass in the intermediate state one should also use a dressed coupling constant instead of the bare

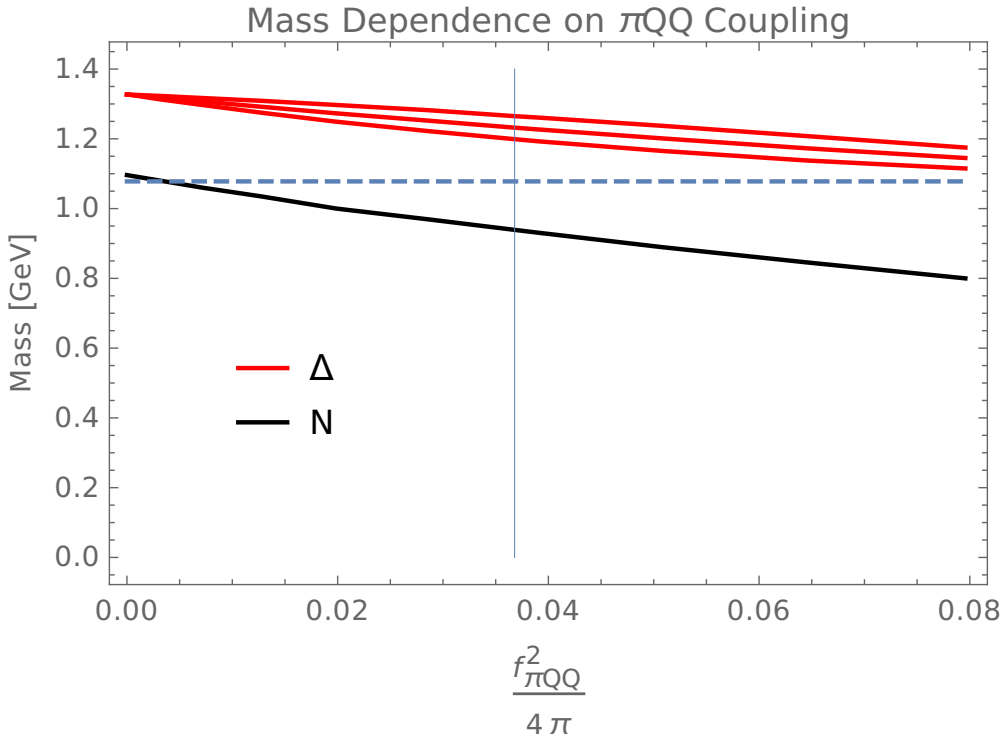

Figure 9.6.: Mass dependence on πQQ coupling constant. Same description as in Fig. 9.5. The decay width of the Δ is shown by the breadth of the red band (see also the text).

one. In Ref. [SL96] it is found that the dressed coupling constant, $f_{\pi N\Delta}$, is 1.3 times the bare one: $f_{\pi N\Delta} = 1.3\, f_{\pi\widetilde{N}\widetilde{\Delta}}$. Using this result we may now also assume the dressed coupling constants 1.3 times larger than the bare ones. The corresponding results for bare masses and decay widths are given in Tab. 9.8. If one compares Tab. 9.8 with Tab. 9.7 one recognizes that now the dressing effect on both the real part and on the imaginary part of the Δ mass eigenvalue is increased. The experimental value for the resonance decay width is well reached by the CC parametrization and the results for Γ are also much enhanced in the other cases. The dressing effects for the KNLS model remains still small, because the $\pi\widetilde{N}\widetilde{\Delta}$ coupling constant is small from the very beginning (cf. Tab. 9.5).

As in the previous discussions, the mass eigenvalues can again be plotted against the πQQ coupling, see Fig. 9.7. The threshold is the same as before but the coupling to the decay channel is 1.3 times larger. Consequently, the decay width, indicated by the band between the highest and lowest red line, is larger as compared to the one in Fig. 9.6. At the assumed πQQ coupling of $\frac{f^2_{\pi QQ}}{4\pi} = 0.037$, indicated by the vertical blue line, the experimentally measured Δ decay width $\Gamma \sim 117$ MeV is obtained. Again, when the coupling becomes too strong and consequently the decay threshold is reached, the de-

cay width is vanishing.

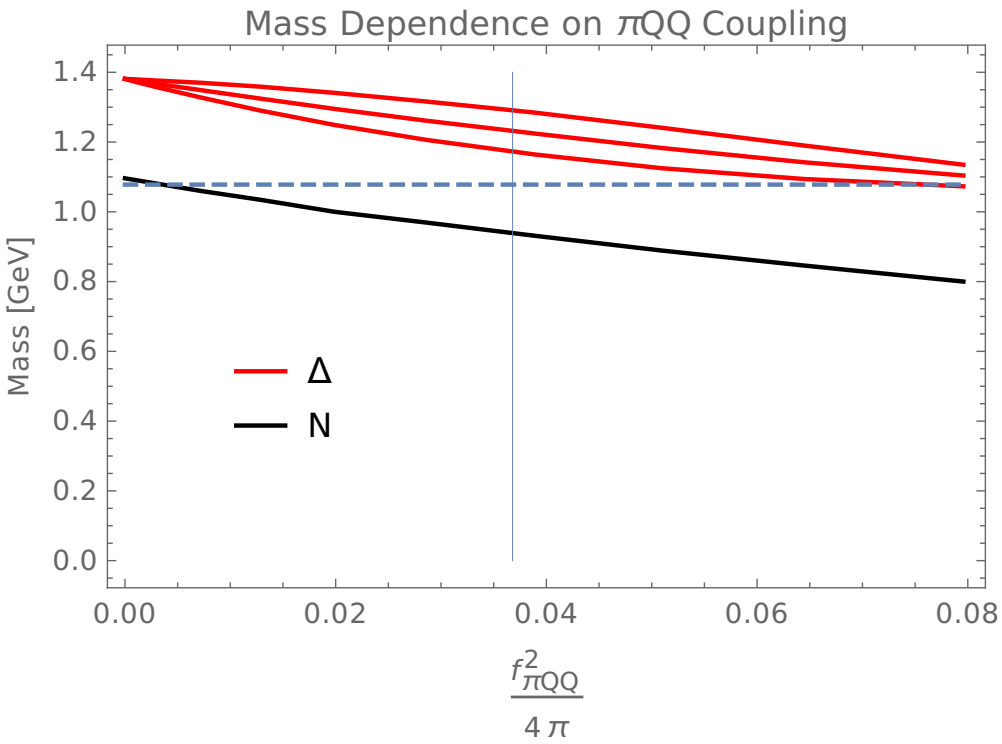

Figure 9.7.: Mass dependence on πQQ coupling constant. Same description as in Fig. 9.5. The decay width of the Δ is shown by the breadth of the red band (see also the text). Now $f_{\pi N\Delta} = 1.3 f_{\pi\widetilde{N}\widetilde{\Delta}}$ is used.

9.5. $\mathcal{F}_{\pi\widetilde{\Delta}\widetilde{N}}$ and $\mathcal{F}_{\pi\widetilde{\Delta}\widetilde{\Delta}}$ Vertex Form Factors

Finally we present the results for the bare $\mathcal{F}_{\pi\widetilde{\Delta}\widetilde{N}}$ and $\mathcal{F}_{\pi\widetilde{\Delta}\widetilde{\Delta}}$ vertex form facotrs defined in Eqs. (8.52) and (8.55), respectively. The numerical data of the $\mathcal{F}_{\pi\widetilde{\Delta}\widetilde{N}}$ are shown in Fig. 9.8 together with the parametrization after Eq. (9.1). The correspronding parameters are collected in Tab. 9.9.

It is interesting to compare $\mathcal{F}_{\pi\widetilde{\Delta}\widetilde{N}}$ to the $\mathcal{F}_{\pi\widetilde{N}\widetilde{\Delta}}$ form factor from Sec. 9.4 above, see Fig. 9.9. Obviously neither the bare coupling constants nor the momentum dependences of the bare form factors are the same for $\pi\widetilde{\Delta}\widetilde{N}$ and $\pi\widetilde{N}\widetilde{\Delta}$ (cf. also Tabs. 9.9 and 9.4). This is a direct consequence of the definitions in Eqs. (8.52) and (8.55).

The $\mathcal{F}_{\pi\widetilde{\Delta}\widetilde{\Delta}}$ form factor is plotted in Fig. 9.10 together with its parameterization after Eq. (9.1). The corresponding parameters are quoted in Tab. 9.10.

We compare the $\pi\widetilde{\Delta}\widetilde{\Delta}$ form factor extracted in the CC model to the KNLS parametrization in Fig. 9.11 and they agree very well. However, the coupling constants differ a lot. The CC one is about a factor six higher than the KNLS one as can be seen in

	RCQM	SL	KNLS	PR Gauss	PR Multipole	CC
m_N	939	939	939	939	939	939
$Re[m_\Delta]$	1232	1232	1232	1232	1232	1232
$m_{\widetilde{\Delta}}$	1356	1319	1279	1387	1418	1381
$Re[m_\Delta] - m_{\widetilde{\Delta}}$	-124	-87	-47	-155	-186	-149
$2\,Im[m_\Delta] = \Gamma$	83	106	45	94	97	118
$\Gamma_{exp}(\Delta \to \pi N)$			~ 117			

Table 9.8.: π loop effects on the Δ mass m_Δ from coupling to the πN channel where dressed coupling constants, $f_{\pi N\Delta} = 1.3\, f_{\pi\widetilde{N}\widetilde{\Delta}}$, have been used. $m_{\widetilde{\Delta}}$ and m_N are the bare $\widetilde{\Delta}$ and physical N masses, respectively. All values given in MeV. The π mass is assumed to be $m_\pi = 139$ MeV.

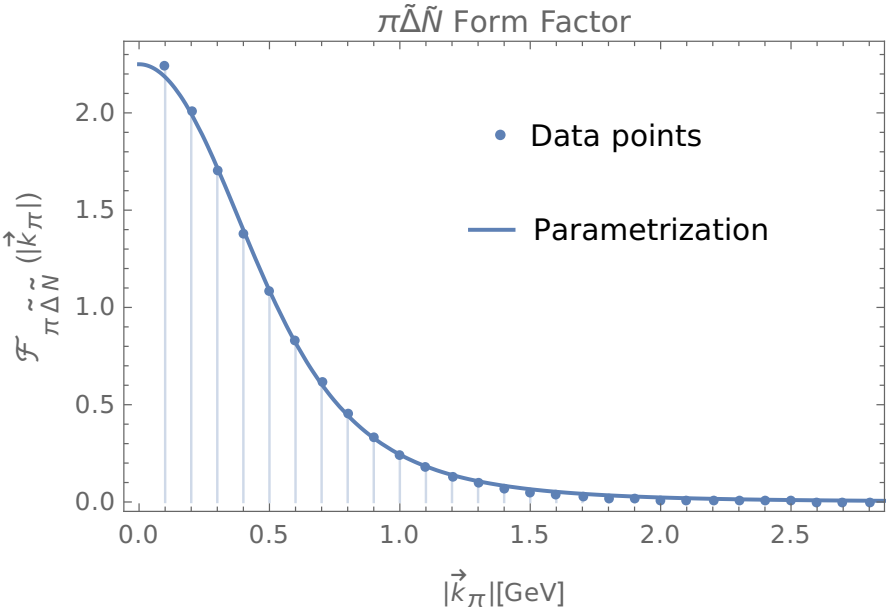

Figure 9.8.: Bare $\pi\widetilde{\Delta}\widetilde{N}$ form factor resulting from the CC approach at the microscopic quark level together with its parametrization according to Eq. (9.1).

Tab. 9.10. The small coupling constant of the KNLS model obviously comes about, because therein many more coupled channels are taken into account.

a	2.25
$\frac{f^2_{\pi\widetilde{\Delta}\widetilde{N}}}{4\pi}$	0.186
λ_1	0.581
λ_2	0.66

Table 9.9.: Parameters of the bare CC $\pi\widetilde{\Delta}\widetilde{N}$ form factor fitted with Eq. (9.1).

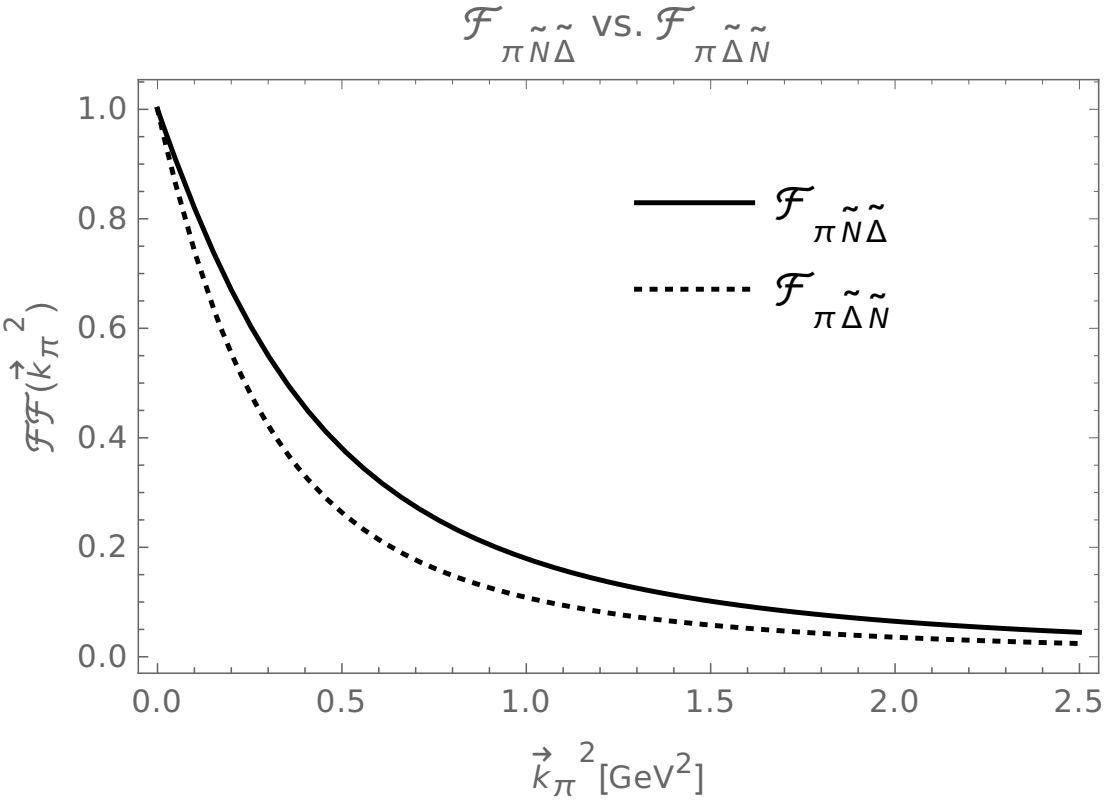

Figure 9.9.: Comparison of $\mathcal{F}_{\pi\widetilde{N}\widetilde{\Delta}}$ and $\mathcal{F}_{\pi\widetilde{\Delta}\widetilde{N}}$ vertex form factors from the CC approach.

	RCQM	KNLS
a	1.586	
$\frac{f^2_{\pi\widetilde{\Delta}\widetilde{\Delta}}}{4\pi}$	0.093	0.014
λ_1	0.57	
λ_2	0.656	
Λ		0.703

Table 9.10.: Parameters of the bare CC $\pi\widetilde{\Delta}\,\widetilde{\Delta}$ form factor fitted with Eq. (9.1). For reasons of comparison, the parameters of the KNLS parametrization, Eq. (4.56) are given here too.

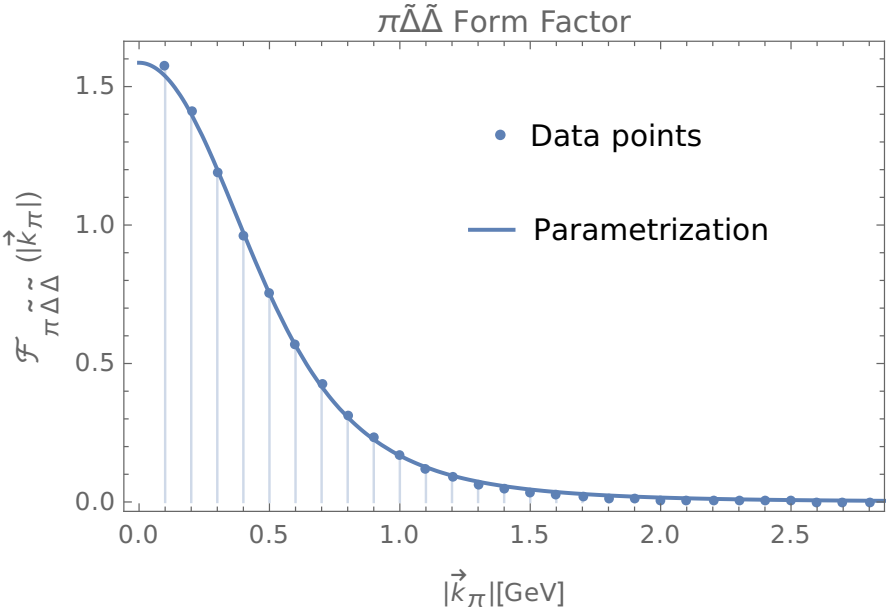

Figure 9.10.: Bare $\pi\widetilde{\Delta}\,\widetilde{\Delta}$ form factor resulting from the CC approach at the microscopic quark level together with its parametrization according to Eq. (9.1).

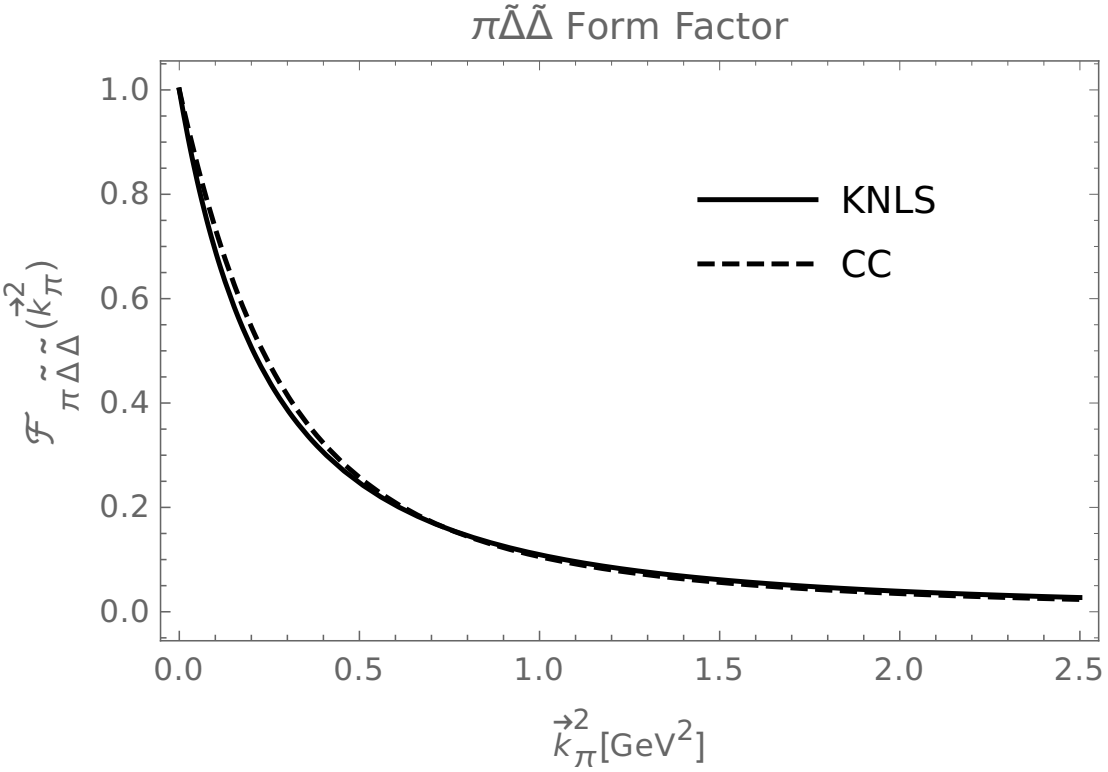

Figure 9.11.: Comparison of the $\mathcal{F}_{\pi\widetilde{\Delta}\,\widetilde{\Delta}}$ form factor extracted in the CC approach and the $\mathcal{F}_{\pi\widetilde{\Delta}\,\widetilde{\Delta}}$ form factor obtained in the phenomenological KNLS model.

Part V.

Summary and Outlook

In this thesis we have presented a coupled-channels aproach for baryon ground and resonant states within the point form of relativistic quantum mechanics. It has been applied in particular to the N and Δ states with π degrees of freedom.

The CC treatment makes it feasible to take mesonic effects in baryon states explicitly into account. The theory relies on a Poincaré-invariant CC mass operator, which provides for the coupling to channels with additional mesons. A Feshbach reduction is applied to reduce the CC eigenvalue equation in matrix form to finally end up with a non-Hermitian problem. The corresponding eigenvalue equation is no longer linear, since the eigenvalue appears also in the optical potential. The latter describes the meson dressing of the baryon.

This type of approach had already been applied before to a simplified (spinless) model for mesons with promising results [Kle10]. Here we were interested, if coupling mesonic channels to baryons led also to a more realistic description of three-quark ground and resonant states.

First, the approach has been applied at the hadronic level to the N and the Δ. There, the CC mass-operator eigenvalue equations have been set up, such that a bare baryon, either a N or a Δ, is explicitly coupled to an interaction-free πN channel. For the coupling to the latter a pseudovector Lagrangian density has been applied. To take the microscopic structure at the vertex into account, strong vertex form factors have been employed from different models in the literature. The eigenvalue equations have then been solved to produce the bare and the dressed (physical) masses of the N and Δ. These quantities result in agreement with phenomenology.

The bare masses of the N turned out to lie about 100 MeV higher than the dressed masses more or less for all form-factor models considered. The dressing effects on the real part of the Δ mass vary in a broader range. A finite Δ decay width is naturally produced. Since the Δ is to almost 100% decaying into a πN system, we assumed its CC mass operator to consist of a Δ channel and a πN channel only. In the first instance, when we considered a bare N in the exit channel the decay width resulted unreasonably small, because of the threshold $m_\pi + m_{\widetilde{N}}$ lying much too high due to the relatively big mass of the bare N.

In a next step we have thus replaced the bare N masses by the physical one and so the threshold has been lowered. Thereby the bare Δ masses have only been slightly altered, but already half of the experimentally measured decay width has been obtained. In this way we have achieved a more realistic description of the Δ decaying into πN.

In addition, π degrees of freedom beyond one-loop contributions have been considered both for the N and Δ in order to check, if the results for dressing the masses and producing the decay widths will alter. In all cases higher π contributions caused only minor effects of at most a few MeV, and they can readily be considered as negligible.

To be able to study in a consistent way pionic effects in the N and Δ masses as well as in the Δ decay width, we set up a microscopic CC mass operator on the quark level. In this way vertex form factors have been extracted from the quark dynamics at the microscopic level. With regard to the πNN and $\pi N\Delta$ vertices they are compared together with the corresponding coupling constants to the form-factor models from the litera-

ture used before. In addition, our approach has also allowed to consistently produce the strong form factors for the $\pi\Delta N$ and $\pi\Delta\Delta$ vertices. As a result all (bare) strong form factors and the pertinent coupling constants occurring in a setting with N, Δ and π are now available from a microscopic theory.

Applying the CC form factors and corresponding couplings at the πNN and $\pi N\Delta$ vertices, the dressing effects on the N and Δ have then been studied. We have obtained quite similar results as before with the new form factors derived here. Only the Δ decay width remained zero, if the threshold was set to $m_\pi + m_{\widetilde{N}}$, the reason lying in the bare N mass being too high. The situation has been remedied by assuming a physical N in the πN decay channel, and more than half of the experimental decay width has then been achieved.

The result for the decay width is further improved, if a dressed coupling constant is used for the πN coupling instead of a bare one. Following suggestions in the literature, for instance, in Ref. [SL96] we have thus assumed a dressed coupling constant 1.3 times stronger. This has finally led to results, where the dressing effect on the real part of the Δ mass is enhanced and the π decay width also becomes larger. In fact, in case of the CC model a decay width completely compatible with the experimental value is generated.

By the present work we have laid the basis for explicitly taking into account meson degrees of freedom for baryons in a relativistic CC theory. The framework is suitable for application on a macroscopic (hadronic) as well as a microscopic (quark) level and for an arbitrary number of particles and channels. Beyond the concrete studies presented here for the cases of the N and the Δ it would be very interesting to investigate further baryon resonances, such as N^* states or resonances with strangeness, notably the $\Lambda(1405)$. For some resonances it will not be sufficient to consider couplings to channels with only one additional meson. However, as proven already here with evaluating two-π degrees of freedom, our approach will be mighty enough to account also for such situations, where several mesonic channels and/or interactions among them will be needed.

Part VI.

Appendices

A. Basic Relations and Notation

In this chapter we are summarizing all the relations and basic tools that are needed for the theoretical framework of the present work.

A.1. Minkowski Space Relations

Since we are working in Minkowski space an arbitrary four-vector is given by

$$x^\mu = (x^0, x^1, x^2, x^3) = (x^0, \vec{x}). \tag{A.1}$$

This contravariant version corresponds to the following covariant one

$$x_\mu = (x_0, x_1, x_2, x_3) = (x^0, -\vec{x}) = g_{\mu\nu} x^\nu \tag{A.2}$$

with $g_{\mu\nu}$ being the metric tensor defined as

$$g_{\mu\nu} = \begin{pmatrix} 1 & 0 & 0 & 0 \\ 0 & -1 & 0 & 0 \\ 0 & 0 & -1 & 0 \\ 0 & 0 & 0 & -1 \end{pmatrix}. \tag{A.3}$$

Hence, the invariant scalar product between two four-vectors is defined as

$$x \cdot y = x^\mu y_\nu = x^\mu g_{\mu\nu} y^\nu = x^0 y^0 - \vec{x}\,\vec{y}. \tag{A.4}$$

A.2. Dirac and Rarita-Schwinger Spinors

Dirac Spinors for Spin-$\frac{1}{2}$ Particles

The standard representation of the Dirac matrices is given by

$$\gamma^0 = \begin{pmatrix} \mathbb{1}_2 & 0 \\ 0 & -\mathbb{1}_2 \end{pmatrix}, \quad \gamma = \begin{pmatrix} 0 & \vec{\sigma} \\ -\vec{\sigma} & 0 \end{pmatrix}, \quad \text{and} \quad \gamma^5 = \begin{pmatrix} 0 & \mathbb{1}_2 \\ \mathbb{1}_2 & 0 \end{pmatrix} \tag{A.5}$$

with

$$\sigma_1 = \begin{pmatrix} 0 & 1 \\ 1 & 0 \end{pmatrix}, \quad \sigma_2 = \begin{pmatrix} 0 & -i \\ i & 0 \end{pmatrix}, \quad \text{and} \quad \sigma_3 = \begin{pmatrix} 1 & 0 \\ 0 & -1 \end{pmatrix} \tag{A.6}$$

being the common forms of the Pauli matrices. In using this standard representations a canonical boost in the (4×4) matrix representation of the group SL(2,$\mathbb{C}$) can be written as

$$S[B_c(\vec{v})] = \sqrt{\frac{k^0+m}{2m}} \begin{pmatrix} \mathbb{1}_2 & \frac{\vec{\sigma}\cdot\vec{k}}{k^0+m} \\ \frac{\vec{\sigma}\cdot\vec{k}}{k^0+m} & \mathbb{1}_2 \end{pmatrix} \qquad \text{with} \qquad \vec{v} = \frac{\vec{k}}{m}. \tag{A.7}$$

The SL(2,$\mathbb{C}$) is the covering group of the Pioncaré group and a detailed discussion thereof can be found in Ref. [Bie11].

In the rest frame of a massive spin-$\frac{1}{2}$ particle with mass m, the solutions of the Dirac equation, namely the Dirac spinors for spin up and spin down are given as, Ref. [IZ06]

$$u\left(\vec{0}, s = +\frac{1}{2}\right) = \begin{pmatrix} 1 \\ 0 \\ 0 \\ 0 \end{pmatrix} \qquad \text{and} \qquad u\left(\vec{0}, s = -\frac{1}{2}\right) = \begin{pmatrix} 0 \\ 1 \\ 0 \\ 0 \end{pmatrix}. \tag{A.8}$$

These can be boosted by a canonical boost, given in Eq. (A.7), from rest up to a certain velocity $\vec{v}$,

$$u(\vec{k}, s) = \frac{k_\mu \gamma^\mu + m}{\sqrt{m+k^0}} u(\vec{0}, s) = \begin{pmatrix} \sqrt{k^0+m}\,\chi^s \\ \frac{\vec{\sigma}\cdot\vec{k}}{\sqrt{m+k^0}}\chi^s \end{pmatrix} \qquad \text{with} \qquad s = \pm\frac{1}{2} \tag{A.9}$$

with s denoting either spin up or spin down. The conjugate spinors are defined as

$$\bar{u}(\vec{k}, s) = \bar{u}(\vec{0}, s) \frac{k_\lambda \gamma^\lambda + m}{\sqrt{k^0+m}} \tag{A.10}$$

with χ^s being the so called Pauli spinors

$$\chi^{s=+\frac{1}{2}} = \begin{pmatrix} 1 \\ 0 \end{pmatrix} \tag{A.11}$$

and

$$\chi^{s=-\frac{1}{2}} = \begin{pmatrix} 0 \\ 1 \end{pmatrix}. \tag{A.12}$$

Rarita-Schwinger Spinors for Spin-$\frac{3}{2}$ Particles

To construct Rarita-Schwinger spinors for spin-$\frac{3}{2}$ particles one has to combine the Dirac spinors for spin-$\frac{1}{2}$ particles and spin-1 polarization vectors.

The spin-$\frac{1}{2}$ spinors at rest are given in Eq. (A.8) and the ones that are boosted up to a velocity $\vec{v}$ are given in Eqs. (A.9) and (A.10).

Spin-1 rest frame polarization vectors are defined in spherical representation, [Pil79], as

$$\epsilon^\mu(0, M) \quad = \quad (0, e(M)), \tag{A.13}$$

where for different $M = 0, \pm 1$ they read as

$$e(+1) := -\frac{1}{\sqrt{2}}(1, i, 0), \tag{A.14}$$

$$e(-1) := \frac{1}{\sqrt{2}}(1, -i, 0), \tag{A.15}$$

$$e(0) := (0, 0, 1). \tag{A.16}$$

Polarization vectors with arbitrary momentum $\vec{k}$ are obtained from the rest-frame vectors by applying a canonical boost

$$\epsilon^{\mu}(\vec{k}, M) = B_c(\vec{v})^{\mu}_{\nu} \epsilon^{\nu}(0, M), \tag{A.17}$$

with

$$B_c(\vec{v}) = \begin{pmatrix} v^0 & \vec{v}^{\,T} \\ \vec{v} & 1 + \frac{(v^0 - 1)\vec{v} \cdot \vec{v}^{\,T}}{\vec{v}^{\,2}} \end{pmatrix}, \quad v^0 = \sqrt{1 + \vec{v}^{\,2}} \quad \text{and} \quad \vec{v} = \frac{\vec{k}}{m}. \tag{A.18}$$

After performing the calculation the boosted polarization four-vector reads

$$\epsilon^{\mu}(\vec{k}, M) = \left(\frac{\vec{e}(M) \cdot \vec{k}}{m}, \; \vec{e}(M) + \frac{\vec{k}(\vec{e}(M) \cdot \vec{k})}{m(\omega_k + m)} \right) \tag{A.19}$$

with $\vec{k}$ the momentum of the particle under consideration, m its mass and ω_k the corresponding energy.

The Rarita-Schwinger spinors for spin-$\frac{3}{2}$ particles can be described as products of spin-$\frac{1}{2}$ spinors $u\left(\pm\frac{1}{2}\right)$ and polarization vectors $\epsilon^{\mu}(\pm 1)$ of spin-1 particles with $1 + \frac{1}{2} \to \frac{3}{2}$ Clebsch-Gordan coefficients [Pil79]

$$\begin{aligned} u^{\mu}\left(\pm\frac{3}{2}\right) &= u\left(\pm\frac{1}{2}\right) \epsilon^{\mu}(\pm 1), \\ u^{\mu}\left(\pm\frac{1}{2}\right) &= 3^{-\frac{1}{2}} u\left(\mp\frac{1}{2}\right) \epsilon^{\mu}(\pm 1) + \left(\frac{2}{3}\right)^{\frac{1}{2}} u\left(\pm\frac{1}{2}\right) \epsilon^{\mu}(0). \end{aligned} \tag{A.20}$$

List of Figures

Bibliography

[A+08] C. Amsler et al. Review of Particle Physics. *Phys. Lett.*, B667:1, 2008.

[ABFS56] J. Ashkin, J. P. Blaser, F. Feiner, and M. O. Stern. Pion-Proton Scattering at 150 and 170 Mev. *Phys. Rev.*, 101(3):1149, 1956.

[AFLN52] H. L. Anderson, E. Fermi, E. A. Long, and D. E. Nagle. Total Cross Sections of Positive Pions in Hydrogen. *Phys. Rev.*, 85:936–936, 1952.

[ASWP95] R. A. Arndt, I. I. Strakovsky, R. L. Workman, and M. M. Pavan. Updated Analysis of πN Elastic Scattering Data to 2.1-GeV: The Baryon Spectrum. *Phys. Rev.*, C52:2120–2130, 1995.

[BD64] J. D. Bjorken and S. D. Drell. *Relativistic Quantum Mechanics*. McGraw-Hill, New York, 1964.

[Bie11] E. P. Biernat. *Electromagnetic Properties of Few-Body Systems Within a Point-Form Approach*. PhD thesis, University of Graz, 2011.

[BKSZ08] E. P. Biernat, W. H. Klink, W. Schweiger, and S. Zelzer. Point-Form Quantum Field Theory. *Annals Phys.*, 323:1361–1383, 2008.

[BT53] B. Bakamjian and L. H. Thomas. Relativistic Particle Dynamics. 2. *Phys. Rev.*, 92:1300–1310, 1953.

[Car71] P. A. Carruthers. *Spin and Isospin in Particle Physics*. Gordon and Breach, New York, 1971.

[CG09] R. N. Cahn and G. Goldhaber. *The Experimental Foundations of Particle Physics*. Cambridge University Press, Cambridge, 2009.

[CS00] L. Canton and W. Schadow. Isoscalar Off-Shell Effects in Threshold Pion Production from $p\,d$ Collision. *Phys. Rev.*, C61:064009, 2000.

[Dir49] P. A. M. Dirac. Forms of Relativistic Dynamics. *Rev. Mod. Phys.*, 21:392–399, 1949.

[DST65] A. De-Shalit and I. Talmi. *Nuclear Shell Theory*. Pure and Applied Physics, Rehoboth, Israel, 1965.

[EL07] P. Exner and J. Lipovský. Equivalence of Resolvent and Scattering Resonances on Quantum Graphs. *Adventures in Mathematical Pysics, Proceedings*, 447:73–81, 2007.

[EW88] T. Ericson and W. Weise. *Pions and Nuclei*. Oxford University Press, New York, 1988.

[Fes62] H. Feshbach. A Unified Theory of Nuclear Reactions. *Annals Phys.*, 19:287–313, 1962.

[GPP+98] L. Ya. Glozman, Z. Papp, W. Plessas, K. Varga, and R. F. Wagenbrunn. Effective Q Q Interactions in Constituent Quark Models. *Phys. Rev.*, C57:3406–3413, 1998.

[GPVW98] L. Ya. Glozman, W. Plessas, K. Varga, and R. F. Wagenbrunn. Unified Description of Light and Strange Baryon Spectra. *Phys. Rev.*, D58:094030, 1998.

[GS93] F. Gross and Y. Surya. Unitary, Relativistic Resonance Model for πN Scattering. *Phys. Rev.*, C47:703–723, 1993.

[IZ06] C. Itzykson and J.-B. Zuber. *Quantum Field Theory*. Dover Publ. Inc., London, 2006.

[Kam12] H. Kamano. Results of Nucleon Resonance Extraction via Dynamical Coupled-Channels Analysis from Collaboration@EBAC. *PoS*, QNP2012:011, 2012.

[Kle10] R. Kleinhappel. Resonances and Decay Widths Within a Relativistic Coupled Channel Approach. Master's thesis, University of Graz, 2010.

[Kli98] W. H. Klink. Relativistic Simultaneously Coupled Multiparticle States. *Phys. Rev.*, C58:3617–3626, 1998.

[Kli03] W. H. Klink. Constructing Point Form Mass Operators from Interaction Lagrangians. *Nucl. Phys.*, A716:123–135, 2003.

[KNKJ04] N. G. Kelkar, M. Nowakowski, K. P. Khemchandani, and S. R. Jain. Time Delay Plots of Unflavoured Baryons. *Nucl. Phys.*, A730(1):121 – 140, 2004.

[KNLS13] H. Kamano, S. X. Nakamura, T. S. H. Lee, and T. Sato. Nucleon Resonances Within a Dynamical Coupled-Channels Model of πN and γN Reactions. *Phys. Rev.*, C88(3):035209, 2013.

[KP91] B. D. Keister and W. N. Polyzou. Relativistic Hamiltonian Dynamics in Nuclear and Particle Physics. *Adv. Nucl. Phys.*, 20:225–479, 1991.

[Kra01] A. Krassnigg. *A Relativistic Point-Form Approach to Quark-Antiquark Systems*. PhD thesis, University of Graz, 2001.

[LMCPV12] T. Ledwig, J. Martin-Camalich, V. Pascalutsa, and M. Vanderhaeghen. The Nucleon and $\Delta(1232)$ Form Factors at Low Momentum-Transfer and Small Pion Masses. *Phys. Rev.*, D85:034013, 2012.

[MCP09] T. Melde, L. Canton, and W. Plessas. Structure of Meson-Baryon Interaction Vertices. *Phys. Rev. Lett.*, 102:132002, 2009.

[Moi98] N. Moiseyev. Quantum Theory of Resonances: Calculating Energies, Widths and Cross-Sections by Complex Scaling. *Phys. Rep.*, 302(5):212 – 293, 1998.

[P+16] C. Patrignani et al. Review of Particle Physics. *Chin. Phys.*, C40(10):100001, 2016.

[Pil79] H. M. Pilkuhn. *Relativistic Particle Physics*. Springer-Verlag, Berlin, 1979.

[PR05a] H. Polinder and Th. A. Rijken. Soft-Core Meson-Baryon Interactions. I. One-Hadron-Exchange Potentials. *Phys. Rev.*, C72:065210, 2005.

[PR05b] H. Polinder and Th. A. Rijken. Soft-Core Meson-Baryon Interactions. II. πN and K^+N Scattering. *Phys. Rev.*, C72:065211, 2005.

[PT00] V. Pascalutsa and J. A. Tjon. Pion Nucleon Interaction in a Covariant Hadron Exchange Model. *Phys. Rev.*, C61:054003, 2000.

[SCPS17] R. A. Schmidt, L. Canton, W. Plessas, and W. Schweiger. Baryon Masses and Hadronic Decay Widths with Explicit Pionic Contributions. *Few Body Syst.*, 58(2):34, 2017.

[Sen06] B. Sengl. *Mesonic Baryon Resonance Decays in Relativistic Constituent Quark Models*. PhD thesis, University of Graz, 2006.

[SL96] T. Sato and T.-S. H. Lee. Meson Exchange Model for πN Sscattering and γN —> πN Reaction. *Phys. Rev.*, C54:2660–2684, 1996.

[SV98] Y. Suzuki and K. Varga. Stochastic Variational Approach to Quantum-Mechanical Few Body Problems. *Lect. Notes Phys. Monogr.*, 54:1–310, 1998.

[Tay83] J. R. Taylor. *Scattering Theory*. R. E. Krieger Publishing Company, Malabar, 1983.

[Tho98] T. Thonhauser. Meson Spectra in a Chiral Constituent Quark Model. Master's thesis, University of Graz, 1998.

[TWDP01] L. Theußl, R. F. Wagenbrunn, B. Desplanques, and W. Plessas. Hadronic Decays of N and Δ Resonances in a Chiral Quark Model. *Nucl. Phys.*, A689:394–397, 2001.

[VMK88] D. A. Varshalovich, A. N. Moskalev, and V. K. Khersonskii. *Quantum Theory of Angular Momentum*. World Scientific, Singapore, 1988.

[Wag98] R. Wagenbrunn. *Chiral Constituent-Quark Model for Light and Strange Baryons*. PhD thesis, University of Graz, 1998.

B. Acknowledgements

I thank Alexander, Nora, and Klara not only for giving me some extra time to finish my PhD.

I thank my supervisor Willibald Plessas for the continuous support. His guidance helped me in all the years of research and writing this thesis.

I thank Wolfgang Schweiger for his time, his constructive suggestions and helpful ideas.

I thank Luciano Canton for his hospitality during my stay in Padova and especially for always being available for discussions.

I thank the FWF for my funding within the doctoral college "Hadrons in Vacuum, Nuclei and Stars".